This technical report has been made
electronically available on
the World Wide Web
through a contribution from

an Anonymous Donor

U.S. DEPARTMENT OF
ENERGY

Office of Science

osti.gov

Severe Accidents in Spent Fuel Pools in Support of Generic Safety Issue 82

DO NOT MICROFILM
COVER

Prepared by V. L. Sailor, K. R. Perkins, J. R. Weeks, H. R. Connell

Brookhaven National Laboratory

NOTICE

Availability of Reference Materials Cited in NRC Publications

Most documents cited in NRC publications will be available from one of the following sources:

1. The NRC Public Document Room, 1717 H Street, N.W.
   Washington, DC 20555

2. The Superintendent of Documents, U.S. Government Printing Office, Post Office Box 37082,
   Washington, DC 20013-7082

3. The National Technical Information Service, Springfield, VA 22161

Although the listing that follows represents the majority of documents cited in NRC publications, it is not intended to be exhaustive.

Referenced documents available for inspection and copying for a fee from the NRC Public Document Room include NRC correspondence and internal NRC memoranda; NRC Office of Inspection and Enforcement bulletins, circulars, information notices, inspection and investigation notices; Licensee Event Reports; vendor reports and correspondence; Commission papers; and applicant and licensee documents and correspondence.

The following documents in the NUREG series are available for purchase from the GPO Sales Program: formal NRC staff and contractor reports, NRC-sponsored conference proceedings, and NRC booklets and brochures. Also available are Regulatory Guides, NRC regulations in the *Code of Federal Regulations*, and *Nuclear Regulatory Commission Issuances*.

Documents available from the National Technical Information Service include NUREG series reports and technical reports prepared by other federal agencies and reports prepared by the Atomic Energy Commission, forerunner agency to the Nuclear Regulatory Commission.

Documents available from public and special technical libraries include all open literature items, such as books, journal and periodical articles, and transactions. *Federal Register* notices, federal and state legislation, and congressional reports can usually be obtained from these libraries.

Documents such as theses, dissertations, foreign reports and translations, and non-NRC conference proceedings are available for purchase from the organization sponsoring the publication cited.

Single copies of NRC draft reports are available free, to the extent of supply, upon written request to the Division of Information Support Services, Distribution Section, U.S. Nuclear Regulatory Commission, Washington, DC 20555.

Copies of industry codes and standards used in a substantive manner in the NRC regulatory process are maintained at the NRC Library, 7920 Norfolk Avenue, Bethesda, Maryland, and are available there for reference use by the public. Codes and standards are usually copyrighted and may be purchased from the originating organization or, if they are American National Standards, from the American National Standards Institute, 1430 Broadway, New York, NY 10018.

DISCLAIMER

This report was prepared as an account of work sponsored by an agency of the United States Government. Neither the United States Government nor any agency Thereof, nor any of their employees, makes any warranty, express or implied, or assumes any legal liability or responsibility for the accuracy, completeness, or usefulness of any information, apparatus, product, or process disclosed, or represents that its use would not infringe privately owned rights. Reference herein to any specific commercial product, process, or service by trade name, trademark, manufacturer, or otherwise does not necessarily constitute or imply its endorsement, recommendation, or favoring by the United States Government or any agency thereof. The views and opinions of authors expressed herein do not necessarily state or reflect those of the United States Government or any agency thereof.

Severe Accidents in Spent Fuel Pools in Support of Generic Safety Issue 82

Prepared by
V. L. Sailor, K. R. Perkins, J. R. Weeks, H. R. Connell

Department of Nuclear Energy
Brookhaven National Laboratory
Upton, New York 11973

MASTER

ABSTRACT

This investigation provides an assessment of the likelihood and consequences of a severe accident in a spent fuel storage pool - the complete draining of the pool. Potential mechanisms and conditions for failure of the spent fuel, and the subsequent release of the fission products, are identified. Two older PWR and BWR spent fuel storage pool designs are considered based on a preliminary screening study which tried to identify vulnerabilities. Internal and external events and accidents are assessed. Conditions which could lead to failure of the spent fuel Zircaloy cladding as a result of cladding rupture or as a result of a self-sustaining oxidation reaction are presented. Propagation of a cladding fire to older stored fuel assemblies is evaluated. Spent fuel pool fission product inventory is estimated and the releases and consequences for the various cladding failure scenarios are provided. Possible preventive or mitigative measures are qualitatively evaluated. The uncertainties in the risk estimate are large, and areas where additional evaluations are needed to reduce uncertainty are identified.

TABLE OF CONTENTS

LIST OF TABLES

LIST OF FIGURES

PREFACE

This study is an initial attempt by Brookhaven National Laboratory to characterize the radiological risks posed by storage of spent reactor fuel at commercial reactor sites in the United States. This work was done at the request of the U.S. Nuclear Regulatory Commission in support of their technical analysis related to Generic Safety Issue 82, "Beyond Design Basis Accidents in Spent Fuel Pools." The method of analysis used in this study was to a) survey the spent fuel pool configurations at commercial reactor sites in terms of the characteristics that are important to risk and b) perform detailed analyses of those spent fuel configurations for which the risk appeared to be potentially significant. The detailed analyses were performed by using the methodology of probabilistic risk assessment that has been used extensively in the assessment of power plant risks during normal operation. Thus, this initial study, while limited in resources, required the integration of several technologically distinct disciplines (e.g., seismic analysis, fuel degradation analysis, offsite consequence analysis). Although these disciplines have been integrated before in the normal operation risk assessments, the application to the spent fuel problem posed novel and uncertain conditions not encountered in the normal operation risk assessments. The present study did not address: the potential for recriticality; the fuel damage process during a slow pool drainage; and the fuel reconfiguration after a clad fire. The results of this study have additional uncertainty, beyond those characteristic of traditional risk assessment studies for reactor operations, which is associated with the novel aspects of the phenomenology and the limitations of the data base.

ACKNOWLEDGEMENTS

S.1 INTRODUCTION

Generic Safety Issue 82, "Beyond Design Basis Accidents in Spent Fuel Pools," was assigned a MEDIUM priority in November 1983.[1] In this prioritization, the NRC staff considered three factors that had not been included in earlier risk assessments:[2]

1. Spent fuel is currently being stored rather than shipped for reprocessing or repository disposal, resulting in much larger inventories of spent assemblies in reactor fuel basins than had previously been anticipated,

2. In order to accommodate the larger inventory, high density racking is necessary, and

3. A theoretical model[3,4] suggested the possibility of Zircaloy fire, propagating from recently discharged assemblies to lower power assemblies in the event of complete drainage of water from the pool.

The Reactor Safety Study,[2] commonly referred to as WASH-1400, concluded that the risks associated with spent fuel storage were extremely small in comparison with accidents associated with the reactor core. That conclusion was based on design and operational features of the storage pools which made the loss of water inventory highly unlikely. In addition it was assumed that the pool inventory would be limited to about one-third of a core.

Subsequent to the Reactor Safety Study, A.S. Benjamin et al.[3,4] investigated the heatup of spent fuel following drainage of the pool. A computer code, SFUEL, was developed to analyze thermal-hydraulic phenomena occurring when storage racks and spent assemblies become exposed to air.

Calculations with SFUEL indicated that, for some storage configurations and decay times, the Zircaloy cladding could reach temperatures at which the exothermic oxidation would become self-sustaining with resultant destruction of the cladding and fission product release. The possibility of propagation to adjacent assemblies (i.e., the cladding would catch fire and burn at a high enough temperature to heat neighboring fuel assemblies to the ignition point) was also identified. Under certain conditions, the entire inventory of stored fuel could become involved. Cladding fires of this type could occur at temperatures well below the melting point of the UO_2 fuel. The cladding ignition point is about 900°C compared to the fuel melting point of 2880°C.

There is no case on record of a significant loss of water inventory from a domestic, commercial spent fuel storage pool. However, two recent incidents have raised concern about the possibility of a partial draindown of a storage pool as a result of pneumatic seal failures.

The first incident occurred at the Haddam Neck reactor during preparations for refueling with the refueling cavity flooded. An inflatable seal bridging the annulus between the reactor vessel flange and the reactor cavity bearing plate extruded into the gap, allowing 200,000 gallons of borated water to drain out of the refueling cavity into the lower levels of the containment

building in about 20 minutes. Gates to the transfer tube and the fuel storage pool were in the closed position, so no water drained from the pool.[6]

The second pneumatic seal failure incident occurred in the Hatch spent storage pool/transfer canal, (the seal failure at Hatch was not in the refueling cavity) which released approximately 141, 000 gallons of water and resulted in a drop in water level in the pool of about five feet.[7]

However, the BNL review of these events indicates that they are unique to the plants involved and such events are unlikely to cause a substantial loss of pool inventory for other plants. However, pneumatic seal failures may expose individual fuel bundles during refueling and these events are being investigated as part of Generic Issue 137, "Refueling Cavity Seal Failure."

S.2 OBJECTIVE

The objective of this investigation is to provide an assessment of the potential risk from possible accidents in spent fuel pools. The risks are defined in terms of:

- the probabilities of various initiating events that might compromise the structural integrity of the pool or its cooling capability,
- the probability of a system failure, given an initiating event,
- fuel failure mechanisms, given a system failure,
- potential radionuclide releases, and
- consequences of a specified release.

This study generally follows the logic of a typical probabilistic risk analysis (PRA); however, because of the relatively limited number of potential accident sequences which could result in the draining of the pool, the analyses have been greatly simplified.

The configurations of spent fuel storage pools vary from plant to plant. In BWR's, the pools are located within the reactor building with the bottom of the pool at about the same elevation as the upper portion of the reactor pressure vessel. During refueling the cavity above the top of the pressure vessel is flooded to the same elevation as the storage pool, so that fuel assemblies can be transferred directly from the reactor to the pool via a gate which separates the pool from the cavity. In PWR plants, the storage pool is located in an auxiliary building. In some cases the pool surface is at about grade level, in others the pool bottom is at grade. The refueling cavities are usually connected to the storage pool by a transfer tube. During refueling the spent assembly is removed from the reactor vessel and placed in a container which then turns on its side, moves through the transfer tube to the storage pool, is set upright again and removed from the transfer container to a storage rack. Various gates and weirs separate different sections of the transfer and storage systems. A screening study was performed to identify potentially risk significant sequences involving spent fuel pools, the pool design features of the commercial power plants were reviewed and summarized.

In order to prioritize the present risk analysis, a preliminary risk assessment was performed for spent fuel pools using the RSS methodology[2] and the results of the above screening study. This preliminary study indicated that a seismic initiated failure of the pool was the dominant risk

contributor. Based on this assessment, two older BWR and PWR plants were selected for more detailed studies based on their perceived vulnerability to seismic events. Specifically, Millstone 1 and Ginna, were selected because of availability of data, fuel pool inventory, and the relative familiarity of the BNL staff with the various candidate sites. The operating histories of the two plants were modeled to obtain a realistic radioactive inventory in the various spent fuel batches.

S.3 ACCIDENT INITIATING EVENTS AND PROBABILITY ESTIMATES

Accident initiating events that have been considered include both internal and external events:

- pool heatup due to loss of cooling water circulation capability,
- structural failure of pool due to seismic events or missiles,
- partial draindown of pool due to pneumatic seal failure, and
- structural failure of pool due to a heavy load drop.

Accidents leading to complete pool draining that might be initiated by loss of cooling water circulation capability, missiles, and pneumatic seal failure were found to have a very low likelihood. However, the frequency estimates for pool draining due to structural failure resulting from seismic events and heavy load drops were found to be quite uncertain. In the case of seismic events, the seismic hazard and structural fragilities both contribute to the uncertainty range. For heavy load drops, human error probabilities, structural damage potentials and recovery actions are the primary sources of uncertainties.

S.4 EVALUATION OF FUEL CLADDING FAILURE

The SFUEL computer code developed at Sandia National Laboratories (SNL) by Benjamin et al.,[3] analyzes the behavior of spent fuel assemblies after an accident has drained the pool. The analyses predict that self-sustaining oxidation of the Zircaloy cladding (i.e., a cladding fire) would occur for a wide range of decay heat levels and storage geometries. Several limitations in the SFUEL analyses had been recognized in Reference 3 and have been addressed in a modified version of the code, SFUEL1W.[4]

The BNL evaluations of SFUEL1W have led to the conclusions that the modified code gives a reasonable estimate of the potential for propagation of a cladding fire from high power to low power spent fuel while the fuel is intact. The code therefore provides a valuable tool for assessing the likelihood of a cladding fire for a variety of intact spent fuel configurations in the event that the pool is drained.

S.5 CONSEQUENCE EVALUATION

Radioactive releases are estimated for the two plants for cladding failure scenarios predicted by SFUEL calculations involving cladding fires. Partial drainage events where the cladding may rupture and release the rod gap inventory (without a fire) are also presented.

The radioactive inventories contained in the spent fuel pools (as of April 1987) for Millstone 1 and Ginna were calculated using the ORIGEN2

computer code,[8] based on the operating histories of each of the plants (Appendix A). The calculated data included the 1987 inventories for each fuel batch discharged at each refueling over the operating history.

Fractional releases for various groups of radionuclides were estimated based on the physical parameters characterizing the SFUEL failure scenario. Thus, source terms were estimated corresponding to the seven accident scenarios: five involving cladding fire for various amounts of fuel, and two involving cladding rupture (without a fire).

Off-site radiological consequences were calculated using the CRAC2 computer code.[9] Because of several features in the health physics modeling in the CRAC2 code, the population dose results are not very sensitive to the estimated fission product release. A more sensitive measure of the accident severity appears to be the interdiction area (contaminated land area) which in the worst cases was about two hundred square miles. While the long-term health effects (i.e., person-rem) are potentially large, it is important to note that no "prompt fatalities" were predicted and the risk of injury was also negligible.

S.6 RISK PROFILE

The likelihood and consequences of various spent fuel pool accidents have been combined to obtain the risks which are summarized in Table S.1. The population dose results are insensitive to the fission product release because they are driven by decontamination levels assigned within the CRAC2 code. The health physics models in CRAC2 assign a maximum allowable dose for each individual before the contaminated area is reoccupied. This allowable dose for the returning population is the dominant contributor to total exposure and limits the utility of the dose calculation. Thus the land interdiction area is included in Table S.1 as a more sensitive representation of the severity of the postulated accident.

The unique character of fuel pool accidents (potentially large releases of long lived isotopes) makes it difficult to compare directly to reactor core melt accidents. There are no early health effects. The long-term exposure calculations are driven by assumptions in the CRAC modeling and the results are not very sensitive to the severity of the accident. There is substantial uncertainty in the fission product release estimates. These uncertainties are due to both uncertainty in the accident progression (fuel temperature after clad oxidation and fuel relocation occurs) and the uncertainty in fission product decontamination.

S.7 CONSIDERATION OF MEASURES WHICH MIGHT REDUCE CONSEQUENCES

A number of potential preventive and mitigative measures were identified, but because of the large uncertainty ranges in Table S.1, the potential benefits of such measures are also uncertain and plant specific. A cost benefit analysis has not been performed. Rather, the phenomenological insights, developed during the investigation, have been used to generate a list of possible risk reduction measures. Calculations with the SFUEL code indicate that, for those plants that use a high density storage rack configuration, a factor of five reduction in the fire probability (given loss of pool inventory) can be achieved by improved air circulation capability. This reduction

factor is based upon the time period after discharge for which SFUEL predicted that the decay heat is sufficient to initiate a clad fire. Considering the large uncertainty in risk, a plant specific cost/benefit analyses should be performed before such risk reduction measures are implemented.

S.8 CONCLUSIONS

This limited risk assessment, which was performed for two older spent fuel pools, indicates that the risk estimates are quite uncertain and could potentially (under worst case assumptions) be significant. The uncertainty in risk is dominated by the estimated uncertainty in the likelihood of the loss of pool integrity due to beyond design basis seismic events. This uncertainty is, in turn, driven by the uncertainty in the seismic hazard and the spent fuel pool fragility. These risk ranges are consistent with the current medium priority assigned to the issue by the NRC.[1] It is not clear that these uncertainty ranges are directly applicable to other plants because the plants selected for detailed study were chosen specifically for their perceived vulnerability to seismic events after an extensive screening process (refer to Section S.2). For example, if the fragility estimates for plants, which meet the new seismic design criteria, were used, a significant reduction in the predicted likelihood of seismically initiated pool failure would result. In addition many of the new plants have pool configurations and administrative procedures which would preclude cask drop accidents. Therefore, in order to determine whether other plants have a significant risk profile, a plant specific evaluation would be required. A key part of such an evaluation would be to obtain a realistic seismic fragility estimate for the specific spent fuel pool.

S.9 REFERENCES FOR SUMMARY

1. "A Prioritization of Generic Safety Issues," Division of Safety Technology, Office of Nuclear Reactor Regulation, U.S. Nuclear Regulatory Commission, NUREG-0933, December 1983, pp. 3.82-1 through 6.

2. "Reactor Safety Study, An Assessment of Accident Risks in U.S. Commercial Nuclear Power Plants," U.S. Nuclear Regulatory Commission, NUREG-75/014 (WASH-1400), October 1975, App. I, Section 5.

3. A.S. Benjamin, D.J. McClosksy, D.A. Powers, and S.A. Dupree, "Spent Fuel Heatup Following Loss of Water During Storage," prepared for the U.S. Nuclear Regulatory Commission by Sandia Laboratories, NUREG/CR-0649 (SAND77-1371), May 1979.

4. N.A. Pisano, F. Best, A.S. Benjamin and K.T. Stalker, "The Potential for Propagation of a Self-Sustaining Zirconium Oxidation Following Loss of Water in a Spent Fuel Storage Pool," prepared for the U.S. Nuclear Regulatory Commission by Sandia Laboratories, (Draft Manuscript, January 1984) (Note: the project ran out of funds before the report was published.)

5. IE Bulletin No. 84-03: "Refueling Cavity Water Seal," U.S. Nuclear Regulatory Commission, Office of Inspection and Enforcement, August 24, 1984.

6. Licensee Event Report, LER No. 84-013-00, Haddam Neck, Docket No. 50-213, "Failure of Refueling Pool Seal," 09/21/84.

7. Nucleonics Week, December 11, 1986, pg. 3-4.

8. A.G. Croff, "ORIGEN2: A Versatile Computer Code for Calculating the Nuclide Composition and Characteristics of Nuclear Materials," Nuclear Technology, Vol. 62, pp. 335-352, September 1983.

9. L.T. Ritchie, J.D. Johnson and R.M. Blond, Calculations of Reactor Accident Consequences Version 2, CRAC2: Computer Code User's Guide, prepared by Sandia National Laboratories for the U.S. Nuclear Regulatory Commission, NUREG/CR-2326 (SAND81-1994), February 1983.

Table S.1 Estimated Risk for the Two Spent Fuel Pools from the Two Dominant Contributors

Accident Initiator	Spent Fuel Pool Fire Probability/Ry	Health Risk[1] (Man-rem/Ry)	Interdiction[1] Risk (Sq. Mi./Ry)
Seismic induced PWR pool failure	$2.6 \times 10^{-4} - 1.6 \times 10^{-10}$	600-Neg.*	.011-Neg.
Seismic induced BWR pool failure	$6.5 \times 10^{-5} - 4 \times 10^{-11}$	156-Neg.	.003-Neg.
Cask drop[2] induced PWR pool failure	$3 \times 10^{-5} - 3 \times 10^{-12}$	70-Neg.	.001-Neg.
Cask drop[2] induced BWR pool failure	$8 \times 10^{-6} - 8 \times 10^{-13}$	20-Neg.	4×10^{-4}-Neg.

*Neg. - Negligible.

[1]The upper end of the risk ranges assumes no fire propagation from the last fuel discharge to older fuel. However, the fission products in the last fuel discharge were assumed to be released during the fire with no fission product decontamination on structures.

[2]After removal of accumulated inventory resumes. Presently, most plants are accumulating spent fuel in the pool without shipping to permanent storage. (Note that many new plants have pool configurations and administrative procedures which would preclude this failure mode.)

1. INTRODUCTION

Generic Safety Issue 82, "Beyond Design Basis Accidents in Spent Fuel Pools," was assigned a MEDIUM priority in November 1983.[1] In this prioritization, the NRC staff considered three factors that had not been included in earlier risk assessments:[2]

1. Spent fuel is currently being stored rather than shipped for reprocessing or repository disposal, resulting in much larger inventories of spent assemblies in reactor fuel basins than had previously been anticipated;

2. In order to accommodate the larger inventory, high density racking is necessary, and

3. A theoretical model[3] suggested the possibility of Zircaloy fire, propagating from assembly to assembly in the event of complete drainage of water from the pool.

1.1 Previous Investigations

The Reactor Safety Study,[2] commonly referred to as WASH-1400, concluded that the risks associated with spent fuel storage were extremely small in comparison with accidents associated with the reactor core. That conclusion was based on design and operational features of the storage pools which made the loss of water inventory highly unlikely, e.g.,

- The pool structures were designed to withstand safe shutdown earthquakes,
- The fuel racks were designed to preclude criticality,
- Pool design and instrumentation precluded inadvertent and undetected loss of water inventory,
- Procedures and interlocks prevented the drop of heavy loads on stored assemblies, and
- The storage structures were designed to accommodate the forces and missiles generated by violent storms.

Probabilities of pool failures due to external events (earthquakes, missiles) or heavy load drops were estimated to be in the range of 10^{-6}/year. Radioactive release estimates were based on melting of 1/3 of a core for various decay periods, with and without filtration of the building atmosphere (see Ref. 2, Table I 5-2).

Subsequent to the Reactor Safety Study, A.S. Benjamin et al.[3] investigated the heatup of spent fuel following drainage of the pool. A computer code, SFUEL, was developed to analyze thermal-hydraulic phenomena occurring when storage racks and spent assemblies become exposed to air. The computer model takes into account decay time, fuel assembly design, storage racks design, packing density, room ventilation and other variables that affect the heatup of the fuel.

Calculations with SFUEL indicated that, for some storage configurations and decay times, the Zircaloy cladding could reach temperatures at which the exothermic oxidation would become self-sustaining with resultant destruction

1

of the cladding and fission product release. The possibility of propagation to adjacent assemblies (i.e., the cladding would catch fire and burn at a hot enough temperature to heat neighboring fuel assemblies to the ignition point) was also identified. Under certain conditions, the entire inventory of stored fuel could become involved. Cladding fires of this type could occur at temperatures well below the melting point of the UO_2 fuel. The cladding ignition point is about 900°C compared to the fuel melting point of 2880°C.

Uncertainties in the SFUEL calculations were primarily attributed to uncertainties in the zirconium oxidation rates.

Further work was done to refine the SFUEL computer model and to compare calculated results with experimental data.[4] These more recent results have generally confirmed the earlier concepts of a Zircaloy fire which, given the right conditions, will propagate to neighboring assemblies. However, comparisons to out-of-pile heat-up data have not shown good agreement with the code. As discussed in Section 3, the SNL authors noted that more work in several areas was needed to define more precisely the conditions and configurations which allow or prevent propagation.

Several studies have been conducted on alternative spent fuel storage concepts. Among these is a report published by the Electric Power Research Institute (EPRI), which applies probabilistic risk assessment techniques to several storage concepts.[5] While this study does not directly address Generic Safety Issue 82, it does provide useful insight on appropriate analytical methodology as well as useful data on an in-ground (on-site) storage pool.

1.2 Related Events

There is no case on record of a significant loss of water inventory from a domestic, commercial spent fuel storage pool. However, two recent incidents have raised concern about the possibility of a partial draindown of a storage pool as a result of pneumatic seal failures.

The first incident occurred at the Haddam Neck reactor during preparations for refueling.[6] An inflatable seal bridging the annulus between the reactor vessel flange and the reactor cavity bearing plate extruded into the gap, allowing 200,000 gallons of borated water to drain out of the refueling cavity into the lower levels of the containment building in about 20 minutes. Gates to the transfer tube and the fuel storage pool were in the closed position, so no water drained from the pool.[7] Had these gates been open at the time of the leak, and had they not been closed within 10 to 15 minutes, the pool would have drained to a depth of about 8.5 feet, exposing the upper 3 feet of the active fuel region in the spent fuel assemblies.[7] Also, had the transfer of spent fuel been in progress with an assembly on the refueling machine, immediate action would have been necessary to place the assembly in a safe location under water to limit exposure to personnel. The NRC has identified this aspect of a seal failure accident as potential Generic Issue 137, "Refueling Cavity Seal Failure."[8] The current schedule for evaluation of the issue is December 1987.

The NRC Office of Inspection and Enforcement required all licensees to promptly evaluate the potential for refueling cavity seal failures.[6] Responses indicated that the refueling cavity configuration at Haddam Neck is

unique in that the annulus between the reactor flange and the cavity bearing plate is more than 2 feet wide. In most plants this gap is only about 2 inches wide.[9] About 40 operating (or soon to operate) reactors use inflatable seals in the refueling cavity. However, because of design differences, the Haddam Neck failure does not appear to be directly applicable to the other plants. It is noted that most BWR plants have permanent steel bellows seals to fill the gap between the reactor flange and the cavity bearing plate. This issue is discussed more fully in Section 2.3.

The second pneumatic seal failure incident occurred in the Hatch spent storage pool/transfer canal in December 1986.[10] In this incident, a pair of pneumatic seals deflated when the compressed air supply was inadvertently shut off. The seals involved were in the transfer canal flexible seismic joint. The leak detection annunciator failed to alarm and the leak was not discovered for about 7-1/2 hours. Approximately 141,000 gallons of water leaked from the storage fuel and the water level dropped about 5-1/2 feet.

1.3 Risk Potential

This study addresses beyond design basis accidents in spent fuel pools that might result in the complete loss of pool water due to structural failure, massive leaks or boil-off of inventory due to prolonged failure of cooling systems. The risk potentials are defined in terms of

- the probabilities of various initiating events that might compromise the structural integrity of the pool or its cooling capability,
- the probability of a system failure, given an initiating event,
- fuel failure mechanisms, given a system failure,
- potential radionuclide releases, and
- consequences of a specified release.

The analyses generally follow the logic of typical probabilistic risk analyses (PRA); however, because of the relatively limited number of potential accident sequences, which could result in the draining of the pool, the analyses have been greatly simplified.

1.4 Discussion of Spent Fuel Storage Pool Designs and Features

The general design criteria for spent fuel storage facilities are stated in Appendix A of 10 CFR 50,[11] and are discussed more fully in Regulatory Guide 1.13.[12]

The pool structures, spent fuel racks and overhead cranes must be designed to Seismic Category I standards. It is required that the systems be designed (1) with capability to permit appropriate periodic inspection and testing of components important to safety, (2) with suitable shielding for radiation protection, (3) with appropriate containment, confinement, and filtering systems, (4) with a residual heat removal capability having reliability and testability that reflects the importance to safety of decay heat and other residual heat removal, and (5) to prevent significant reduction in fuel storage coolant inventory under accident conditions.[11]

As part of the preliminary screening study for accident vulnerabilities, the design features of the spent fuel pools for the commercial power plants

3

were reviewed and assembled. The configurations of spent fuel storage pools vary from plant to plant. Table 1.1 summarizes this information for each of the pools.

In BWRs the pools are located within the reactor building with the bottom of the pool at about the same elevation as the upper portion of the reactor pressure vessel. (For example, at Oyster Creek the bottom of the pool is at elevation 80'6", and the top at 119'3". The water depth is 38 feet.) During refueling, the cavity above the top of the pressure vessel is flooded to the same elevation as the storage pool, so that fuel assemblies can be transferred directly from the reactor to the pool via a gate which separates the pool from the cavity.

In PWR plants the storage pool is located in an auxiliary building. In some cases the pool surface is at about grade level, in others the pool bottom is at grade. The refueling cavities are usually connected to the storage pool by a transfer tube. During refueling the spent assembly is removed from the reactor vessel and placed in a container which then turns on its side, moves through transfer tube to storage pool, set upright again and removed from the transfer container to a storage rack. Various gates and weirs separate different sections of the transfer and storage systems. More details concerning various configurations are given in Section 2.3.

1.5 More Detailed Studies

The overall objective of the present investigation was to determine whether possible severe accidents involving spent fuel pools posed a significant risk to the public. In order to prioritize the investigation a preliminary risk assessment was performed using RSS[2] methodology to identify the potentially important accident sequences and the characteristics of specific fuel pools which could lead to unusually high vulnerability to accidents. This preliminary risk assessment indicated that seismically induced structural failure of the pool appeared to dominate the spent fuel pool risk. This appeared to be particularly true for older plants in the eastern states where recent studies have indicated an increase in the estimated seismic hazard. Based on this preliminary study, two older BWR and PWR plants were selected for more detailed studies because of their perceived vulnerability to seismic events. Specifically, Millstone 1 and Ginna, were selected because of availability of data, fuel pool inventory, and the relative familiarity of the BNL staff with the various candidate sites. The operating histories of the two plants were modeled to obtain a realistic radioactive inventory in the various spent fuel batches. Details of the modeling procedures and a listing of the calculated radionuclide content are presented in Appendix A.

It should be noted that both plants have relatively large inventories of spent fuel assemblies in their spent fuel pools.

1.6 Report Content

Accident initiating events and their probabilities are covered in Section 2. Fuel cladding failure scenarios based on the SFUEL1W Computer Code are evaluated in Section 3. Included are sensitivity analyses of the failure scenarios arising from uncertainties in Zircaloy oxidation reaction rate data, and hardware configuration assumptions. Section 4 presents data on the

4

potential for releases of radionuclides under various cladding failure scenarios and compares the projected releases with releases associated with severe core accident sequences. In Section 5, risk profiles are developed in terms of person-rem population doses for several accident sequences. Section 6 considers measures that might mitigate pool draining and/or Zircaloy fire propagation.

1.7 References for Section 1

1. "A Prioritization of Generic Safety Issues," Division of Safety Technology, Office of Nuclear Reactor Regulation, U.S. Nuclear Regulatory Commission, NUREG-0933, December 1983, pp. 3.82-1 through 6.

2. "Reactor Safety Study, An Assessment of Accident Risks in U.S. Commercial Nuclear Power Plants," U.S. Nuclear Regulatory Commission, NUREG-75/014 (WASH-1400), October 1975, App. I, Section 5.

3. A.S. Benjamin, D.J. McClosksy, D.A. Powers, and S.A. Dupree, "Spent Fuel Heatup Following Loss of Water During Storage," prepared for the U.S. Nuclear Regulatory Commission by Sandia Laboratories, NUREG/CR-0649 (SAND77-1371), May 1979.

4. N.A. Pisano, F. Best, A.S. Benjamin and K.T. Stalker, "The Potential for Propagation of a Self-Sustaining Zirconium Oxidation Following Loss of Water in a Spent Fuel Storage Pool," prepared for the U.S. Nuclear Regulatory Commission by Sandia Laboratories, (Draft Manuscript, January 1984) (Note: the project ran out of funds before the report was published.)

5. D.D. Orvis, C. Johnson, and R. Jones, "Review of Proposed Dry-Storage Concepts Using Probabilistic Risk Assessment," prepared for the Electric Power Research Institute by the NUS Corporation, EPRI NP-3365, February 1984.

6. IE Bulletin No. 84-03: "Refueling Cavity Water Seal," U.S. Nuclear Regulatory Commission, Office of Inspection and Enforcement, August 24, 1984.

7. Licensee Event Report, LER No. 84-013-00, Haddam Neck, Docket No. 50-213, "Failure of Refueling Pool Seal," 09/21/84.

8. "Generic Issue Management Control System - First Quarter FY-87 Updates," Memorandum from T.P. Speis, Director, Division of Safety Review and Oversight, to H.R. Denton, Director, Office of Nuclear Reactor Regulation, U.S. Nuclear Regulatory Commission, February 13, 1987.

9. Licensee Responses to NRC IE Bulletin No. 84-03.

10. U.S. Nuclear Regulatory Commission, "Morning Report - Region II," December 5, 1986.

11. Code of Federal Regulations, Title 10, Part 50, "Domestic Licensing of Production and Utilization Facilities, Appendix A, 'General Design Criteria for Nuclear Power Plants,' General Design Criterion 61, 'Fuel Storage and Handling and Radioactivity Control'."

12. U.S. Nuclear Regulatory Commission, Regulatory Guide 1.13, "Spent Fuel Storage Facility Design Basis," December 1981.

Table 1.1 BWR's: DATA ON SPENT FUEL STORAGE BASINS. Included are spent fuel storage inventories as of December 1984, fractions of core in storage, comparisons with the "reference case" of radionuclide inventory, locations of spent fuel basins, and seismic design bases of pools.

Plant	Thermal Power (MWt)	Number of Fuel Assemblies in Core[a]	Spent Fuel Stored Inventory[a] (No. of Assemblies)	Stored Inventory Fractions of Core[b]	Radioactivity Relative to Reference Case[c] (per cent)	Storage Pool Location[d]	Seismic Design Basis[e]
Big Rock Point	240	84	172	2.05	4.9	AB, grd	DBE=0.05g
Browns Ferry-1	3293	764	1068	1.40	46.1	RB, ele	DBE=0.20g
Browns Ferry-2	3293	764	889	1.16	38.2	RB, ele	DBE=0.20g
Browns Ferry-3	3293	764	1768	2.31	76.1	RB, ele	DBE=0.20g
Brunswick-1	2436	560	1056[f]	1.89	46.0	RB, ele	DBE=0.16g
Brunswick-2	2436	560	924[g]	1.65	40.2	RB, ele	DBE=0.16g
Cooper	2381	548	985	1.80	42.9	RB, ele	DBE=0.2g
Dresden-1	700	464	221	0.48	3.36		DBE=0.20g
Dresden-2	2527	724	2014[h]	2.78[h]	70.3[h]	RB, ele	DBE=0.2g
Dresden-3	2527	724	-	-	-	RB, ele	DBE=0.2g
Duane Arnold	1658	368	576	1.57	26.0	RB, ele	DBE=0.12g
Fitzpatrick	2436	560	816	1.46	35.6	RB, ele	DBE=0.15g
Grand Gulf-1	3833	N/A[i]	0	0.00	0.0	N/A	
Hatch-1	2436	560	140	0.25	6.1	RB, ele	DBE=0.15g

7

Table 1.1 (Cont'd)

Plant	Thermal Power (MWt)	Number of Fuel Assemblies in Core[a]	Spent Fuel Stored Inventory[a] (No. of Assemblies)	Stored Inventory Fractions of Core[b]	Radioactivity Relative to Reference Case[c] (per cent)	Storage Pool Location[d]	Seismic Design Basis[e]
Hatch-2	2436	560	1284	2.29	55.8	RB, ele	DBE=0.15g
Humboldt Bay	220	172	251	1.46	3.2	N/A	DBE=0.50g
LaCrosse	165	72	207	2.88	4.8	AB, grd	DBE=0.12g
LaSalle-1	3323	N/A	0	0.00	0.0	RB, ele	SSE=0.20g
LaSalle-2	3323	N/A	0	0.00	0.0	RB, ele	SSE=0.20g
Limerick-1	3293	N/A	0	0.00	0.0	RB, ele	SSE=0.13g
Millstone-1	2011	580	1346	2.32	46.7	RB, ele	DBE=0.17g
Monticello	1670	484	1137	2.35	39.2	RB, ele	DBE=0.12g
Nine Mile Point-1	1850	532	1244	2.34	43.3	RB, ele	DBE=0.11g
Oyster Creek	1930	560	1375	2.46	47.5	RB, ele	DBE=0.22g
Peach Bottom-2	3293	764	1361	1.78	58.6	RB, ele	DBE=0.12g
Peach Bottom-3	3293	764	1212	1.59	52.4	RB, ele	DBE=0.12g
Pilgrim-1	1998	580	1128	1.94	38.8	RB, ele	DBE=0.15g
Quad Cities-1	2511	724	1730	2.39	60.0	RB, ele	DBE=0.24g
Quad Cities-2	2511	724	412	0.57	14.3	RB, ele	DBE=0.24g

Table 1.1 (Cont'd)

Plant	Thermal Power (MWt)	Number of Fuel Assemblies in Core[a]	Spent Fuel Stored Inventory[a] (No. of Assemblies)	Stored Inventory, Fractions of Core[b]	Radioactivity Relative to Reference Case[c] (per cent)	Storage Pool Location[d]	Seismic Design Basis[e]
Susquehanna-1	3293	764	0	0.00	0.0	RB, ele	SSE=0.1g
Susquehanna-2	3293	764	0	0.00	0.0	RB, ele	SSE=0.1g
Vermont Yankee	1593	368	1174	3.19	50.8	RB, ele	DBE=0.14g
Wash. Nucl.-2	3323	N/A	0	0.00	0.0	N/A	SSE=0.32g

Footnotes

a) Source: U. S. Nuclear Regulatory Commission, Licensed Operating Reactors, NUREG-0020, Vol. 9, No. 1, January 1985.

b) (Stored Assemblies)/(Assemblies in Core).

c) "Reference Source Term" assumes a thermal power of 3000 MWt, stored inventory from ten annual discharges, last discharge six months ago, total inventory 1750 assemblies. Source term relative to "Reference Source Term" has not been corrected for age of fuel in storage.

d) Location: RB = reactor building, AB = auxiliary building, grd = pool at grade level, ele = pool at high elevation in building.

e) Seismic design basis as a function of the gravitational acceleration (g): DBE = design basis earthquake, or equivalent as used for older vintage plants; SSE = safe shutdown earthquake as defined in 10 CFR 100, App. A. Entry shown is the horizontal component.

f) Brunswick-1 has in storage 160 PWR + 656 BWR assemblies, equivalent to 1056 BWR assemblies.

g) Brunswick-2 has in storage 144 PWR + 564 BWR assemblies, equivalent to 924 BWR assemblies.

h) Dresden Units 2 and 3 have two pools in one structure. The data cited are total of the two.

i) N/A = data not available.

Table 1.1 (Cont'd) PWR's: DATA ON SPENT FUEL STORAGE BASINS. Included are spent fuel storage inventories as of December 1984, fractions of core in storage, comparisons with the "reference case" of radionuclide inventory, locations of spent fuel basins, and seismic design bases of pools.

Plant	Thermal Power (MWt)	Number of Fuel Assemblies in Core[a]	Spent Fuel Stored Inventory[a] (No. of Assemblies)	Stored Inventory Fractions of Core[b]	Radioactivity Relative to Reference Case[c] (per cent)	Storage Pool Location[d]	Seismic Design Basis[e]
Arkansas-1	2568	177	388	2.19	56.3	AB, grd	DBE=0.2g
Arkansas-2	2815	177	168	0.95	26.7	AB, grd	DBE=0.2g
Beaver Valley-1	2660	157	104	0.66	17.6	FB, grd	SSE=0.125g
Byron-1	N/A[f]	N/A	0	0.00	0.0	AB, grd	SSE=0.2g
Callaway-1	3411	N/A	N/A	N/A	N/A	AB, grd	SSE=0.2g
Calvert Cliffs-1	2700	217	868[g]	4.00[g]	108.0[g]	AB, grd	DBE=0.15g
Calvert Cliffs-2	2700	217	-	-	-	AB, grd	DBE=0.15g
Catawba-1	N/A	N/A	N/A	N/A	N/A	AB, grd	SSE=0.12g
Cook-1	3250	193	553[g]	2.87[g]	93.1[g]	AB, grd	SSE=0.20g
Cook-2	3411	193	-	-	-	AB, grd	SSE=0.20g
Crystal River-3	2544	177	171	0.97	24.6	AB, grd	SSE=0.10g
Davis Besse-1	2772	177	199	1.12	31.2	AB, grd	DBE=0.15g
Diablo Canyon-1	3338	N/A	N/A	N/A	N/A	AB, grd	DDE=0.4g[j]
Farley-1	2652	157	114	0.73	19.3	AB, grd	SSE=0.10g

Table 1.1 (Cont'd)

Plant	Thermal Power (MWt)	Number of Fuel Assemblies in Core[a]	Spent Fuel Stored Inventory[a] (No. of Assemblies)	Stored Inventory Fractions of Core[b]	Radioactivity Relative to Reference Case[c] (per cent)	Storage Pool Location[d]	Seismic Design Basis[e]
Farley-2	2652	157	62	0.39	10.5	AB, grd	SSE=0.10g
Fort Calhoun	1500	133	305	2.29	34.4	AB, grd	DBE=0.17g
Ginna	1520	121	340	2.81	42.7	AB, grd	DBE=0.20g
Haddam Neck	1825	157	545	3.47	63.4	AB, grd	DBE=0.17g
Indian Point-1	h	0[h]	160	h	h	AB, grd	DBE=0.10g
Indian Point-2	2758	193	332	1.72	47.4	AB, grd	DBE=0.15g
Indian Point-3	3025	193	140	0.73	21.9	AB, grd	DBE=0.15g
Kewaunee	1650	121	268	2.21	36.5	AB, grd	DBE=0.12g
Maine Yankee	2630	217	577	2.66	69.9	AB, grd	DBE=0.10g
McGuire-1	3411	193	91	0.47	16.1	AB, grd	SSE=0.15g
McGuire-2	3411	N/A	N/A	N/A	N/A	AB, grd	SSE=0.15g
Millstone-2	2700	217	376	1.73	46.8	AB, grd	DBE=0.17g
North Anna-1	2775	157	220[g]	1.40[g]	38.9[g]	AB, grd	SSE=0.12g
North Anna-2	2775	157	-	-	-	AB, grd	SSE=0.12g
Oconee-1	2568	177	1037[g]	5.86[g]	150.5[g]	AB, grd	DBE=0.10g

Table 1.1 (Cont'd)

Plant	Thermal Power (MWt)	Number of Fuel Assemblies in Core[a]	Spent Fuel Stored Inventory[a] (No. of Assemblies)	Stored Inventory Fractions of Core[b]	Radioactivity Relative to Reference Case[c] (per cent)	Storage Pool Location[d]	Seismic Design Basis[e]
Oconee-2	2568	177	-	-	-	AB, grd	DBE=0.1g
Oconee-3	2568	177	218	1.23	31.6	AB, grd	DBE=0.1g
Palisades	2530	204	480	2.35	59.5	AB, grd	DBE=0.20g
Palo Verde-1	N/A	N/A	N/A	N/A	N/A	AB, grd	SSE=0.20g
Point Beach-1	1518	121	524[g]	4.33[g]	65.7[g]	AB, grd	DBE=0.18g
Point Beach-2	1518	121	-	-	-	AB, grd	DBE=0.18g
Prairie Island-1	1650	121	601[g]	4.97[g]	82.0[g]	AB, grd	SSE=0.12g
Prairie Island-2	1650	121	-	-	-	AB, grd	SSE=0.12g
Rancho Seco-1	2772	177	260	1.47	40.7	AB, grd	SSE=0.25g
Robinson-2	2300	157	152	0.97	22.3	AB, grd	DBE=0.20g
Salem-1	3338	193	296	1.53	51.2	AB, grd	DBE=0.20g
Salem-2	3411	193	265	1.37	46.8	AB, grd	DBE=0.20g
San Onofre-1	1347	157	94	0.60	8.1	AB, grd	DBE=0.50g
San Onofre-2	3410	217	217	1.00	34.1	AB, grd	SSE=0.67g
San Onofre-3	3390	217	0	0.00	0.0	AB, grd	SSE=0.67g

Table 1.1 (Cont'd)

Plant	Thermal Power (MWt)	Number of Fuel Assemblies in Core[a]	Spent Fuel Stored Inventory[a] (No. of Assemblies)	Stored Inventory Fractions of Core[b]	Radioactivity Relative to Reference Case[c] (per cent)	Storage Pool Location[d]	Seismic Design Basis[e]
Sequoyah-1	3411	193	65	0.34	11.5	AB, grd	SSE=0.18g
Sequoyah-2	3411	193	130	0.67	23.0	AB, grd	SSE=0.18g
St. Lucie-1	2700	217	352	1.62	43.8	AB, grd	DBE=0.10g
St. Lucie-2	2560	N/A	N/A	N/A	N/A	AB, grd	SSE=0.10g
Summer-1	2775	157	52	0.33	9.2	AB, grd	SSE=0.15g
Surry-1	2441	157	608[g]	3.87[g]	94.5[g]	AB, grd	SSE=0.15g
Surry-2	2441	157	-	-	-	AB, grd	SSE=0.15g
Three Mile Island-1	2535	177	208	1.18	29.8	AB, grd	DBE=0.12g
Three Mile Island-2	i	177	0	0.00	0.0	AB, grd	SSE=0.12g
Trojan	3411	193	312	1.62	55.1	AB, grd	DBE=0.25g
Turkey Point-3	2200	157	445	2.83	62.4	AB, grd	DBE=0.15g
Turkey Point-4	2200	157	430	2.74	60.3	AB, grd	DBE=0.15g
Waterford-3	N/A	N/A	N/A	N/A	N/A	AB, grd	SSE=0.10g
Yankee Rowe	600	76	250	3.29	19.7	AB, grd	None

Table 1.1 (Cont'd)

Plant	Thermal Power (MWt)	Number of Fuel Assemblies in Core[a]	Spent Fuel Stored Inventory[a] (No. of Assemblies)	Stored Inventory Fractions of Core[b]	Radioactivity Relative to Reference Case[c] (per cent)	Storage Pool Location[d]	Seismic Design Basis[e]
Zion-1	3250	193	863[g]	4.47[g]	145.3[g]	AB, grd	SSE=0.17g
Zion-2	3250	193	-	-	-	AB, grd	SSE=0.17g

Footnotes

a) Source: U. S. Nuclear Regulatory Commission, Licensed Operating Reactors, NUREG-0020, Vol. 9, No. 1, January 1985.

b) (Stored Assemblies)/(Assemblies in Core).

c) "Reference Source Term" assumes a thermal power of 3000 MWt, stored inventory from ten annual discharges, last discharge six months ago, total inventory 700 assemblies. Source term relative to "Reference Source Term" has not been corrected for age of fuel in storage.

d) Location: RB = reactor building, AB = auxiliary building, FB = fuel building, g = pool at grade level, e = pool at high elevation in building.

e) Seismic design basis as a fraction of the gravitational acceleration (g): DBE = design basis earthquake, or equivalent as used for older vintage plants; SSE = safe shutdown earthquake as defined in 10 CFR 100, App. A. Entry shown is the horizontal component.

f) N/A = data not available.

g) Spent fuel basin shared by two units. Entries shown are totals.

h) Indian Point-1 is permanently shutdown.

i) TMI-2 is indefinitely shutdown.

j) Diablo Canyon originally used the "Double Design Earthquake," DDE acceleration = 2 DBE. Later, more elaborate analysis was done to postulate an earthquake of 0.5g associated with the Hosgri Fault.

2. ACCIDENT INITIATING EVENTS AND PROBABILITY ESTIMATES

2.1 Loss of Water Circulating Capability

The spent fuel basins of U.S. nuclear power stations contain a large inventory of water, primarily to provide ample radiation shielding over the top of the stored spent fuel. Some typical pool dimensions and water inventories are shown in Table 2.1. The heat load from decay heat of spent fuel depends on decay time since the last refueling. Heat loads for the entire spent fuel inventory of the two older plants are shown in Table 2.2 (data extrapolated to the 1987 scheduled refuelings). The cooling systems provided for spent fuel pools typically have a capacity in the range of 15 to 20×10^6 Btu/hr (4.4 to 5.9×10^3 kw).

In the event that normal circulation of the cooling water is disrupted, e.g., due to station blackout, pump failure, pipe rupture, etc., the water temperature of the pool would steadily increase until bulk boiling occurred. (Note: In a situation where the stored inventory was small, an equilibrium temperature, below the boiling point, would be reached at which surface evaporation balanced the decay heat load).

Thermal-hydraulic analyses of the consequences of partial or complete loss of pool cooling capability are a routine part of the safety analysis reports required for licensing and amendments thereto. Generally, these analyses consider several scenarios ranging from typical to extremely conservative conditions. A sampling of conservative results for several plants is given in Table 2.3. The data clearly demonstrate that the time interval from loss of circulation until exposure of fuel to air is quite long. Even in the most pessimistic case cited in Table 2.3 (Docket No. 50-247), the water level in the pool would drop only about 6 inches per hour. Thus, there is considerable time available to restore normal cooling or to implement one of several alternative backup options for cooling.

For licensing purposes, it has been accepted that the time interval for restoring cooling manually from available water sources is adequate without requiring active (automatic) redundant cooling systems.

However, in considering the prioritization of Generic Issue 82, "Beyond Design Basis Accidents in Spent Fuel Pools," the NRC staff recognized that there is a finite probability that cooling could not be restored in a timely manner.[2] The case treated in Ref. 2 was for a BWR. The estimated frequency for the loss of one (of two) cooling "trains" was taken to be 0.1/Ry (the value assumed in WASH-1400).[3] This combined with the conditional probabilities of failure/non-availability of the second "train" yielded a combined frequency of a pool heatup event of 3.7×10^{-2}/Ry. (This estimate appears to be somewhat conservative since no "pool heatup events" are on record after ~10^3 reactor years of accumulated experience).

To escalate from a "pool heatup event" to an event which results in fuel damage requires the failure of several alternative systems that are capable of supplying makeup water (the RHR and condensate transfer systems, or, as a last resort, a fire hose). Estimated frequencies of failure for each of the alternatives, combined with the frequency of a pool heatup event, resulted in an

estimated frequency of 1.4×10^{-6}/Ry for an accident initiated by loss of spent fuel pool cooling.

Originally, the spent fuel pool at the Ginna plant had only one installed cooling train with a "skid-mounted" backup pump and heat exchanger. However, a second cooling train was to have been installed in 1986.[4] Because of the third option for cooling at Ginna (the skid-mounted system) the probability estimate for an accident initiated by a pool heatup event should be reduced to 5×10^{-7}/Ry, i.e., about a factor of 3 smaller than for the BWR case analyzed in Ref. 2. For other PWRs with a typical two train pool cooling system, a somewhat higher failure frequency (about 10^{-6}/Ry) would be expected.

2.2 Structural Failure of Pool

Because of the massive reinforced concrete structure of LWR spent fuel storage pools, designed to Category I seismic criteria, initiating events that would lead to a structural failure are extremely unlikely. On the other hand, a structural failure that resulted in rapid and complete draining of water from the pool would have serious consequences. Probabilities of events that might result in loss of structural integrity are estimated in the following two subsections.

2.2.1 Structural Failure of Pool Resulting from Seismic Events

Procedures and conventions for a detailed probabilistic risk assessment (PRA) of seismically-induced core damage accident sequences have been presented in Ref. 5. The recommended methodology could be applied to spent fuel pools as a separate plant component, or could be coupled to a core damage sequence that might occur simultaneously during a severe earthquake. To date the seismic PRA methodology has not been rigorously applied to spent fuel pools.

Seismic risk analyses consist of three basic steps:

1) portrayal of the seismic hazard in terms of annual frequency of exceedance as a function of some ground motion parameter (e.g., the peak ground acceleration);

2) assessment of the probability that the capacity of a structure or component can survive the seismic event, often expressed in the form of a fragility curve which is the inverse of the capacity for survival; and, finally,

3) a logic model, e.g., an event tree, which relates a seismic-induced failure to a higher order event that results in some category of radioactive release.

In principle, an appropriate convolution of the probability functions derived in steps 1) and 2) yields a probability function for seismic-induced failure. It is recognized that large uncertainties exist in the two input probability functions which are reflected in the function expressing the probability of failure.

16

The three steps and the treatment of the uncertainties have been summarized by Reed,[6] who notes that the largest uncertainties are associated with step 1), i.e., the probabilities of occurrence of severe earthquakes having correspondingly very large ground accelerations. Reed makes the assertion that "due to the large uncertainties in the ground shaking hazard, it is unproductive to refine the structure and equipment capacity calculations to accuracies which are inconsistent with the hazard uncertainty."[6] The specific applicability to spent fuel pools of Reed's assertion is discussed in Section 2.2.1.3.

2.2.1.1 A Review of Seismic Hazard Data

The primary difficulty in characterizing the seismic hazard at specific sites in the Eastern United States (EUS), i.e., sites to the east of the Rocky Mountains is that severe earthquakes are rare events in the EUS. A systematic analysis of recorded earthquakes and their relationship to geological features has yielded seismic zonation maps of the EUS.[7] However, such information cannot readily be translated into the type of seismic hazard functions needed as input for PRA. Consequently, available historical data alone are insufficient for obtaining meaningful site specific estimates of the frequency of severe events.

During the past 6 or 7 years, the methodologies for seismic hazard analyses have been under intensive development. Hence, the analyses presented in this report must be considered provisional and subject to future refinement. At the present time, an intensive effort to refine the methodology is in progress under the auspices of the Electric Power Research Institute (EPRI).[8] The methods, input parameters, computer programming and users' manuals are presented in a ten volume report which is currently in the process of distribution.[8] This is referred to as the Seismicity Owners Group (SOG) seismic hazard methodology development program, or SOG Methodology. Unfortunately the SOG Methodology was not available for the calculations carried out in this report.

The SOG Methodology is a refinement and elaboration of the methodologies developed earlier at Lawrence Livermore National Laboratory (LLNL) by D.L. Bernreuter and his colleagues under NRC sponsorship. The initial study was a part of the NRC's Systematic Evaluation Program (SEP).[9] The methodology has been expanded and modified in a subsequent study, "EUS Seismic Hazard Characterization Project" (SHCP).[10,11]

Since the SHCP results are used for the seismic hazard estimates, some further discussion of the Bernreuter methodology is appropriate. Three basic steps are involved:

1. Expert opinion was elicited to delineate and characterize seismically active zones in the EUS, and to define earthquake ground motion models. The experts also provided estimates of uncertainties associated with their assumptions.

2. Seismic zonation, seismicity and ground motion inputs are integrated into hazard functions at specified sites.

17

3. Modeling and parameter uncertainties are reflected in the form of "best estimates" and 15th, 50th and 85th percentile seismic hazard curves.

The various steps are carried out in a highly disciplined and systematic manner. Provision is made at various stages for peer review of the methods and input opinion, feedback to the experts and critical evaluation of the results.

In step 1, each expert prepares a "best estimate" map which delineates the seismic zones. Each zone is characterized by a set of parameters that give the maximum earthquake intensity to be expected for that zone (upper magnitude cut-off), the expected frequency of earthquakes, and the magnitude recurrence relation. For each input (zone boundaries, seismic parameters), the expert provides a measure of his degree of confidence. Also each expert is given the option of submitting alternative maps of differing zonations and characterizations (up to as many as 30 maps). The data from each expert are evaluated separately through step 2.

In step 2, the contribution at a given site from each zone is integrated over the zone area and then over all zones. This requires the use of ground motion models for which a range of alternative models are employed to yield a set of alternative hazard curves. A "Ground Motion Panel" of experts have selected several alternative models to be used, each having a weighting factor (see Ref. 10, App. C). Also each ground motion model incorporates a site specific correction to account for local geology.

In step 3, the results of the individual experts are combined to obtain a "best estimate" hazard curve and the uncertainty bands are computed in several alternative ways.

It is obvious that the methodology requires a massive data collection and computer effort. In its present state, the final results are not in a form to be easily applied to a specific PRA by a non-expert in seismology. Further work is needed to develop a more convenient format for presenting the final results. In particular, numerical tabulations of the sets of hazard curves (such as those shown in Figs. 2.1 and 2.2) and their derivatives, $|dH/da|_i$, for each reactor site would be helpful. Also, it appears that the local site geology needs more rigorous consideration in the derivation of the hazard curves (see below).

Members of the Peer Review Panel have suggested several ways in which the methodology could be refined (see Ref. 11, Section 7 and Appendices D.1-D.4). Many of these suggestions were implemented in the final feedback process and were included in the final results reported in Ref. 11.

In order to illustrate the hazard curves, their range of uncertainties and comparison with other studies, a series of figures taken from Ref. 11 for the Millstone site is reproduced in Figs. 2.1-2.4.

Figure 2.1 is the hazard curve obtained from averaging the "best estimate" results for all experts in the SHCP study (including the seismic and the ground motions panels). The curve plots frequency of exceedance per year vs. peak ground acceleration.

18

Figure 2.2 illustrates the uncertainties in the hazard curve (15, 50, and 85 percentiles) derived from the spread in expert opinion and the self-confidence factors in the input parameters. It can be seen that the spread between the 15 and 85 percentiles is about a factor of 20 at low PGA increasing to about 50 at the high PGA. Comparison of Figs. 2.1 and 2.2 shows that the "best estimate" curve is considerably higher than the 50 percentile, i.e., the mean > median.

Figure 2.3 illustrates the spread in the "best estimate" hazard curves for all of the experts participating in either the SEP[9] or the SHCP[10] studies, or both (6 experts participated in both studies). The spread ranges from about one order of magnitude at lower PGA to about 1.5 orders of magnitude at the higher PGA. The curve marked "A," which falls considerably below the main grouping, was derived from data input in the SEP study by one of the experts who participated in both studies. The revised input for this expert in the SHCP project raised the derived curve by about an order of magnitude at the low accelerations and almost two orders of magnitude at the higher PGA. This raises the obvious questions of whether the experts were somehow influenced by the opinions of their colleagues, or whether the revision resulted from a more careful consideration of the various geological factors that were taken into account in preparing the input parameters. The question of testing the results for inadvertent biases of this nature was addressed by the Peer Review Panel members, but their recommendations could not be fully implemented in the final report due to limited time and budget (Ref. 11, pg. 7-3).

Figure 2.4 compares the "best estimate" hazard curves for the individual SHCP experts with curves generated from zonation maps prepared by the U.S. Geological Survey (USGS)[12] and historical data of the past 280 years. As can be seen, the USGS hazard curve (denoted by "X") lies above the SHCP data. Bernreuter et al. attribute the difference between the SHCP and the USGS curves to the variations in the equations used for conversions from intensity to magnitude and in the values for the rate of earthquake recurrence (Ref. 11, pg. 8-1 et seq.). As would be expected the 280 year historical hazard curve (denoted by "H") falls below the SHCP data because it does not include postulated stronger earthquakes with return times much greater than the time span of the historical record.

It should be noted that recent research has raised significant questions concerning the frequency of strong earthquakes in the coastal zone of the EUS.[13] The speculation has arisen from paleoseismic field studies originally focused on the region of the strong earthquake near Charleston, SC, in 1886, which produced many "sand blows."[14,15] These result from the liquefaction and venting to the surface of sub-surface water-saturated sediment. Several sand blow craters have been found for which radiocarbon dating indicates that moderate to large earthquakes have recurred in the Charleston region on an average of about every 1800 years.[16] The latest (prior to 1886) occurred about 1100 years ago.[16] Sand blows from prehistoric earthquakes have been unearthed recently in the region extending from near Savannah, GA as far north as Myrtle Beach, SC.[17] The broad extent of sand blows suggests that Charleston-type earthquakes might be associated with some tectonic feature which extends for some distance along the east coast and not uniquely centered near Charleston. Up to the present time, no systematic field search has been made for sand blows outside of the Savannah to Myrtle Beach region.[18] Recently Thorson et al. reported the existence of apparent sand blow craters in eastern

Connecticut.[19] These craters were recently examined by a USGS field team and assessed as not being of the same nature as those observed in South Carolina.[18]

2.2.1.2 Seismic Hazard Estimates for Eastern United States Sites

The "best estimate" and the median, 15 and 85 percentile seismic hazard curves developed by the SHCP project for the Millstone site are shown in Figs. 2.1 and 2.2.[11] An NRC staff evaluation of the seismic hazard curves for the Millstone site was performed as part of the Millstone Risk Evaluation[20] (Appendix D). Included in the staff evaluation were discussions of seismic hazard curves generated by contractors of the Licensee and used in the Millstone 3 Probabilistic Safety Study (PSS). The PSS 16, 50 and 84 fractile hazard curves are shown in Fig. D.1 of Ref. 20 together with the 15, 50 and 85 fractile curves from the initial phase of the SHCP project.[10] The staff noted that the PSS hazard curves were about an order of magnitude below the SHCP curves. However, the final revisions of the SHCP data[11] decreased the discrepancy by more than a factor of two. The revised SHCP curves are compared with the PSS 50 fractile curve in Fig. 2.5. It will be seen that the PSS 50 fractile curve almost coincides with the SHCP 15 fractile.

Although the hazard curves shown in Figs. 2.1 through 2.5 are intended to be "site specific" for the Millstone site, comparison with curves generated for other EUS sites, generally fall within the range of uncertainty reflected by the spread in Fig. 2.5. Therefore, the spread of these seismic hazard curves can be regarded as "generic" rather than site specific.

The data in the four SHCP hazard curves were used for the calculations presented in Section 2.2.1.4. The PSS 50 fractile curve was included in the sensitivity cases presented in Section 2.2.1.5.

A fundamental problem in attempting to use the hazard curves is the need for extrapolation to higher peak ground accelerations, e.g., to values as high as 2000 cm/sec^2 (~2g). The NRC staff evaluation[20] recognizes the validity of choosing an upper magnitude cutoff for each seismic zone but underscores the uncertainty in such parameters (see Ref. 20, pg. D-3). The choice of the upper magnitude cutoffs is one of several factors that determine how fast the tails of the hazard curves drop at peak ground accelerations in excess of about 600-700 cm/sec^2. In order to illustrate how the seismic failure probabilities might be affected, we have extrapolated the four SHCP curves to >2g using an exponential tail tangent to the point where the hazard curves terminate in Figs. 2.1 and 2.2. The results are presented in Section 2.2.1.5.

2.2.1.3 Seismic Fragility of Pool Structures

Fragility curves specifically for spent fuel pools have never been developed.[21] It is necessary therefore, to rely on fragility assessments for other structures which appear to be of similar construction to spent fuel storage pools. It must be recognized that this procedure introduces an additional element of uncertainty in the final risk estimates -- an uncertainty that is difficult to quantify. Another source of uncertainty is the degree to which the stainless steel lining of a pool would enhance the seismic strength capacity (i.e., reduce the fragility). Conceivably, the reinforced concrete structure of the pool could crack without loss of integrity of the pool lining.

The dilemma of selecting an appropriate fragility for a BWR plant is aggravated by the fact that the pool structure extends typically from the 60 to the 100 foot elevations above grade with the resultant amplification of the seismic bending stresses relative to the lower elevations of the structure.[22]

For the present analyses, two, somewhat diverse sets of fragility estimates, have been used:

1) the fragility curve developed by R.P. Kennedy et al.[23] for the Oyster Creek reactor building; and

2) the fragility of the Zion plant auxiliary building shear walls (north-south ground motion).[24]

For the sensitivity studies presented in Section 2.2.1.5, a third fragility curve has been added which is for a 36 inch thick reinforced concrete shear wall.[25]

In each case, the fragility curve is defined by the following equation:

$$F(a) = \Phi \left[\ln(a/\tilde{A})/\beta_R \right] , \qquad (2.1)$$

where $F(a)$ is the probability of structural failure given a peak ground acceleration, PGA $= a$. $\Phi( )$ is the normal distribution function, $\tilde{A}$ is the median fragility level (i.e., the acceleration at which there is a 50% probability of failure) and β_R is the logarithmic standard deviation expressing the randomness in the value of $\tilde{A}$. A third parameter, β_u, is used to express the uncertainty in the median value and is used to generate upper and lower confidence limits. For example, it can be shown that the substitution for $\tilde{A}$ in Eq. 2.1 of $\tilde{A}' = \tilde{A} \, e^{+\beta_u}$ and $\tilde{A}' = e^{-\beta_u}$ generate respectively the 84 and 16 percentile curves.

Thus, a set of fragility curves can be generated from three parameters, $\tilde{A}$, β_R and β_u. The data used for generating the "Kennedy" and the "Zion" curves are given in Table 2.4.

Kennedy notes that the estimated median fragility value of about 0.75g is considered applicable to plants designed in the U.S. in the mid 1960's. The Kennedy fragility curve is shown in Fig. 2.6, with the 84 and 16 percentile limits. The corresponding Zion curves appear in Fig. 22, pp. 3-35 of Ref. 24. (Note: the Zion curves are expressed in terms of floor slab acceleration, rather than ground acceleration.)

It has been noted by Kennedy et al.[23] that the

"use of the lognormal distribution for estimating very low failure frequencies of components or structures associated with the tails of the distribution is considered to be conservative since the low probability tails of the lognormal distribution generally extend further from the median than actual structural response data might extend since such data generally show cut-off limits beyond which there is essentially zero probability of occurrence."

In other words, Kennedy indicates that a more realistic analysis should truncate the lower end of the fragility curve as indicated by experimental data. (We chose to truncate when $F(a) < 10^{-4}$ in Equation 2.1).

2.2.1.4 Seismically-Induced Failure Probabilities

The convolution of the derivative of a seismic hazard curve (e.g., Fig. 2.1) with a fragility curve, yields the annual probability of a seismically-induced failure. This can be expressed by the equation:

$$P_{i,j} = \int_0^{a_{max}} \left|\frac{dH}{da}\right|_i F(a)_j \, da \, , \qquad (2.2)$$

where $P_{i,j}$ is the failure probability obtained from the convolution of hazard curve i with fragility curve j, $|dH/da|_i$ is the derivative of the hazard curve i (i.e., the annual frequency of occurrence of peak ground acceleration, a, and $F(a)_j$ is failure probability at acceleration, a, for fragility curve j. Since the seismic hazard curve is not an analytic function, the derivative dH/da and the integration are carried out numerically.

Given many hazard and fragility curves from which to choose, and there being no a priori basis for choosing a particular pair, the convolution expressed in Eq. 2.2 can be carried out for each pair of curves with weighting factors assigned to each of the curves in each set. The resultant collection of $P_{i,j}$ gives a probability distribution which expresses the uncertainties in the analysis. The probability density distribution obtained for the generic site is shown in Fig. 2.7.

At least in principle, the various hazard and fragility curves (sets i and j) do not have an equal likelihood of being correct. Therefore, a weighting factor (ω_i or ω_j) should be assigned to each curve which reflects an "engineering judgement" of its relative validity for a specific site. The mean probability for failure is then derived from the following expression,

$$\overline{P}_f = \sum \omega_i \omega_j P_{i,j} \, / \, \sum \omega_{i,j} \, , \qquad (2.3)$$

where $\sum \omega_i = 1$, $\sum \omega_j = 1$ and $\sum \omega_{i,j} = \sum \omega_i \omega_j = 1$. For the purposes of illustration, the weighting factors listed in Table 2.5 were selected. Results for each convolution without weighting factors are listed in Table 2.6. As can be seen from the table, the "best estimate" hazard curve has been assigned a weighting factor of 0.5 with the remaining 0.5 distributed among the median, 15 and 85 percentile curves. The "Kennedy" set of fragility curves were assigned a total weighting factor of 0.75 with the remaining 0.25 distributed among the "Zion" set. Assuming an upper limit cutoff of 1.0 g, the mean probability of failure, $\overline{P}_f$, derived from the 24 sets of $P_{i,j}$, using the weighting factors listed in Table 2.5 and Equation 2.3, would be

$$\overline{P}_f = 2.2 \times 10^{-5}/\text{year} \, .$$

22

2.2.1.5 Sensitivity Studies

In order to better understand the limitations in assessing the probability of seismically-induced structural failures in spent fuel pools the results of the convolutions of each pair of curves (seismic hazard against fragility) are listed in Table 2.6. Each of the five hazard curves were convoluted with seven fragility curves. Results range from

$$P_f = 2.6 \times 10^{-4} \text{ to } \ll 1 \times 10^{-10}/\text{Ry} \ .$$

The primary contributors to the wide spread in the results are:

• uncertainties in how the tails of seismic hazard curves drop off at PGA's < 700 cm/sec^2.

• uncertainties in pool structural fragilities.

2.2.1.6 Conclusions on Seismic Risk

Available seismic hazard and fragility data are inadequate to assess the probability of seismically-induced structural failure of spent fuel pools within a factor of 1000. The present results indicate that the pool failure probability may be as high as $2.6 \times 10^{-4}/\text{Ry}$, or as low as $1 \times 10^{-10}/\text{Ry}$. Further work is need to narrow the uncertainties.

2.2.2 Structural Failures of Pool Due to Missiles

Missiles generated by tornadoes, aircraft crashes or turbine failure could penetrate the pool structure and result in structural failure.

The probability of tornado missiles depends on the frequency of tornadoes at the site, the target area presented to the missile and the angle of impact. An analysis made by Orvis et al.[26] for an average U.S. site derives a probability of $<1 \times 10^{-8}$/year for structural loss of pool integrity due to a tornado missile (Ref. 26, pg. 4-44). (WASH-1400 estimated $<5 \times 10^{-6}/\text{yr}$.[3])

Similarly, the analysis for structural failure of a pool from an aircraft crash yielded a probability of $<1 \times 10^{-10}$/year (Ref. 26, pg. 4-58).

The damage caused by Missiles generated by turbine failure depends on the orientation of the turbine axis relative to the structure, as well as the frequency of turbine failure. An analysis by Bush yields a probability of $\sim 4 \times 10^{-7}$/year for spent fuel pool damage from a turbine failure missile.[3,27] In the case of Ginna, the probability would be several orders of magnitude smaller (i.e., essentially zero) because the spent fuel pool is shielded from turbine missiles by the primary containment.

2.3 Partial Draindown of Pool Due to Refueling Cavity Seal Failures

On August 21, 1984, the Haddam Neck Plant experienced a failure of the refueling cavity water seal, while the refueling cavity was flooded. The water level in the refueling cavity dropped by about 23 feet to the top of the reactor vessel flange within 20 minutes -- a loss of approximately 200,000 gallons, or a leak rate of about 10,000 gallons per minute.[28] At the time of

the event, refueling had not begun. The gates of the transfer tube connecting the refueling cavity to the spent fuel storage pool were closed.

Although the seal failure did not result in an accident or in the release of radioactivity, the incident raised the question of whether similar failures might occur while spent fuel was being transferred or while transfer gates to the spent fuel basin were open, either case of which might result in exposure of spent fuel to air and possible clad failure.

All licensed plants were instructed to evaluate the potential for and consequences of a refueling cavity seal failure.[28]

Refueling cavity seals seal the gap between the reactor vessel flange and a flange on the inner periphery of the reactor cavity, or the floor of the cavity.

Most BWR's have a permanently installed stainless steel bellows to seal the gap, and are thus not subject to failure of the Haddam Neck type.

Many PWR's seal the gap with gaskets held down by a bolted flat steel ring. Such systems have experienced difficulties in achieving tight seal because of surface irregularities and small vertical and concentric offsets in the two flanges. Consequently, many plants have converted to inflatable (pneumatic) rubber seals. Also, it should be noted that pneumatic rubber seals are often used to seal the gates in transfer tubes or canals.

Licensee responses to the IE Bulletin indicate that the Haddam Neck cavity configuration is unique in that the width of the annular gap between the reactor flange and the cavity flange is about two feet, whereas, in most plants the gap is of the order of <1" to ~3". As of summer 1985 some 45 units used pneumatic seals in the refueling cavity.[29]

Typical pneumatic seals are illustrated in Figures 2.8-2.10. There are many variations in the details of the designs, e.g., some plants have various types of retainers to support the rubber seals (e.g., see Figure 2.10), others rely on the rubber seal alone (e.g., see Figure 2.9). According to the responses of the licensees, even if a pneumatic seal should deflate, the leakage would be expected to be small or negligible, because the wedged shaped upper section would maintain a good seal (refer to Figure 2.8), i.e., the deflated seal would not distort enough under the hydrostatic head to extrude through the gap.

Aside from the Haddam Neck 1984 incident, a few cases have been reported in which inflated seals have failed, either in the refueling cavity or transfer gates. None of these events had significant radiological consequences. The most serious loss of pool water inventory occurred December 3, 1986 at the Hatch 1 & 2 spent fuel pool when a pair of pneumatic seals in the seismic gap of the transfer canal deflated. About 141,000 gallons of water was lost from the pool and the pool level dropped about five and one half feet before the leak was detected.[30]

Several seal failure events are listed in Table 2.7. It is likely that this list is not exhaustive. To the best of the authors' knowledge no data base has been compiled (or is available) of the failure rate of pneumatic

24

seals and their pressurizing systems of the types used in nuclear power plants, or of similar seals used in non-nuclear industries.

Based on the limited experience cited in Table 2.7, the historical failure rate in seals/systems is in the range of ~1×10^{-2}/Ry. Because of advances in design, increased awareness and surveillance, the present failure rate is estimated to be an order of magnitude smaller, i.e., ~1×10^{-3}/Ry.

As is obvious from Table 2.7, a seal failure does not necessarily result in the rapid loss of water inventory from spent fuel transit or storage locations. The limited experience indicates that the most probable time for a refueling cavity seal to fail is shortly after installation, while the cavity volume is being filled with water. According to the analyses supplied by licensees in response to IE Bulletin No. 84-03, the failure of a pneumatic refueling cavity seal in most PWR plants would not result in massive leaks because of the relatively narrow gap to be sealed and the geometric shape of the seal. Also, leaks from seal failures in transfer tube/canal gates would be limited, in most cases, because the leakage would be into a confined volume, e.g., from the storage pool into a drained up-ender sump. Taking these factors into consideration, it is estimated that the frequency of a serious loss of pool water inventory resulting from a pneumatic seal failure to be in the range of ~1×10^{-5}/Ry.

Even a large loss of water inventory from the spent fuel pool does not necessarily result in uncovering and subsequent failure of fuel. Most spent fuel pools are constructed with weirs below the transfer gates which preclude complete drainage of the pool, even in the event of a Haddam Neck type failure with the transfer tube/canal gates open. In most cases, the water level would remain a foot or more above the active zone of the spent fuel assemblies. In a few cases, the upper several inches of the fuel could uncover. (Note: Licensee responses to IE Bulletin 84-03 did not always provide information about the elevations of weirs and tops of stored assemblies.)

In the event of a draindown of the pool to near the top of the fuel assemblies, there would still be time (1/2 to 1 hour) to close gates and restore a supply of water before the residual water inventory reached the boiling point. However, as noted in one licensee response, even if the fuel remained covered "dose rate in the vicinity of the spent fuel pool would, however, be high, complicating recovery from the event."[31]

A pool heatup event similar to the partial draindown scenario described above was considered by the NRC staff in Ref. 2. A conditional probability for failure to restore adequate makeup water was taken to be 5×10^{-2}. Combining this restoration failure frequency with the initiating frequency (1×10^{-5}/Ry), the probability of a pneumatic seal failure which results in exposure to air of stored spent fuel with possible clad failure is estimated to be of the order of

$$P \approx 5 \times 10^{-7}/\text{Ry}.$$

2.4 Pool Structural Failure Due to Heavy Load Drop

WASH-1400 considered the probability of structural damage to the pool due to the dropping of a fuel transfer cask (Ref. 3, pg. I-97). In the analysis,

it was anticipated that one spent fuel shipment per week would be the equilibrium shipping rate. The estimated rate for a drop resulting in pool failure (for a single unit plant) was 4.5×10^{-7}/Ry.

The above frequency was based on a crane failure probability of 3×10^{-6} per operating hour. It was further assumed that each lift was of 10 minutes duration and for a 10 second period per lift the cask would be in a position to cause gross structural damage to the pool wall if a crane failure occurred. Human error was not considered.

Since very little spent fuel is currently being shipped, the likelihood of such an accident is very low. However, at some point in the future as the fuel pools are filled, spent fuel will have to be removed from the reactor spent fuel pools, either to some onsite storage facility, or eventually to a high level waste repository. At that time, the frequency of removal of spent fuel will be correspondingly greater.

Orvis et al.[25] have reexamined the cask drop probability and have used the following probabilities:

Mechanical failure of crane = 3×10^{-6}/operating hour

Electrical control failure of crane = 3×10^{-6}/operating hour

Human error = 6×10^{-4}/lift.

As can be seen, human error dominates the Orvis estimates for probability of a cask drop. The Orvis datum for human error was based on a study by Garrick et al.[30] which concerned human reliability in the positioning of heavy objects. The applicability of the Garrick study to crane operations is not obvious. Nevertheless, a human failure rate in the range of 10^{-3} to 10^{-4} per operation appears to be consistent with data listed in the NRC handbook on human reliability analysis[31] for cases in which the operation has one or more people who serve as "checkers" and involves some degree of personal risk to the operating personnel.

Obviously, not all human failures associated with the lifting and moving of a spent fuel shipping cask would result in structural damage to the pool. The section of the pool where the cask is set down generally has an impact pad to absorb the impulse of a dropped cask. Accidents in unloading the cask from or reloading on the transport vehicle would not involve the pool.

Only horizontal movements of the cask above a structurally critical section of the pool would pose the threat of structural damage. As noted above, WASH-1400 assumed that the sensitive section is the vertical wall at the pool edge. It was implicitly assumed that all load drops on the pool edge would result in structural failure. This assumption appears to be too simplistic and consequently too conservative for the following reasons:

- many "load drops" would be partially attenuated by crane mechanisms which limit descent rates, and reduce impact energy,

- in case of some "off-center" hits, the full potential impact energy would not be absorbed by the pool edge (cask tilted, one end strikes floor first), and

- account should be taken of exterior cask fittings (e.g., cooling vanes) which absorb some impact energy.

No rigorous structural analyses have been performed to scope the range of damage to a pool edge from a cask drop. In the absence of such analyses, it has been necessary to estimate the conditional probability of structural damage given a cask drop in the vicinity of the pool edge. It is estimated that the conditional probability is less than 100% and greater than 1%. A conditional probability of 10% has been selected for the hazard calculation and 100% and 1% used for defining the range of uncertainties.

Since human error, rather than mechanical or electrical failure, appears to dominate the hazard arising from shipping cask movements, the various steps in the crane operation have been identified in Table 2.8, which also lists the types of human error associated with each step. The distribution of failure frequency in the various steps has been estimated and listed in the last column of Table 2.8. (This distribution was subjected to "peer review" by BNL rigging personnel and managers who oversee operations of this type[34] as well as human factors analysts.[35])

It will be noted that most steps in the crane operation do not jeopardize the structural integrity of the pool. Only in steps 5a and 5b (see Table 2.8) could the cask strike the pool edge. An accident of the type listed in 5a (horizontal movement with cask not high enough to clear the pool edge) would probably not cause serious damage because of the limited kinetic energy of the cask associated with the slow velocity of horizontal crane movements. Thus, only step 5b in Table 2.8 is considered in the hazard calculation.

For purposes of calculating the cask drop hazard, i.e., the probability of structural damage to the pool resulting from a cask dropping on the pool edge, the assumptions listed in Table 2.9 were used. Table 2.9 also lists the uncertainty ranges for each of the parameters. The results are as follows:

Probability of structural failure due to cask drop on pool edge caused by mechanical or electrical failure of crane = 3.5×10^{-7}/Ry.

Probability of structural failure due to cask drop on pool edge caused by human error = 3.1×10^{-5}/Ry.

If the failure rates summarized in Table 2.9 are assumed to be statistically independent, then the uncertainty in the overall failure rate is dominated by the uncertainty in the probability of pool failure. Thus the overall uncertainty is about a factor of ten in either direction.

The NRC has proposed[36] a number of improvements in handling of heavy loads which they estimate will substantially reduce the likelihood of load drop accidents. With the recommended improvements in procedures and equipment in place, the NRC estimated[36] that the likelihood of a cask drop or other heavy load drop over the spent fuel pool would be between 2×10^{-5} and 2×10^{-9} per reactor year. This is a substantial reduction in the likelihood of a load

drop. With the previous estimate of pool failure per cask drop (0.001) the pool failure rate would be 2×10^{-8} to 2×10^{-12} per reactor year due to load drop accidents.

2.5 Summary of Accident Probabilities

The probability estimates made in Sections 2.1-2.4 are summarized in Table 2.10. These include only those accidents that result in the complete loss of pool water inventory. It will be seen that shipping cask drop resulting from human error and seismic induced failures dominate in the hazards. As previously discussed the uncertainty in both of these probabilities is quite large and has been estimated to be an order of magnitude in either direction.

2.6 References for Section 2

1. The data cited in Table 2.3 were culled from submissions by the licensees of the respective dockets in support of license amendments for expanded spent fuel storage limits.

2. "A Prioritization of Generic Safety Issues," Division of Safety Technology, Office of Nuclear Reactor Regulation, U.S. Nuclear Regulatory Commission, NUREG-0933, December 1983, pp. 3.82-1 through 6.

3. "Reactor Safety Study, An Assessment of Accident Risks in U.S. Commercial Nuclear Power Plants," U.S. Nuclear Regulatory Commission, NUREG-75/014 (WASH-1400), October 1975, App. I, Section 5.

4. Rochester Gas and Electric Corporation, Docket No. 50-244, "Design Criteria, Ginna Station, Spent Fuel Cooling System," EWR 1594, Revision 1, October 10, 1979; U.S. Nuclear Regulatory Commission, Safety Evaluation by the Office of Nuclear Reactor Regulation Supporting Amendment No. 65 to Provisional Operating License No. DPR-18, Rochester Gas and Electric Corporation, R.E. Ginna Nuclear Plant, Docket No. 50-244, November 14, 1984.

5. M. McCann, J. Reed, C. Ruger, K. Shiu, T. Teichmann, A. Unione, and R. Youngblood, Probabilistic Safety Analyses Procedures Guide, Vol. 2, prepared for the U.S. Nuclear Regulatory Commission by Brookhaven National Laboratory, NUREG/CR-2815 (BNL-NUREG-51559) Vol. 2, Rev. 1, August 1985.

6. John W. Reed, "Seismic Probabilistic Risk Assessment for Critical Facilities," preprint of paper presented at the 1985 ASCE Spring Convention, Denver Colorado, April 29 - May 3, 1985.

7. N.L. Barstow, K.G. Brill, O.W. Nuttli and P.W. Pomeroy, An Approach to Seismic Zonation for Siting Nuclear Electric Power Generating Facilities in the Eastern United States, prepared for the U.S. Nuclear Regulatory Commission by Rondout Associates, Inc., NUREG/CR-1577, May 1981.

8. J. Moore, "Breaking New Ground in Seismic Research," the EPRI Journal, pp. 20-29, September 1986, and Seismic Hazard Methodology for Nuclear Facilities in the Eastern United States, Vols. 1-10, Report for RPP101,

sponsored by EPRI and the Seismicity Owners Group, EPRI NP-4726, July 1986.

9. U.S. Nuclear Regulatory Commission, NUREG/CR-1582, Seismic Hazard Analysis, 5 Volumes:

    Volume 1, Overview and Executive Summary, D.L. Bernreuter and C. Minichino, April 1983.

    Volume 2, A Methodology for the Eastern U.S., Lawrence Livermore National Laboratory/ TERA Corporation, August 1980.

    Volume 3, Solicitation of Expert Opinion, Lawrence Livermore National Laboratory/ TERA Corporation, August 1980.

    Volume 4, Application of Methodology, Results and Sensitivity Studies, D.L. Bernreuter, Lawrence Livermore National Laboratory, October 1981.

    Volume 5, Review Panel, Ground Motion Panel and Feedback Results, D.L. Bernreuter, Lawrence Livermore National Laboratory, 1981.

10. D.L. Bernreuter, J.B. Savy, R.W. Mensing and D.H. Chung, Seismic Hazard Characterization of the Eastern United States: Methodology and Interim Results for Ten Sites, prepared for the U.S. Nuclear Regulatory Commission by Lawrence Livermore National Laboratory, NUREG/CR-3756 (UCRL-53527), April 1984.

11. D.L. Bernreuter, J.B. Savy, R.W. Mensing, J.C. Chen and B.C. Davis, Seismic Hazard Characterization of the Eastern United States, Vol. 1, "Methodology and Results for Ten Sites," Lawrence Livermore National Laboratory, UCID-20421, April 1985.

12. S.L. Algermissen, D.M. Perkins, P.C. Thenhaus, S.L. Hangen and B.L. Bender, Probabilistic Estimates of Maximum Acceleration and Velocity in Rock in the Cartiguous United States, U.S. Geological Survey, open file report 821033 (1982).

13. E.g., see R.A. Kerr, "Charleston Quakes are Larger or Widespread," Science, 233, p. 1154, September 12, 1986; and R.A. Kerr, "Eastern Quakes Pinned Down?," Science, 227, January 25, 1985.

14. S.F. Obermeier, G.S. Gohn, R.E. Weems, R.L. Gelinas and M. Rubin, "Geologic Evidence for Recurrent Moderate to Large Earthquakes Near Charleston, South Carolina," Science, 227, pp. 408-411, January 25, 1985.

15. E.g., see P. Talwani and J. Cox, "Paleoseismic Evidence for Recurrence of Earthquakes near Charleston, South Carolina," Science, 229, pp. 379-381, July 26, 1985.

16. R.E. Weems, S.F. Obermeier, M.J. Pavich, G.S. Gohn, M. Rubin, R.L. Phipps and R.B. Jacobson, "Evidence for Three Moderate to Large Prehistoric Holocene Earthquakes Near Charleston, SC," Proceedings of the Third U.S. National Conference on Earthquakes Engineering, August 24-28, 1986,

Charleston, South Carolina, pp. 3-14, (published by the Earthquake Engineering Research Institute).

17. S.F. Obermeier, R.B. Jacobson, B.S. Powars, R.E. Weems, B.C. Hallbick, G.S. Gohn and H.W. Markewich, "Holocene and Late Pleistocene (?) Earthquakes Induced Sand Blows in South Carolina," Proceedings of the Third U.S. National Conference on Earthquake Engineering, August 24-28, 1986, Charleston, SC, pp. 197-208 (published by the Earthquake Engineering Research Institute).

18. S.F. Obermeier, private communication, Sept. 26, 1986.

19. R.M. Thorson, W.S. Playton and L. Seeber, "Geological Evidence for a Large Prehistoric Earthquake in Eastern Connecticut," Geology, 14, pp. 463-467, June 1986.

20. G. Kelly, R. Barrett and A. Buslik, Millstone 3 Risk Evaluation Report, U.S. Nuclear Regulatory Commission, NUREG-1152, June 1986, Appendix D.

21. A proposal for such studies has been submitted to the NRC by the Structural Analysis Group of BNL.

22. E.g. see Figs. 12 and 13, pp. 3-22 and 3-23, of Ref. 24.

23. R.P. Kennedy, C.A. Cornell, R.D. Campbell, S. Kaplan and H.F. Perla, "Probabilistic Seismic Safety Study of an Existing Nuclear Power Plant," Nuclear Engineering and Design, 59, (1980) 315-338.

24. L.E. Cover, M.P. Bohn, R.D. Campbell and D.A. Wesley, Handbook of Nuclear Power Plant Seismic Fragilities, prepared for the U.S. Nuclear Regulatory Commission by Lawrence Livermore National Laboratory, NUREG/CR-3558 (UCRL-53455), June 1985.

25. P.C. Wang, H. Hwang, J. Pires, K. Nakai and M. Reich, Reliability Analysis of Shear Wall Structures, prepared for the U.S. Nuclear Regulatory Commission by Brookhaven National Laboratory, NUREG/CR-4293 (BNL-NUREG-51900), January 1986.

26. D.D. Orvis, C. Johnson and R. Jones, Review of Proposed Dry-Storage Concepts Using Probabilistic Risk Assessment, prepared by NUS Corporation for the Electric Power Research Institute, EPRI NP-3365, Feb 1984.

27. S.H. Bush, "Probability of Damage to Nuclear Components Due to Turbine Failures," Nuclear Safety, 14, No. 3, May-June, 1973.

28. U.S. Nuclear Regulatory Commission, Office of Inspection and Enforcement, IE Bulletin No. 84-03: "Refueling Cavity Water Seal," August 24, 1984. (This was subsequently followed up by more detailed instructions for evaluation: "Inspection Requirements for IE Bulletin 84-03, "Refueling Cavity Water Seals," Temporary Instruction 2515/66, Inspection and Enforcement Manual, USNRC, Office of Inspection and Enforcement, issue date 12/17/84.)

29. The total count was based on licensee responses to IE Bulletin No. 84-03. As of mid-1985 a few licensees had not yet filed responses.

30. U.S. Nuclear Regulatory Commission, "Morning Report" Region II, December 5, 1986.

31. Response of Baltimore Gas and Electric to IE Bulletin No. 84-03.

32. B.J. Garrick et al., "The Effect of Human Error and Static Component Failure on Engineered Safety System Reliability," Holmes & Narver, Inc., HN-194, November 1967.

33. A.D. Swain and H.E. Guttmann, Handbook of Human Reliability Analysis with Emphasis on Nuclear Power Plant Applications, prepared for the U.S. Nuclear Regulatory Commission by Sandia National Laboratories, NUREG/CR-1278 (SAND80-0200), August 1983.

34. Personal Communications Between D. Rorer and V.L. Sailor, Brookhaven National Laboratory, October 1986.

35. Personal Communications Between W.J. Luckas and K.R. Perkins, Brookhaven National Laboratory, June 1987.

36. H. George, "Control of Heavy Loads at Nuclear Power Plants," U.S. Nuclear Regulatory Commission, NUREG-0612, July 1980.

Table 2.1 Typical Spent Fuel Pool Dimensions and
Water Inventories

Length/Width/Depth (feet)	Pool Volumes (cubic feet)	Nominal Water Inventory (cubic feet)
40/26/39[a]	4.1×10^4	3.5×10^4
43/22.25/40.25[b]	3.4×10^4	3.3×10^4

[a]BWR, Vermont Yankee.
[b]PWR, Ginna.

Table 2.2 Decay Heat as a Function of Time Since Last
Refueling (Data from Appendix A)

	Decay Heat Load (10^6 Btu/hour)			
	Decay Time Since Last Shutdown for Refueling			
Plant	30 days	90 days	0.5 years	1.0 year
Millstone-1	4.43	3.10	2.38	1.76
Ginna	2.62	1.96	1.59	1.25

Table 2.3 Examples of Thermal-Hydraulic Transient Parameters,
Assuming Complete Loss of Pool Coolant Circulation

Docket No.[a]	Rate of Temp. Increase (°F/hr)	Time of Boiling[b] (hours)	Boil-Off Rate (gpm)	Boil-Off Rate (ft³/hr)
50-325	5.0	13.5	28	262
50-250	9.7	9.3	N.A.	-
50-271	<3	>20	14	131
50-247	13.0	4.8	57	534
50-344	<6.3	>11	34	318

[a]See Ref. 1.
[b]Hours after complete loss of cooling capability.

32

Table 2.4 Fragility Parameters Assumed in This Study
for Spent Fuel Storage Pools

Structure	A (g)	β_R	β_u	Ref.
Oyster Creek Reactor Building[a]	0.75	0.37	0.38	23
Zion Auxiliary Building Shear Walls (N-S motion)[b]	1.1	0.12	0.20	24
36-inch Thick Reinforced Concrete Shear Wall	2.15	0.22	--	25

[a]Designated as the "Kennedy" fragility curves in the text.
[b]Designated as the "Zion" fragility curves in the text.

Table 2.5 Weighting Factors Assigned to the Various
Hazard and Fragility Curves for the
"Weighted" Analysis

Seismic Hazard Curves:	ω_i
"Best Estimate"	0.50
15% Confidence Curve	0.10
Median Curve	0.30
85% Confidence Curve	0.10
$\sum \omega_i$ =	1.00

Fragility Curves:	ω_j
"Kennedy", Median	0.45
" , 16%	0.15
" , 84%	0.15
"Zion", Median	0.15
" , 16%	0.05
" , 84%	0.05
$\sum \omega_j$ =	1.00

Table 2.6 Summary of Convolutions of Seismic Hazard Curves with Fragility Curves. The Seismically-Induced Failure Probabilties were Calculated from the Various Pairs of Curves Using Equation 2.2

Fragility Curve / Hazard Curve	PROBABILITY OF FAILURE PER YEAR						
	K16	K50	K84	Z16	Z50	Z84	SW36
SHCP 85	2.6E-4	8.8E-5	2.9E-5	3.0E-5	1.6E-5	6.4E-6	5.9E-7
SHCP "BE"	8.4E-5	2.9E-5	9.2E-6	1.0E-5	5.0E-6	2.0E-6	1.6E-7
SHCP 50	3.1E-5	9.3E-6	2.4E-6	2.0E-6	7.8E-7	2.4E-7	1.6E-8
SHCP 15	3.1E-6	7.0E-7	1.3E-7	6.4E-8	5.6E-8	3.5E-9	1.6E-10
PSS 50	4.8E-6	9.3E-7	1.4E-7	1.5E-8	2.9E-10	neg.[a]	neg.[a]

[a]neg. = $<10^{-10}$

Key to seismic hazard curves:

SHCP 85: Ref. 11, 85 percentile (see Fig. 2.2).
SHCP "BE": Ref. 11, "best estimate" (see Fig. 2.1).
SHCP 50: Ref. 11, 50 percentile (see Fig. 2.2).
SHCP 15: Ref. 11, 15 percentile (see Fig. 2.2).
PSS 50: Ref. 20, 50 fractile (see Fig. 2.5).

Key to fragility curves:

K16, 50, 84: Ref. 23, 16, 50 and 84 percentiles (see Fig. 2.6).
Z16, 50, 84: Ref. 24, (Zion auxiliary building shear wall), 16, 50 and 84 percentiles.
SW36: Ref. 25 (36" thick reinforced concrete shear wall).

Table 2.7 Events in Which Inflated Seals Have Failed

Date	Plant	Seal Location	Cause	Total Leakage
9/72	Pt. Beach[1]	Transfer Gate	Failure of air supply	11,689 gal.
10/76	Brunswick 2	Inner Pool Gate	Air leak in seal plus compressor power supply failure	(Pool level dropped 5")
5/81	Arkansas Nuclear One - 2	Transfer Gate	Maintenance error, air supply shutoff	1000 gal/min
8/84	Haddam Neck	Cavity Seal	Design weakness, seal shifted	200,000 gal. in 20 min.
10/84	San Onofre 2[1]	Gate Seal	Air compressor power failure	20,000 gal.
11/84	San Onofre 2[1]	Cavity Seal[2]	Manufacturing defect, seal rupture	----
12/86	Hatch[3]	Pool-Canal Flexible Joint	Valve to compressed air supply closed	141,000 gal.

[1]No spent fuel was in the storage pool.
[2]Failure occurred during installation and leak testing.
[3]The leak went undetected for about 7-1/2 hours.

Table 2.8 Estimated Distribution of Human Error in Heavy
Crane Operations. These Estimates, Made by BNL
Staff,[34],[35] are Based on Engineering Judgement
and are Not Supported by Actuarial Data

Operational Step	Possible Human Errors	Estimated Fraction of Total Error Frequency[a] (Per Cent)
1. Install rigging	Wrong slings (e.g., hoist rigging not qualified for task)	10
	Improper installation (shackle, pins, etc.)	10
2. Positioning of crane over load, apply tension	Crane hook not over center of gravity (load upset as tension applied)	15
3. Lift load	Control error (wrong hoisting speed, unintentional reversal of direction)	10
4. Start horizontal travel	Control error (move wrong direction, lift or lower instead of move)	10
5a. Horizontal travel load not high enough to clear obstacles	Control error (unintentional reversal of motion, overshoot stopping point)	4
5b. Horizontal travel	Control error or delayed rigging failure resulting in load drop of cask on fuel pool wall	1
6. Lower load	Control error (wrong direction, descent too fast)	10
7. Positioning of crane over receiving cradle and set-down load	Inaccurate positioning cradle capsizes during set-down	20
	Set down too rapid	10

[a]It is assumed that the movement of a spent fuel shipping cask is carried out by a qualified rigging crew consisting of a foreman, two or more riggers, and a crane operator. The foreman and riggers check each step and crane movements are signaled to the operator by the foreman who stands in a location providing adequate surveillance of the load, and can be clearly seen by the operator.

Table 2.9 Assumptions Used in Calculating the Hazard of
Catastrophic Structural Damage to Pool
Resulting from the Drop of a Shipping Cask

Item	Assumed Value	Uncertainty Range
Number of fuel shipments (eventual rate to reduce accumulated inventory) per week	2	--
Number of passes over pool edge per shipment	2^a	0
Fraction of horizontal movement when cask is above pool edge	0.25	0.1 to 0.5
Total operational time in each movement, minutes per lift	10	8 to 30
Time over pool edge per lift, seconds per lift	10	5 to 20
Mechanical failure rate of crane, per operating hour	3×10^{-6}	10^{-6} to 10^{-5}
Electrical failure rate of crane, per operating hour	3×10^{-6}	10^{-6} to 10^{-5}
Total accident rate from human error, failures per lift	6×10^{-4}	10^{-4} to 10^{-3}
Fraction of human error cask drop accidents occurring during horizontal motion of crane, fraction of total	0.01	5×10^{-3} to 5×10^{-2}
Conditional probability of structural failure of pool given a cask drop at pool edge location, failures per drop	0.1	10^{-2} to 1.0

^{a}Some spent fuel pools have a special section for the shipping cask separated from the main pool by a wall with a wier or gate. For such a configuration the number of passes over the "pool edge" would be zero and hence the risk to the main pool from a cask drop would be zero.

37

Table 2.10 Summary of Estimated Probabilities for Beyond Design
Basis Accidents in Spent Fuel Pools Due to Complete
Loss of Water Inventory

Accident	Estimated Probability/Ry	
	Millstone	Ginna
Loss of Pool Cooling Capability	1.4×10^{-6}	5.7×10^{-7}*
Seismic Structural Failure of Pool	2.6×10^{-4}-Neg.	2.6×10^{-4}-Neg.
Structural Failure from Tornado Missiles	$<1 \times 10^{-8}$	$<1 \times 10^{-8}$
Structural Failure from Aircrash	$<1 \times 10^{-10}$	$<1 \times 10^{-10}$
Structural Failure from Turbine Missile	4×10^{-7}	~ 0**
Loss of Pool Water Due to Pneumatic Seal Failure	0***	5×10^{-7}
Structural Failure from Cask Drop[1]	3.1×10^{-5}	3.1×10^{-5}
Structural Failure from Cask Drop after improvements recommended by Generic Issue A-36 resolution.	$<2 \times 10^{-8}$	$<2 \times 10^{-8}$

Neg. - Negligible.
[1]After removal of accumulated inventory resumes.
*With credit for third cooling system. Other PWRs which typically have two
spent fuel cooling systems would have an estimated fuel uncovery frequency
of about 1×10^{-6}/Ry.
**Typical PWRs may have a failure frequency due to turbine missiles on the
order of 4×10^{-7} but Ginna's pool is shielded from the turbine.
***Most BWRs cannot lose pool inventory even if refueling cavity leaks.
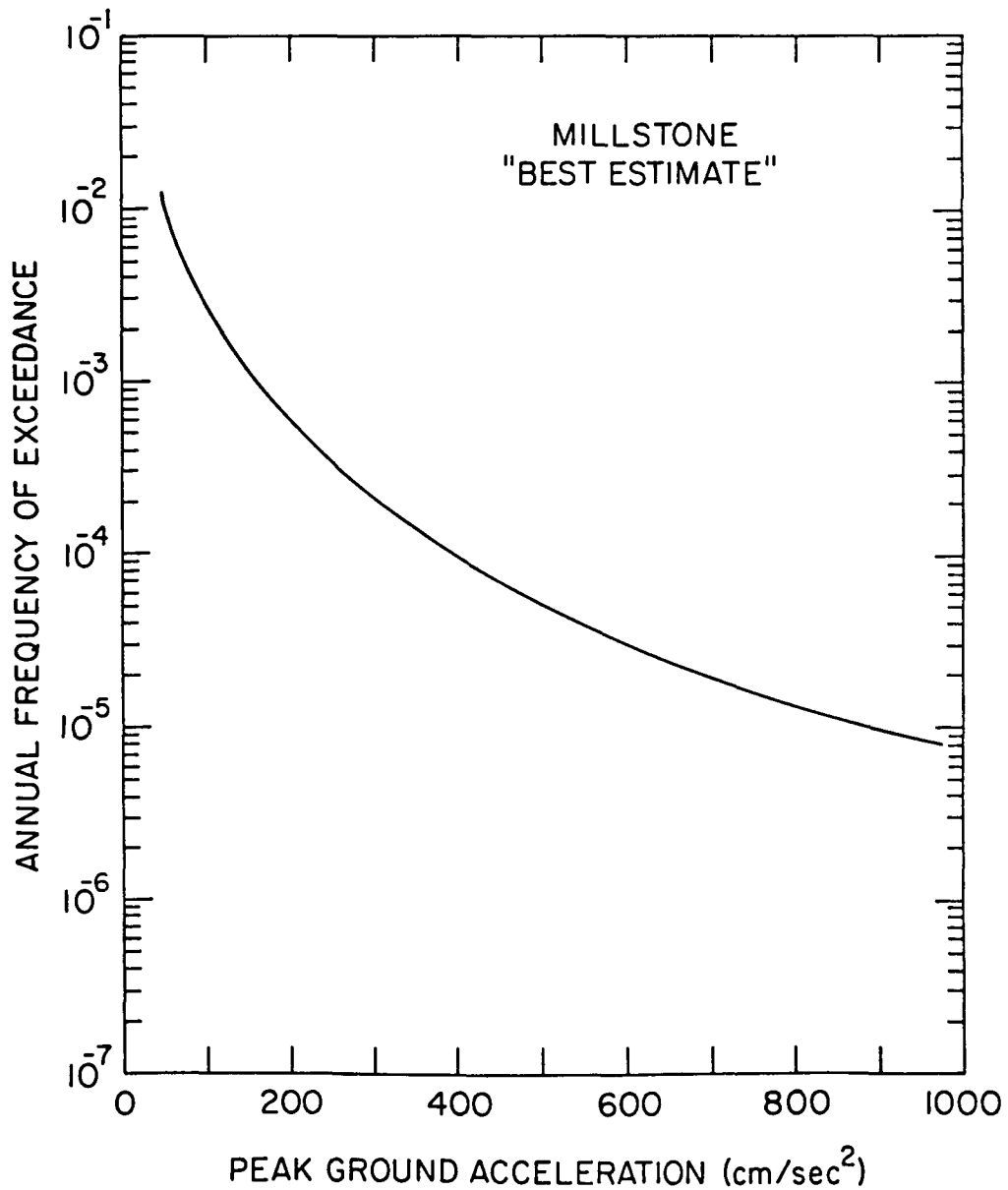
Figure 2.1 Seismic Hazard Curve for the Millstone Site. The curve
shown is the mean of the hazard curves generated from
the "best estimate" input data of the ten experts par-
ticipating in the SHC study combined with the "best es-
timate" model of the ground motion panel. Site correc-
tions are included (Source: Ref. 11, pg. 5-43).
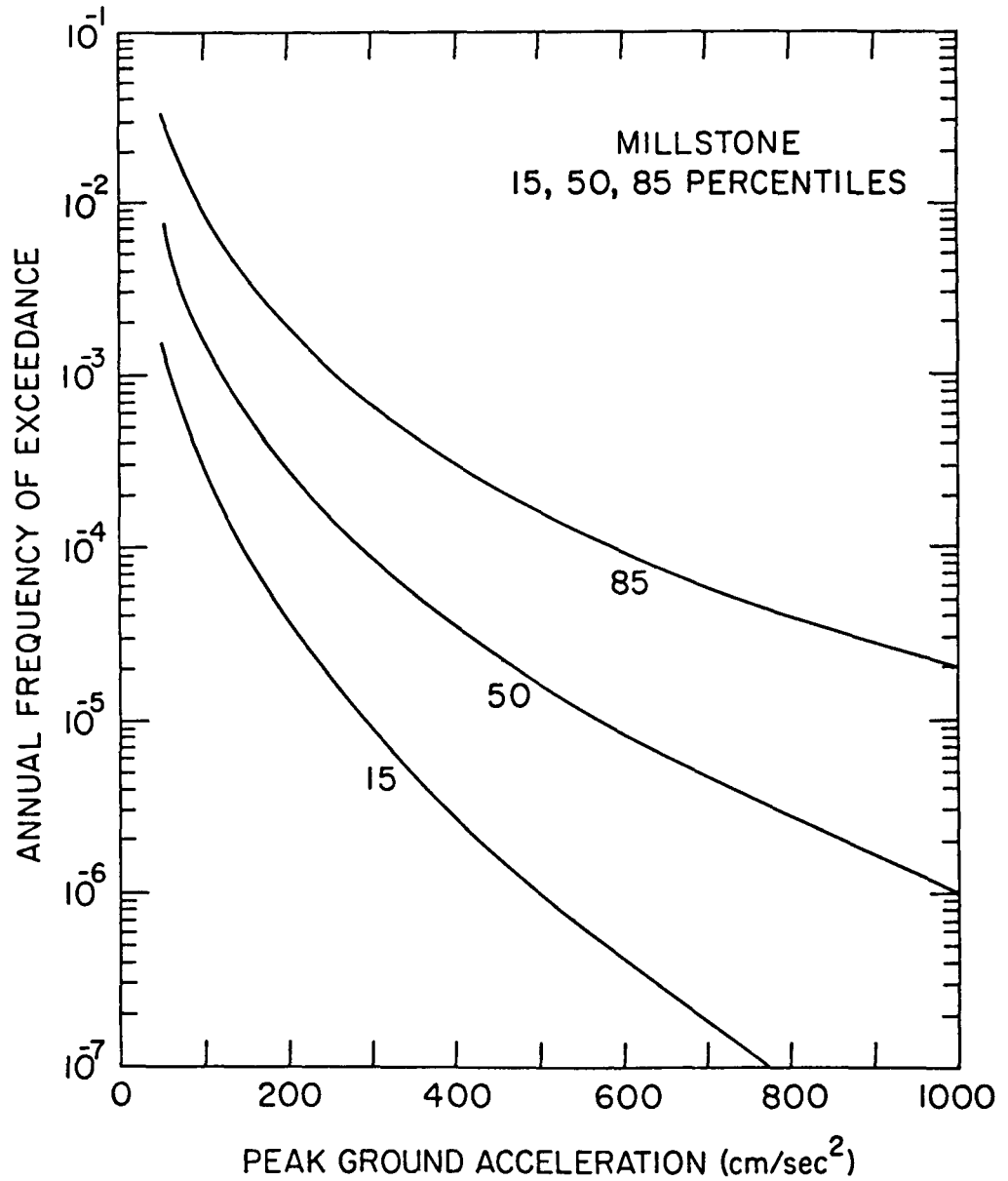
Figure 2.2   The 15, 50 and 85 Percentile Hazard Curves for the
Millstone Site. The data are based on confidence
levels in the input seismicity data of the experts
and uncertainties in the best choice of ground mo-
tion models (Source: Ref. 11, pg. 5-45).

40

-1
10

-2
10

-3
10

-4
10

-5
10

-6
10

-7
10

ACCELERATION CM/SEC**2
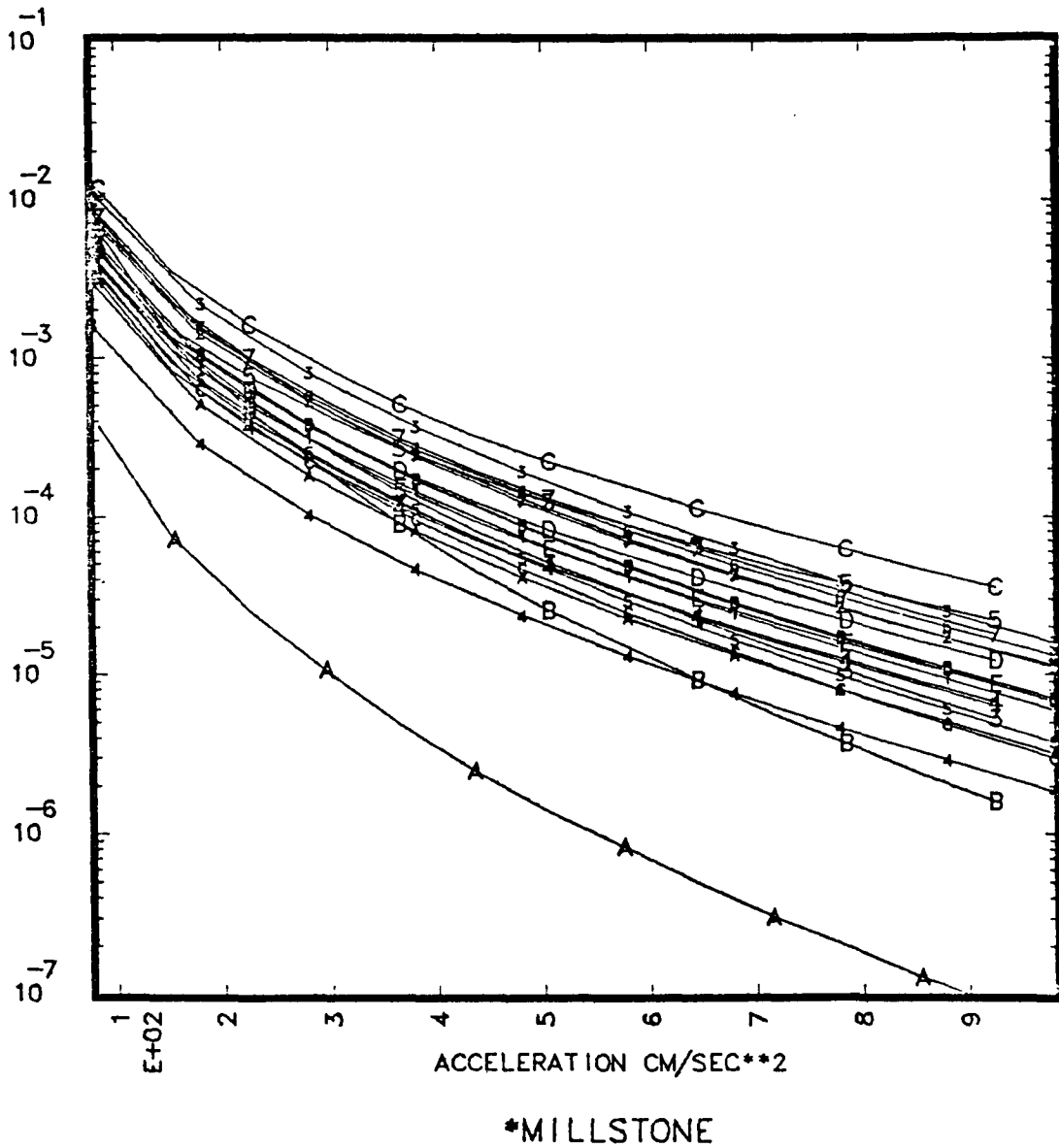
*MILLSTONE

Figure 2.3   Seismic Hazard Curves for Millstone of Each of the Individual Experts Participating in the SEP Studies (Ref. 8) and/or the SHC Studies (Ref. 10). The curves give an indication of the spread in expert opinion (Source: Ref. 11, pg. 209).
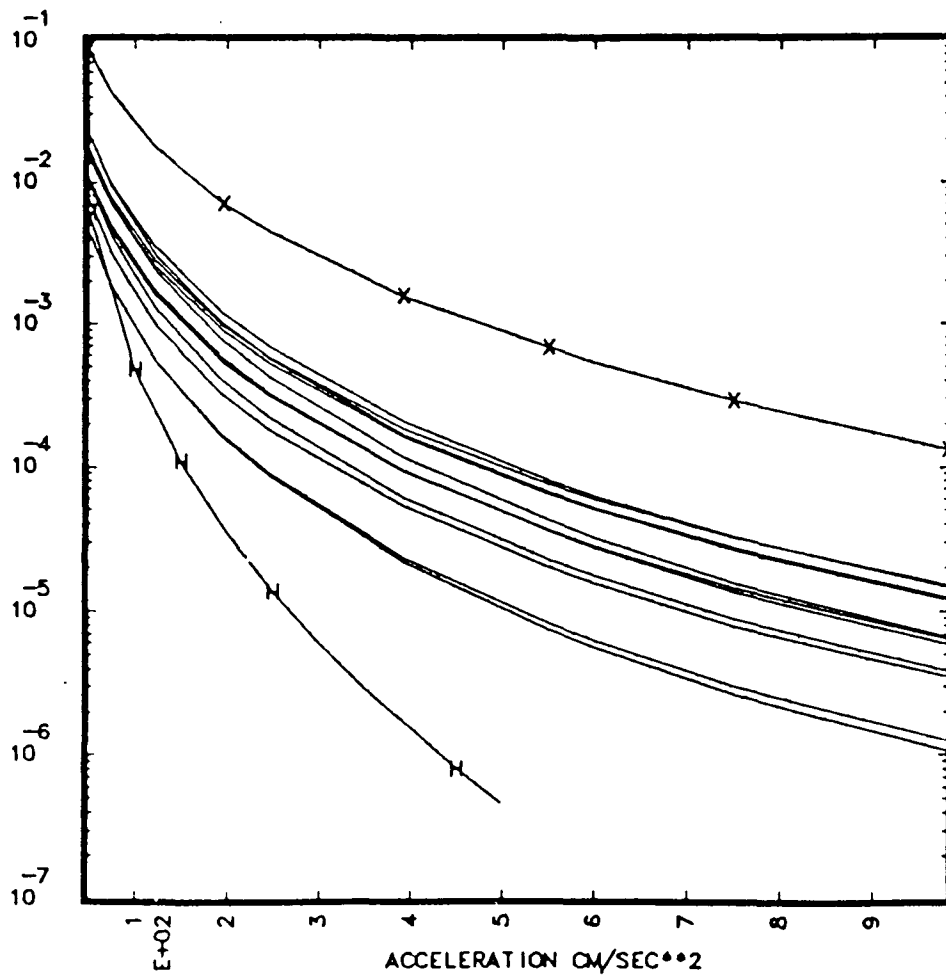
Figure 2.4   Comparison of the Millstone Site Hazard Curves
Generated from the Data Input of the SHC Experts,
with Those Generated from the USGS Data (Curve
"X") and from the Historical Record of the Past
280 Years (Curve H) (Source: Ref. 11, pg. 6-7).

42
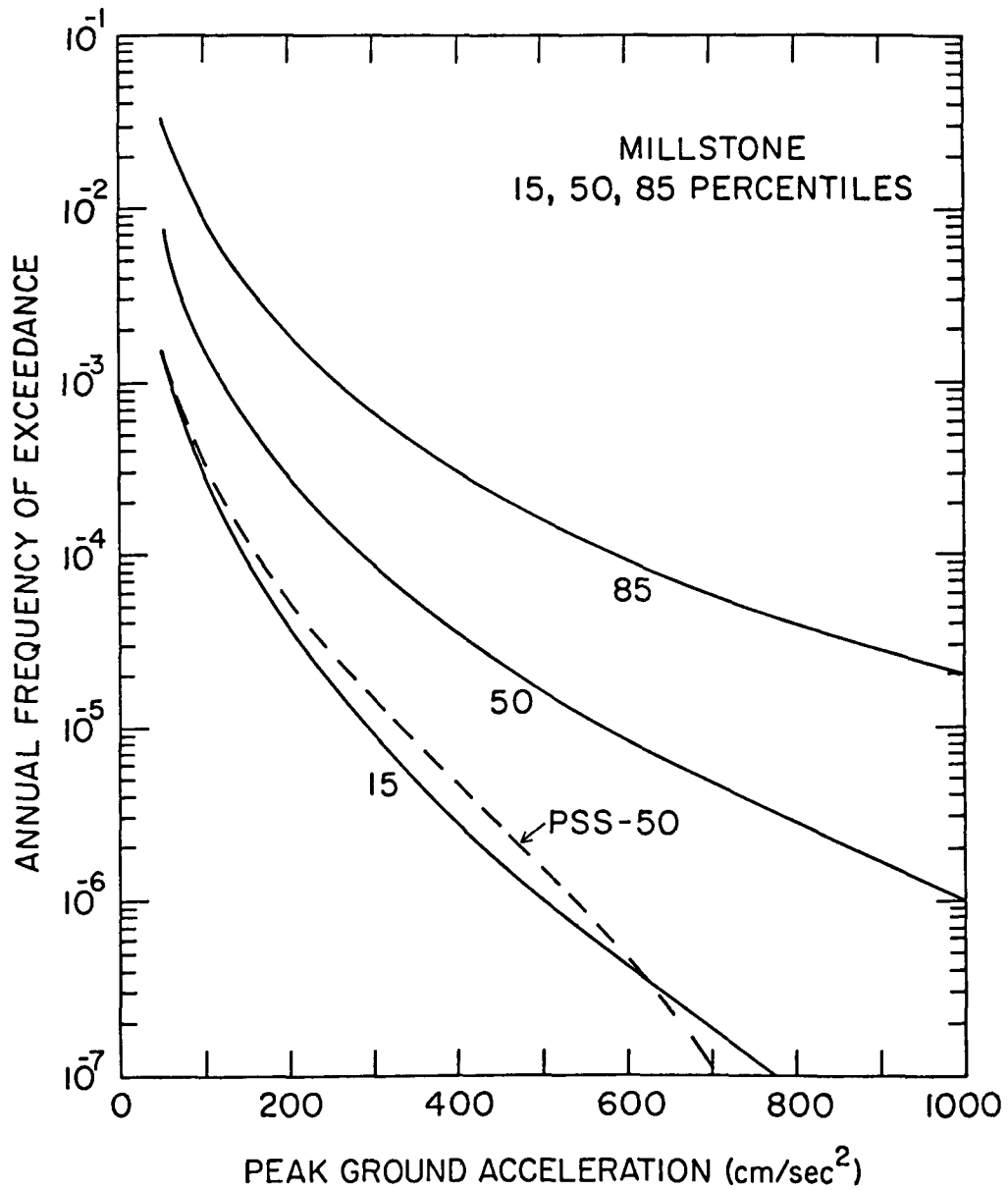
Figure 2.5 SHCP Seismic Hazard Curves of Fig. 2.2 Compared with the 50 Fractile Curve (PSS 50). Derived for the Millstone 3 Probabilistic Safety Study (Ref. 20).

43
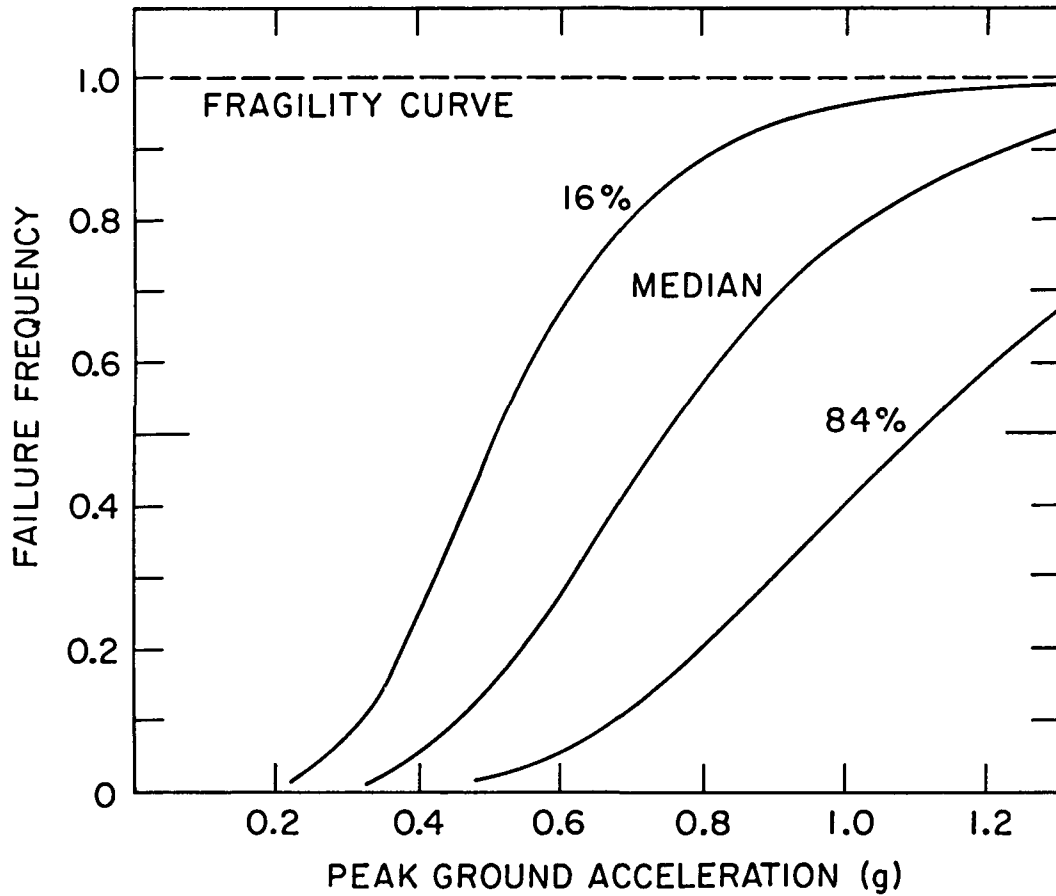
Figure 2.6 Fragility Curves for the Oyster Creek Reactor Building. The curves generated by R.P. Kennedy et al. (Ref. 23) give the frequency of structural failure as a function of peak ground acceleration during an earthquake.
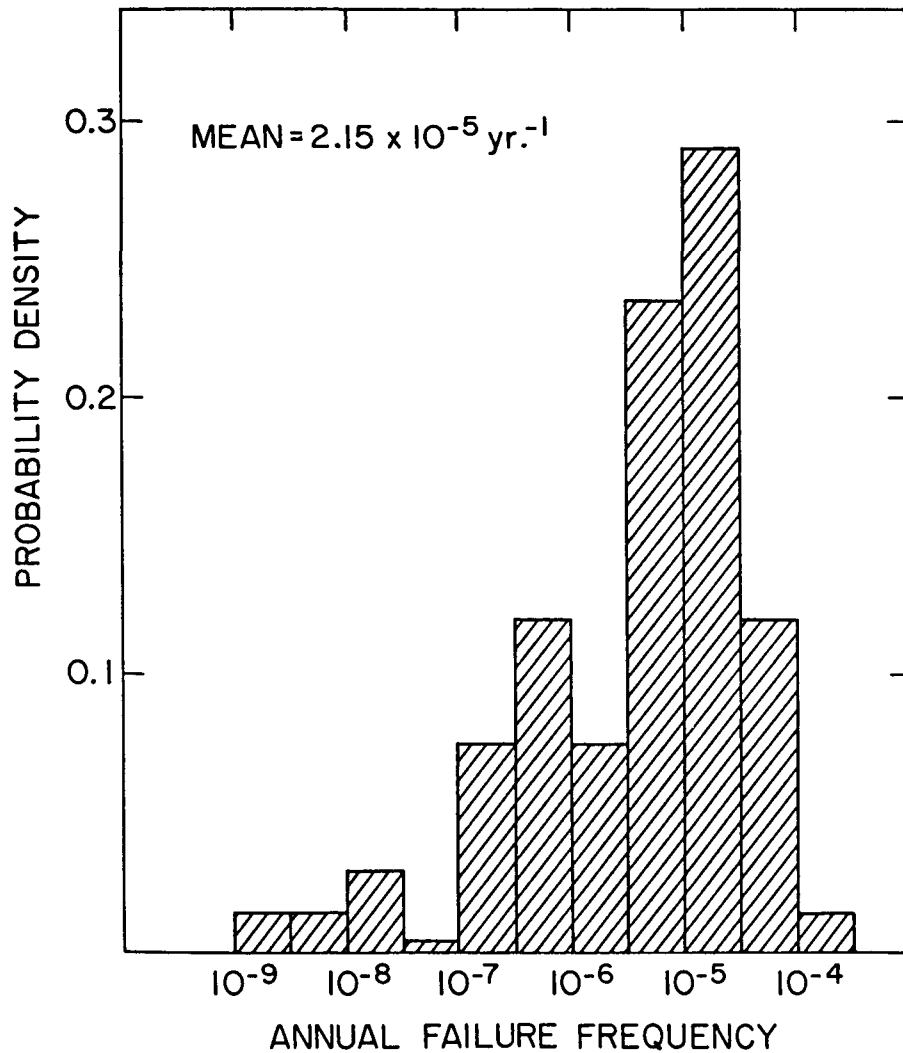
Figure 2.7 Probability Density for Seismically-Induced Failure as a Function of Annual Failure Frequency. The histogram was obtained from 24 convolutions of four hazard curves with six fragility curves and includes the weighting factors assigned to each curve.

45

4"

½"

2"

6 ½"

SEAL SYM ABOUT

1 ½"

B3 - B3
12" = 1'-0"
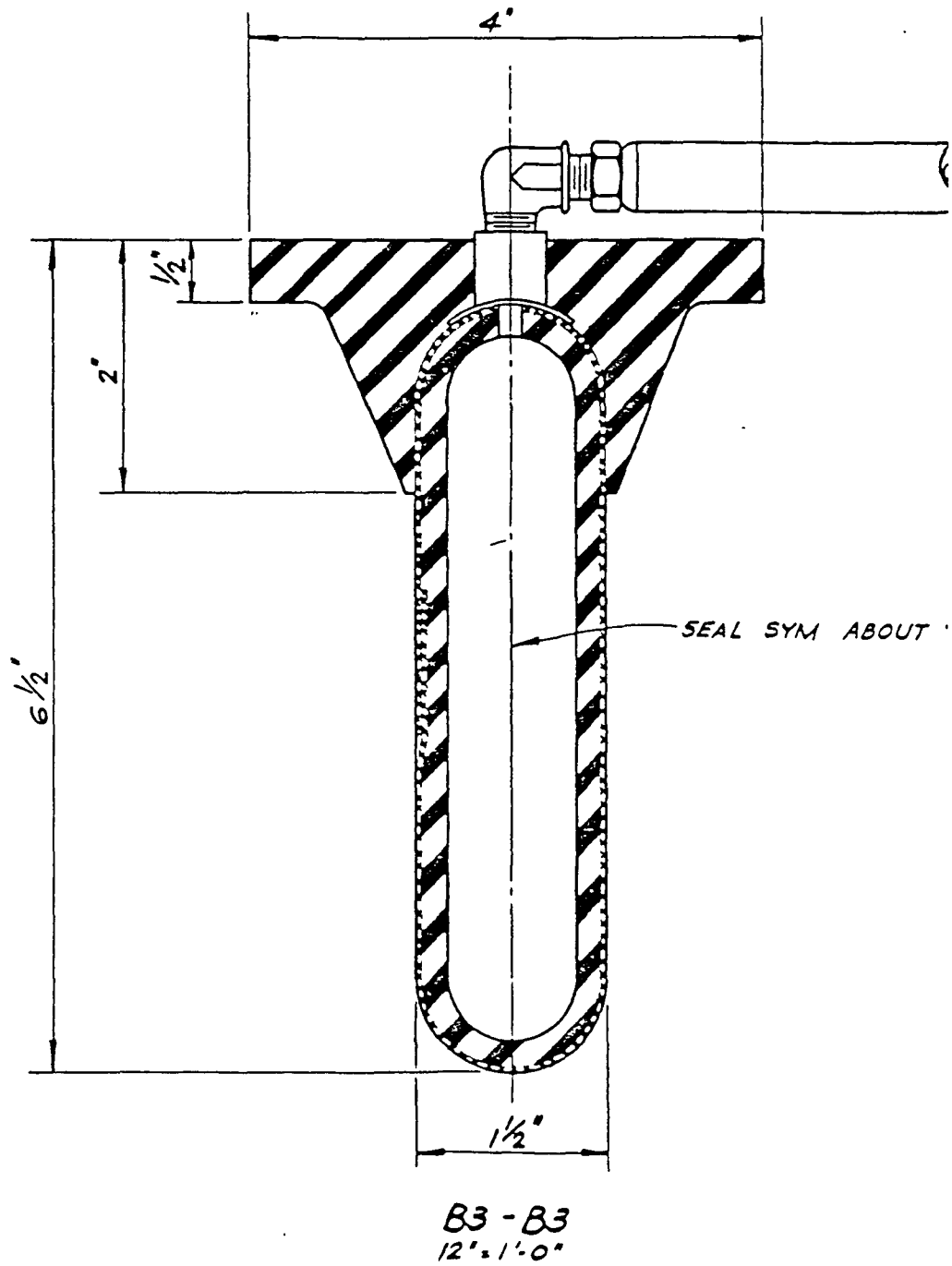
Figure 2.8   Cross Section of a Typical Pneumatic Seal (Source: submission by Sequoyah Nuclear Plant, Docket No. 50-327, 10/26/84 in response to IE Bulletin 84-03.
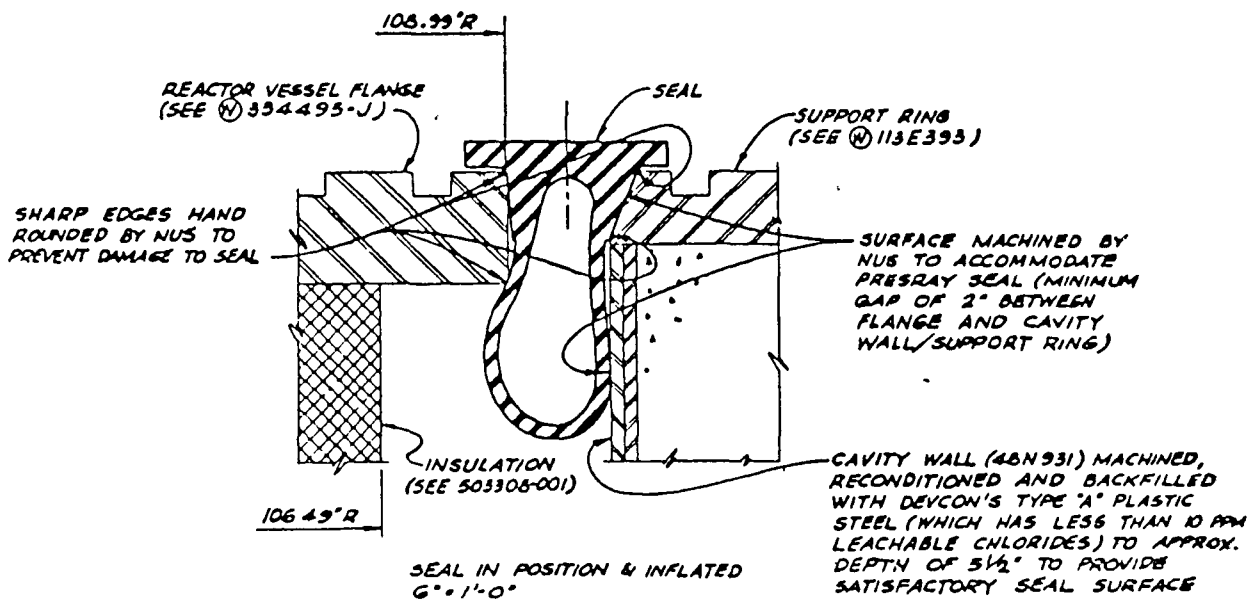
Figure 2.9 Cross Section of Inflated Pneumatic Seal Seated on the Reactor Vessel Flange and Inner Surface of Cavity Wall (Source: submission by Sequoyah Nuclear Plant, Docket No. 50-327, 10/26/84 in response to IE Bulletin 84-03.

47

2 1/4"

S PRS 585-6 INFLATABLE SEAL

REACTOR VESSEL FLANGE

CAVITY FLOOR

2 1/2"

5 1/2"

5 1/2"

W.P.

STATION - *INDIAN POINT 2*
CAVITY SEAL RING

DRAWN BY *A. GAMBUZZA* CHECKED

SCALE *NONE* J.P.

CHIEF
DESIGN
ENG.

ENG.

ENG.

APPROVALS

CONSOLIDATED EDISON CO. OF N.Y. INC.

DWG.
NO. D

RECORDED

REVISIONS
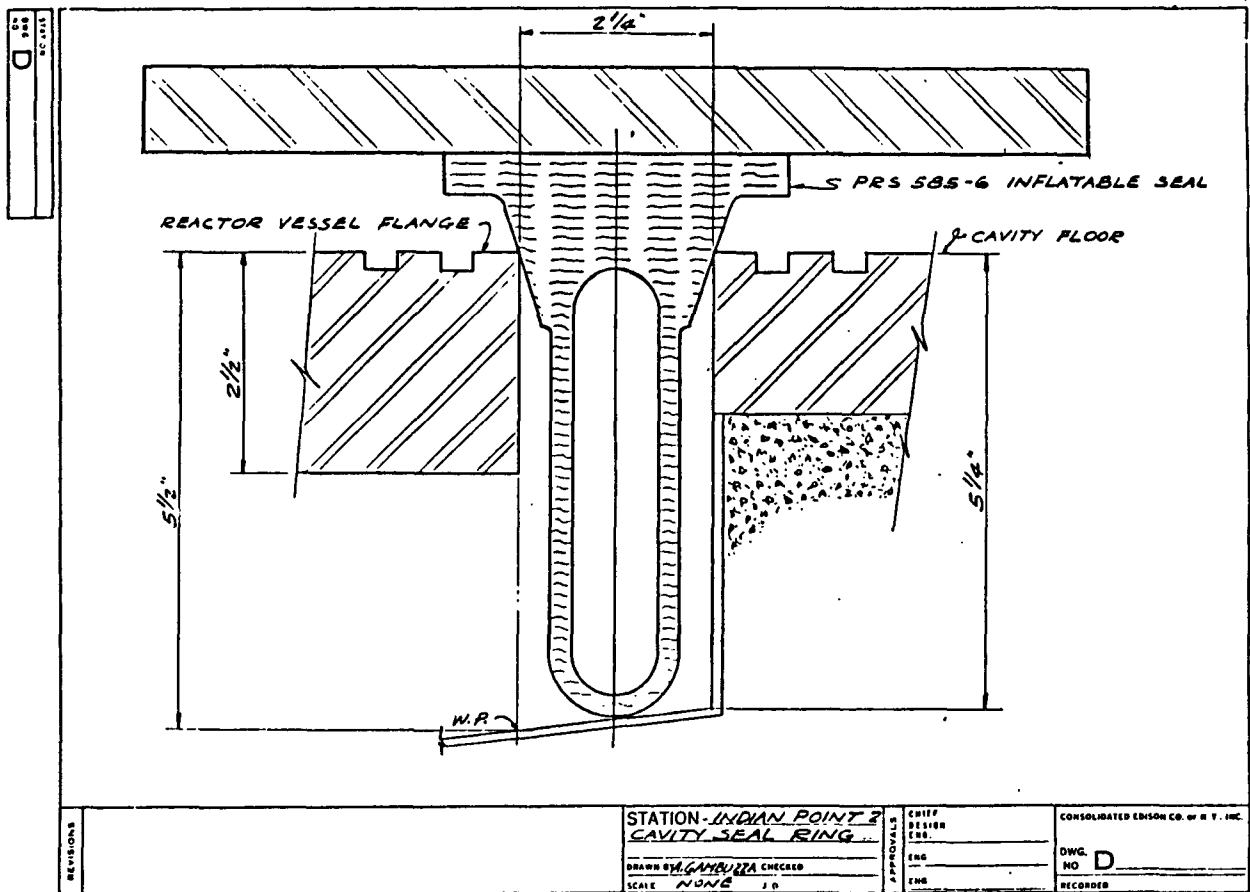
Figure 2.10 Uninflated Pneumatic Seal with Steel Hold-down
Ring (Source: submission by Indian Point Station,
Unit 2, Docket No. 50-247, 11/30/84 in response to
IE Bulletin 84-03).

3. EVALUATION OF FUEL CLADDING FAILURE

Two previous studies[1,2] employing the computer codes SFUEL and SFUEL1W, analyzed the thermal-hydraulic phenomena assuming a complete drainage of the water from a spent fuel pool. The previous section addressed the possible mechanisms for such an accident to occur and provided estimates for the accident frequency. This section provides a reevaluation of the results[1,2] obtained by SFUEL and SFUEL1W calculations and their applicability to beyond design-basis accidents in spent fuel pools.

3.1 Summary of SFUEL Results

The SFUEL code was developed by Benjamin et al.[1] to analyze the behavior of spent fuel assemblies after an accident has drained the pool. The results reported in Reference 1 indicated a wide range of decay power levels for which self-sustaining oxidation of the cladding would be predicted. Several limitations in the SFUEL model were identified and addressed in a subsequent investigation.[2] But comparisons to small scale experiments were not very successful.

Subsequent reviews of Zirconium/Zircaloy reaction rate data indicate that the oxidation equation used in SFUEL is representative of the existing data (see Appendix B). In this analysis it will be shown that self-sustaining oxidation initiation is not very sensitive to the oxidation rate equation but is dependent upon the calculated air flow (related to flow resistance) and the power level. BWR spent fuel with its low power density and open flow configuration must be recently discharged (within about 3 months) for self-sustaining oxidation to be initiated and unless it is a very high power bundle (discharged within 10 days or less) there is only a slight chance of propagation to older low power fuel bundles.

However, PWR spent fuel racks typically have a higher power density in storage and more flow restriction, thus self-sustaining oxidation may be initiated in fuel that has been discharged for one year or more.

3.1.1 Model Description

The SFUEL code was developed at SNL and is described in Reference 1. Basically it is a finite difference solution of the transient conduction equation for heating of the fuel rods considering:

- The heat generation rate from decay heat and oxidation of the cladding.
- Radiation to adjacent assemblies or walls.
- Convection to buoyancy-driven air flows.

The key assumptions in the analysis are:

- The water drains instantaneously from the pool.
- The geometry of the fuel assemblies and racks remains undistorted.
- Temperature variations across the fuel rods are neglected.
- The air flow patterns are one-dimensional.
- The spaces between adjacent basket walls are assumed to be closed to air flow.

49

These assumptions simplify the analysis and may affect the timing and extent of fuel rod failure but they appear to provide a reasonable basis for the present "scoping" calculations. In particular, fuel pool failure, if it occurs, would not cause an instantaneous loss of water. Because of the large water inventory, draining of the pool would occur over several hours or days. The time to drain the pool would have a considerable impact on the likelihood of mitigative action and the timing of the fuel rod heat-up if mitigation were unsuccessful. The idealizations of undistorted geometry and one dimensional flow appear to be reasonable up until the point of clad melting and reloca- tion. Degraded fuel rod phenomenology beyond the melting clad point is beyond the scope of this investigation but may also provide a mechanism for failure propagation to low power assemblies.

The last assumption of no air flow between baskets is accurate for high density configurations but may tend to underestimate cooling flow for some of the older designs (e.g., cylindrical baskets) with large air spaces between each basket.

After the water is drained from the pool the fuel rods heat up until the buoyancy driven air flow is sufficient to prevent further heating. If the decay heat level is sufficient to heat the rods to about 900°C, (1650°F) the oxidation becomes self-sustaining. That is, the exothermic oxidation reaction provides sufficient energy to match the decay heat contribution and the tem- perature rises rapidly.

Reference 2 describes the modification of the SFUEL code to increase cal- culational stability and assess propagation of Zircaloy "fires" from high power to low power assemblies. This version of the code (SFUEL1W) also elimi- nated unrealistically high temperatures* by non-mechanistically removing each node as it reaches the melting point of Zircaloy dioxide (2740°C or 4963°F). In the present investigation, the oxidation cutoff has been reduced to 1900°C (3450°F), which is the melting point of Zircaloy. Recent experiments indicate that Zircaloy relocation will restrict further oxidation occurring above the clad melting point.

3.1.2 Clad Fire Initiation Results

An extensive review of the cladding oxidation models used in SFUEL,[1,2] is given in Appendix B and summarized here:

1. The likelihood of clad fire initiation is not very sensitive to the oxidation equation.

2. The oxidation equation used in SFUEL is a reasonable representation of the data.

3. The likelihood of clad fire initiation is most sensitive to the decay heat level and the storage rack configuration (which controls the ex- tent of natural convection cooling).

---

*Since the code does not explicitly treat melting of the cladding, tempera- tures as high as 3500°C were predicted.[2]

The critical conditions (i.e., the decay heat level which is sufficient to cause a clad fire) for clad fire initiation as determined by SFUEL calculations are summarized in Table 3.1. Note that for the old style cylindrical fuel racks with a large inlet orifice (3 inch diameter) the natural convection cooling in air is predicted to be adequate to prevent self-sustaining oxidation (cladding "fires") after 10 days of decay for BWR assemblies and 50 days for PWR assemblies. However for the new high density fuel racks, natural convective flows are so restricted that even after cooling for a year there is potential for self-sustaining oxidation. As pointed out by Benjamin et al.[1] there are a number of modifications to the fuel rack design which would enhance convective cooling and reduce the potential for cladding fires. However, the limited flow area of the high density designs make it difficult to ensure adequate cooling by natural convection of air.

For the assumption of annual discharges, the critical decay time (the shutdown time which is sufficient to preclude clad fire) can be expressed as a fraction of the fuel cycle and translated into a likelihood of cladding fire for a complete loss of pool water inventory. For the critical cooling times given in Table 3.1 the fraction of time for which the decay heat is sufficiently high to cause self-sustaining oxidation is approximately:

0.0 to 0.5 for BWRs with low density storage racks,

0.0 to 0.7 for PWRs with low density storage racks, and

1.0 for PWRs with high density storage racks.

3.1.3 Clad Fire Propagation

The SNL investigations[1,2] of spent fuel behavior after a loss of pool integrity accident (assumed to result in complete drainage of the pool), identified a range of power levels necessary for the initiation of self-sustaining clad oxidation and substantially lower power levels at which adjacent fuel bundles would oxidize once oxidation had been initiated. However, the phenomenology of propagation is not well understood and there was considerable uncertainty in these estimates. Benjamin et al.,[1] Pisano et al.,[2] Han[3] and Johnsen[4] have pointed out a number of limitations in the previous analyses.[1,2] To put the present results in perspective it is worth mentioning the most important limitations, and what has been done in this study to reduce uncertainties.

1. The oxidation equation allows oxidation to continue beyond 1900°C (3450°F) where clad melting and relocation is expected. PBF and KfK tests show clad relocation at temperatures in the range of 1900° to 2200°C but the analyses have calculated temperatures as high as 3500°C (6330°F) without accounting for clad and fuel melting. At such high temperatures the radiation heat flux becomes very large and it is believed that the potential for propagation to adjacent bundles will be overestimated.

   To provide more realistic estimates of the potential for oxidation propagation, BNL has chosen to terminate oxidation at the Zircaloy melting point since recent severe accident research indicates that Zircaloy relocation will occur and further oxidation will be limited.

51

2. The SFUEL code had not yet been validated successfully against fuel rod oxidation data. A preliminary comparison[2] against SNL data was only partially successful.

   The SFUEL code has been compared to the SNL data in a separate section (3.2) and key portions of the code have been validated. Specifically, the axial heat up (without oxidation) and the temperature at which self sustaining oxidation is reached has been validated. If a low power spent fuel bundle heats up to within one or two hundred °C of self-sustaining oxidation due to its own internal energy there is a high likelihood that the additional energy from an adjacent high power bundle will be sufficient to bring it to the initiation point.

3. The reaction rate equation has been criticized as being too low for long term exposure at low temperatures (when oxide layers may flake off and expose fresh Zircaloy).

   Appendix B has shown that the SFUEL calculations are not very sensitive to the low temperature oxidation rate.

4. The lack of a fuel and clad melting and relocation model has also been criticized.

   The modified SFUEL code (SFUEL1W[2]) has sufficient flexibility to estimate the importance of oxidation propagation via radiation heat transfer to adjacent fuel racks. The subsequent behavior (e.g., fuel rod slumping) after the clad melting temperature is reached may provide an additional mechanism for propagation (heating from below), but this has been treated as an uncertainty in the extent of pool involvement.

5. Johnsen[4] criticized the clad failure criterion used in the SNL analyses.[1,2] He noted that the clad structural failure could occur at temperatures as low as 650°C if the thermal loading is sustained for several hours.

   In view of the large uncertainty in the thermal behavior, we agree that a prediction of temperatures in excess of 650°C should not be viewed as successful cooling of the assembly. At these temperatures cladding failure and fission product release is very likely and the potential for cladding "fires" is high due to the effects of asymmetric heating (from adjacent high power bundles). Two cases for which cladding failure is assumed without self-sustaining oxidation are presented in Chapter 4.

It should be emphasized that SFUEL does not address the question of Zircaloy oxidation propagation after clad melting and relocation. For recently discharged fuel (less than 90 days), or for severely restricted air flow (e.g., high density PWR spent fuel racks) the oxidation reaction is predicted to be very vigorous and failure of both the fuel rods and the fuel rod racks is expected. Thus a large fraction of the fuel rods would be expected to fall to the bottom of the pool forming a large debris bed. If water is not present in the bottom of the pool, the debris bed will remain hot and will tend to heat the adjacent assemblies from below. The investigation of debris bed

formation is beyond the scope of the present study, but it appears to be an additional mechanism for oxidation propagation.

Propagation of cladding "fires" by particulate (i.e., spallation) or zirconium vapor transport has been investigated and eliminated in an approximate separate effects study by Pisano et al.[2] However, the SNL results using the modified SFUEL1W code indicate that propagation due to the heat flux (radiation and convection) from adjacent bundles is likely to occur even to very low power assemblies (at power levels corresponding to 3 years of decays).

With these considerations in mind, a series of SFUEL calculations were performed to establish the range of conditions for which propagation is predicted to occur. Both the power of the initiating bundle and the power of the adjacent bundles have been varied as well as the ventilating conditions of the spent fuel building. An example SFUEL input deck is provided in Appendix C for documentation purposes.

Two fuel building ventilation conditions have been investigated as described below but it must be recognized that both of these assumptions correspond to very idealized conditions that are unlikely to be duplicated in an actual accident. Rather these idealized conditions are provided to demonstrate the sensitivity of the various assumptions. For a beyond design basis seismic event, that ruptures the pool, it seems likely the failure of the fuel building may also occur. Benjamin et al.[1] have shown that a very large hole (at least 77 ft^2) must be opened to approximate the perfect ventilation case.

3.1.3.1 Perfect Ventilation

Under the perfect ventilation condition it is assumed that the fuel building is maintained at ambient conditions by a high powered ventilation system (note that the flow rate must be much higher than typical gas treatment systems) or by a large opening (greater than 77 ft^2) in the building. Oxygen is not depleted and the air entering the pool is assumed not to be heated by the hot gases exiting the fuel assemblies. The conditions necessary to initiate self-sustaining oxidation under perfect ventilation conditions are summarized in Table 3.1 for three typical fuel rack configurations. Note that these are "borderline" conditions in that a slightly lower power level or a larger inlet hole size would predict that self-sustaining oxidation does not occur. Note that the "critical" conditions outlined in Table 3.1 do not imply that fuel rod failure would not occur for power levels below these conditions. The power level must be reduced substantially (about 20%) to ensure that the predicted clad temperature is below 650°C (the minimum temperature at which clad structural failure and fission product release is likely to occur).

For power and flow conditions that are only slightly below the "critical" conditions it should be obvious that the heat flux from a much higher power adjacent bundle would have the potential to push the "non-critical" fuel over the self-sustaining oxidation threshold. Thus the only real propagation question is whether recently discharged (high power) spent fuel will radiate sufficient energy to initiate self-sustaining oxidation in low power fuel bundles that have been cooled for one or more years.

53

In this context two limitations of the SFUEL1W[2] code should be noted:

1. The fuel storage racks are assumed to be immediately adjacent so that no air flow between racks is allowed. (The numerical approach used to calculate the heat transfer is numerically unstable if flow is allowed).

2. All fuel storage racks are assumed to be identical so that the question of propagation from high power cylindrical racks to low power high density racks cannot be addressed.

The first limitation probably represents current storage practices where a number of fuel pools are approaching their design capacity. However, the question of providing deliberate cooling channels between recently discharged fuel and the older fuel cannot be directly addressed. Based on engineering insight, it appears that, under the idealized perfect ventilation conditions, the provision of an air space of 6 to 12 inches around the periphery of recently discharged fuel would minimize the likelihood of oxidation propagation to low power spent fuel assemblies. (Note that the code does allow for an air space adjacent to the pool walls and 6 to 12 inches is found to be adequate if flow through the bundles is not restricted.)

Since high density fuel storage racks are predicted to cause self-sustaining oxidation even after storage for one or more years, it seems clear that it would be undesirable to store spent fuel in high density storage racks if it has been discharged within the last two years. (It may be worth noting that current practice restricts the storage density of low burnup fuel due to nuclear criticality considerations.) Thus the question of propagation from cylindrical fuel racks to high density fuel racks should be addressed, but the second limitation mentioned above precludes intermixing of the storage rack configurations.

The propagation results with perfect ventilation are summarized in Table 3.2 for the high density rack configuration described in Reference 2. Note that the lowest power (11.0 kW/MTU) for self-sustaining clad oxidation corresponds approximately to fuel that has been discharged for one year, but the oxidation reaction will generate sufficient energy to propagate to a fuel bundle that is about 2 years old (6.0 kW/MTU). For a fuel assembly that has been discharged for about 10 days (90 kW/MTU) the high decay heat level causes extensive clad oxidation in the high power bundle and a somewhat higher propensity to propagate to low power fuel assemblies (as low as 5 kW/MTU which corresponds roughly to a 2-1/2 year old discharge).

The propagation results for a low density fuel rack (cylindrical) with a 3 inch diameter inlet hole is summarized in Table 3.3. Note that the range of power for the high power assembly is limited due to the improved free convection within this type of fuel rack. Thus self-sustaining clad oxidation is initiated at decay power levels at or above 30 kW/MTU (corresponding to about 90 days of cooling). Assuming that more than one discharge per year is unlikely, the adjacent low power assembly must be less than or equal to about 19 kW/MTU (180 days of cooling). Thus propagation only occurs for fuel that has been discharged less than 1 year with initiation from fuel that has been discharged within 2 weeks.

For a PWR cylindrical fuel rack with only a 1.5 inch diameter flow hole, the air flow is much more restricted and the possibility of propagation is stronger as indicated in Table 3.4. For the 1.5 inch hole size propagation is predicted to occur for cooling times as long as two years.

3.1.3.2 Inadequate Ventilation

As previously mentioned the case of perfect ventilation implies a very high ventilation rate that is not normally possible. Benjamin et al.[1] extended the SFUEL code to consider limited heat removal to just keep the spent fuel building at constant pressure. Details of the modeling are described in Reference 1, but the main result of the model is that the fuel building atmosphere heats up (due to decay heat and the chemical energy of oxidation) and the oxygen is depleted. Benjamin[1] found that the heat-up of the building increased the likelihood of self-sustaining oxidation (i.e., decreased the decay power level necessary to initiate self-sustaining oxidation). This section is intended to address the question of whether limited ventilation also increases the likelihood of propagation to low power bundles.

Table 3.5 provides a summary of propagation runs under inadequate ventilation conditions. For the analyses the high power assemblies are modeled to represent approximately 1/3 of the core for 1000 MWe plant and the fuel building is taken to have a volume of 150,000 ft^3. The results given in Table 3.5 indicate that propagation is no more likely with inadequate ventilation than with perfect ventilation. In fact propagation does not occur for several conditions listed in Table 3.5 for which propagation was predicted with perfect ventilation. Although this result is somewhat surprising, it is simply a result of the oxygen depletion calculation. That is, the oxidation of the recently discharged assemblies uses up the oxygen supply before the lower power assemblies can be heated to the point of self-sustaining oxidation.

In view of the potential for fuel building failure due to either the assumed initiating event (e.g., a beyond design basis earthquake) or the rapid building pressurization from Zircaloy combustion and decay heat, BNL considers the oxygen depletion calculation to be unrealistic. Thus, in spite of the many uncertainties, the perfect ventilation model is expected to give the best approximation for the potential for propagation.

Conclusions Regarding Propagation

Based on the previous results we have concluded that the modified SFUEL code (SFUEL1W[2]) gives a reasonable estimate of the potential for propagation of self-sustaining clad oxidation from high power spent fuel to low power spent fuel. Under some conditions, propagation is predicted to occur for spent fuel that has been stored as long as 2 years.

The investigation of the effect of insufficient ventilation in the fuel building indicated that oxygen depletion is a competing factor with heating of the building atmosphere and propagation is not predicted to occur for spent fuel that has been cooled for more than three years even without ventilation.

These results are in general agreement with the earlier SNL studies,[1,2] but tend to show a reduced likelihood of clad fire propagation due to the reduced oxidation cutoff temperature (2100°C) used in the BNL analysis.

3.2 Validation of the SFUEL Computer Code

The SNL investigations[1,2] of spent fuel behavior after a loss of pool integrity accident (assumed to result in complete drainage of the pool), identified a range of power levels necessary for the initiation of self-sustaining clad oxidation and substantially lower power levels at which adjacent fuel bundles would oxidize once oxidation had been initiated. However, an attempt[2] to validate the code was only minimally successful in that the post-test analyses were able to match the heat-up rate in helium (without oxidation) but the SFUEL code over-estimated the temperature transient after air was introduced.

The objective of this section is to use the revised[3] oxidation rate equation in SFUEL to analyze the SNL small scale tests to aid in validating the SFUEL code. The SNL tests are described in Reference 2, but in order to put the test results in perspective several important conditions should be highlighted:

1. The test was of a small bundle of electrically heated rods (9 rods) with a short length (38 cm).

2. In order to achieve self-sustaining clad oxidation (>850°C) the rods were heated with a very low flow rate of helium before air was admitted to the test assembly.

Under these test conditions the dominant heat loss is via radiation whereas for the postulated accident the dominant heat loss is via free convection. These test conditions lead to laminar flow (a Reynolds number of about 100) in which oxygen diffusion to the cladding surface limits the reaction rate. Only one test (6) had a sufficiently high air flow rate to allow vigourous oxidation.

Since the free convection and radiation calculations in SFUEL[1,2] were inappropriate to the test configuration, Pisano et al.[2] created a stripped down version called CLAD[2] which used a matrix inversion routine to calculate radiation losses.

After several preliminary attempts to analyze the helium portion of the tests BNL concluded that there were several errors which led to underestimation of the convection portion of the heat losses. Since helium has a much higher heat capacity and conductivity than air it appears to contribute to establishing the initial conditions. In order to provide an adequate simulation of the initial steady-state portion of the test we made two modifications to the CLAD code:

1. Include helium properties with a switch to air properties at the start of the transient.

2. Include an energy balance on each gas control volume to force conservation of energy.

With these changes we were able to obtain an adequate simulation of the initial portion of the tests. Using this revised version of CLAD with the

56

Weeks' oxidation correlation,[3] analysis of both the helium and the air portions of the test looked reasonable, but still tended to over-predict the peak temperatures during oxidation. In order to bring the calculations into reasonable agreement with the small scale data the Weeks' correlation has been reduced by a factor of four (note that this corresponds approximately to the data scatter).

Results

The revised CLAD code has been used to analyze the SNL small scale experiments Tests 4, 5 and 6. The other three tests were intended to simulate propagation with nonuniform heating and structures that CLAD was not capable of modeling. The CLAD results for Test 4 are compared to the data in Figure 3.1. These results still tend to overpredict the temperature in the center of the test rod, but give reasonably good agreement at the top of the rod where radiative heat losses are large.

The peak temperatures calculated by CLAD are summarized in Table 3.6 and compared to the peak measured temperatures for the three tests. Note that CLAD still overpredicts the peak temperature for the low flow rate tests (4 and 5) but gives good agreement with the high flow rate tests where adequate oxygen is available. It should be noted that this "oxygen starvation" phenomenon appears to be a result of the extremely low laminar flow where oxygen must diffuse to the clad surface. CLAD includes an oxygen depletion calculation but assumes that all the oxygen in each volume is immediately available at the surface.

3.3 Conclusions Regarding SFUEL Analyses

After an extensive review of the SFUEL code and comparison to the SNL small scale experiments, BNL concludes that the code provides a valuable tool for assessing the likelihood of self-sustaining clad oxidation for a variety of spent fuel configurations assuming that the pool has been drained.

The SNL small scale data provide a reasonable degree of validation for the heat-up and oxidation models, but the results are extremely sensitive to the natural convection calculation which has not been validated.

When oxidation is terminated at the Zircaloy melting temperature (assuming that the molten Zircaloy is relocated), oxidation propagation only occurs for spent fuel bundles which are already approaching the "critical" conditions for self-sustaining oxidation (see Table 3.1). However, this finding does not mean that oxidation propagation is unlikely. On the contrary, for some high density storage configurations the "critical" conditions are approached for spent fuel that has decayed for two to three years. Thus clad "fire" propagation appears to be a real threat but the basic question remains as to what are the "critical" conditions for initiation of oxidation and what the uncertainty is for a given spent fuel configuration. The critical conditions are summarized in Table 3.1 for several typical spent fuel racks. While the heat-up and oxidation models have been validated to a limited extent by the SNL data (see Section 3.2), the authors believe that the largest source of uncertainty is in the natural convection flow rate. It is recommended that these free convection flow calculations be verified against large scale data. Preferably the

data would be obtained from spent fuel assemblies in typical storage racks (both high and low density).

3.4 References for Section 3

1. A.S. Benjamin, D.J. McCloskey, D.A. Powers, S.A. Dupree, "Spent Fuel Heat-up Following Loss of Water During Storage," NUREG/CR-0649, March 1979.

2. N.A. Pisano, F. Best, A.S. Benjamin, K.T. Stalker, "The Potential for Propagation of a Self-Sustaining Zirconium Oxidation Following Loss of Water in a Spent Fuel Storage Pool," Draft Report, January 1984.

3. J.T. Han, Memo to M. Silberberg, USNRC, May 21, 1984.

4. G.W. Johnsen, Letter to F.L. Sims, EG&G, Idaho, April 4, 1984.

Table 3.1 Summary of Critical Conditions Necessary to
Initiate Self-Sustaining Oxidation

Spent Fuel Rack Configuration	Inlet Orifice Diameter (inches)	Minimum Decay Power (kW/MTU)	Approx. Critical[1] Decay Time (days)
High Density PWR (6 assemblies per rack)	5	6	700
High Density PWR (6 assemblies per rack)	10	11	360
Cylindrical PWR	5	90	10
Cylindrical PWR	3	45	50[2]
Cylindrical PWR	1.5	15	250[2]
Cylindrical BWR	1.5	14	180
Cylindrical BWR	3.0	70	<10

[1] Critical cooling (decay) time is the shutdown time necessary to reach a decay power level below the minimum decay power for self-sustaining oxidation. The cooling time to prevent cladding failure is at least 20% longer.

[2] Note that these critical cooling times are somewhat lower than that found by Benjamin et al.[1] since the orifice loss coefficient was modified at BNL

Table 3.2 Summary of Radial Oxidation Propagation Results for a
High Density PWR Spent Fuel Rack with a 10 Inch Diameter Inlet and Perfect Ventilation

High Power Level (kW/MTU)	Adjacent Power Level (kW/MTU)	Approximate Decay Time (days)	Propagation
11.0	5.9	365	Yes
19.2	5.9	365	Yes
90	5.9	365	Yes
90	4.0	730	No

Table 3.3 Summary of Radial Oxidation Propagation Results for a
Cylindrical PWR Spent Fuel Rack with a 3 Inch Diameter
Hole and Perfect Ventilation

High Power Level (kW/MTU)	Adjacent Power Level (kW/MTU)	Approximate Decay Time (days)	Propagation
90	11.0	365	No
90	19	180	Yes*

*Note that this is an unlikely situation in that the conditions imply a
six month period between discharges.

Table 3.4 Summary of Radial Oxidation Propagation Results for a
Cylindrical PWR Spent Fuel Rack with a 1.5 Inch Diame-
ter Hole and Perfect Ventilation

High Power Level (kW/MTU)	Adjacent Power Level (kW/MTU)	Approximate Decay Time (days)	Propagation
90	11.0	365	Yes
90	5.9	730	Yes
90	3.0	1100	No
15	11.0	365	Yes
15	5.9	730	No

Table 3.5 Summary of Radial Oxidation Propagation Results for
Various PWR Spent Fuel Racks with No Ventilation

Spent Fuel Rack	High Power Level (kW/MTU)	Adjacent Power Level (kW/MTU)	Propagation
Cylindrical with 1.5 inch hole	90	5.9	Yes
Cylindrical with 1.5 inch hole	90	3.0	No (O_2 depletion)
Cylindrical with 3 inch hole	90	5.9	No
Cylindrical with 3 inch hole	19.2	11.0	Yes
High Density with 10 inch hole	90	4.0	No (O_2 depletion)

Table 3.6 Comparison of SNL Small Scale Oxidation
Tests to Calculations with CLAD

Test	Air Flow Rate (1pm)	Peak Temperatures		
		Data (°C)	CLAD (°C)	
			Mid	Top
4	12	1570	1900	1400
5	28.3	~1850	1960	1660
6	56.6	>2000*	2100	1800

*Thermocouple failure.
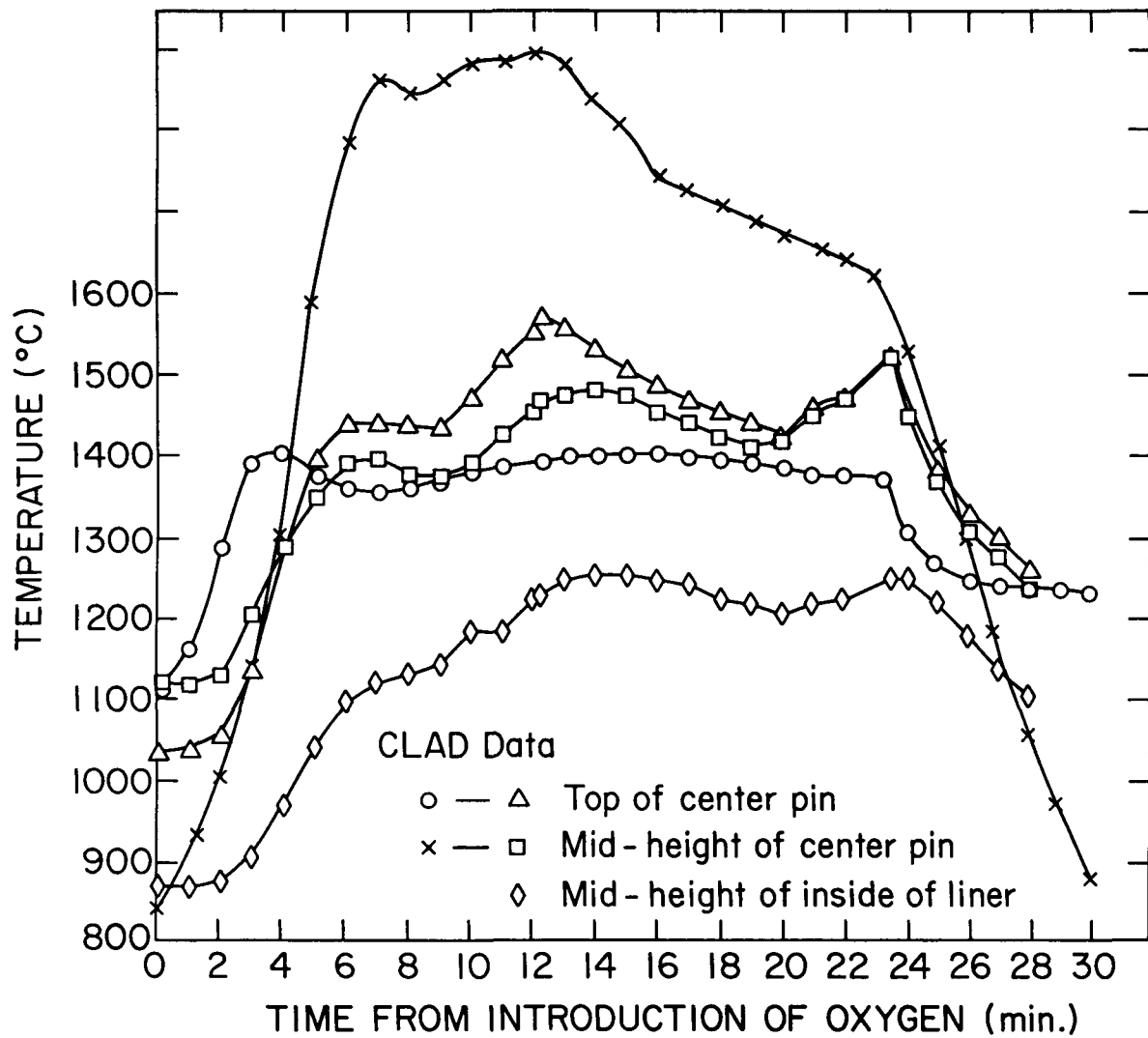
Figure 3.1 Comparison of CLAD to SNL data for Test 4.

4. CONSEQUENCE EVALUATION

A PWR and a BWR reactor were selected for risk evaluation based on a preliminary screening[1] of perceived vulnerability and the spent fuel pool inventory. The reactors selected were Ginna and Millstone 1. Both are older plants that were built before the current seismic design criteria were promulgated and have relatively large inventories of spent fuel.

4.1 Radionuclide Inventories

The radionuclide inventories for both the PWR and BWR pools were calculated using the ORIGEN2 Computer Code[2] for the actual operating and discharge histories for Ginna and Millstone 1. The ORIGEN2 program in use at BNL was verified by comparison with results obtained at ORNL for identical cases.[3]

A description of the assumptions and methods of analysis is given in Appendix A along with the detailed results for each species. The results for the risk significant species are summarized in Table 4.1 (Millstone 1) and Table 4.6 (Ginna).

For both plants, the noble gases and halogens in the spent fuel inventories are a small fraction of the inventory in an equilibrium core at shutdown except for freshly discharged fuel, but cesium and strontium are more than three times the equilibrium inventory (see Tables 4.1 and 4.6).

4.2 Release Estimates

The fission product release fractions have been calculated for two limiting cases in which a Zircaloy fire occurs: In Case 1, the clad combustion is assumed to propagate throughout the pool and the entire inventory is involved. In Case 2 only the most recently discharged fuel undergoes clad combustion.

The release calculations for Cases 1 and 2 make the assumption that if the spent fuel pool suffers a structural failure, coolant inventory will be totally drained, i.e., the leak rate will greatly exceed makeup capability even if the coolant systems are still available. The probability of Zircaloy fire and fission product release has been determined from BNL calculations described in Section 3. In order for a cladding fire to occur the fuel must be recently discharged (about 10 to 180 days for a BWR and 30 to 250 days for a PWR). If a one year refueling cycle is assumed, the SFUEL results in Section 3 indicate that the fraction of time that the fuel must be cooled to preclude overheating leads to a mean conditional probability for a Zircaloy fire of about .25 for a BWR and .4 for a PWR. If the discharged fuel is put into high density racks the air cooling capability is limited such that the critical cooling time is increased to one to three years and the conditional probability of a Zircaloy fire is increased to nearly 1.0.

The BNL reevaluation of the cladding fire propagation calculations with SFUEL (see Section 3) indicates that there is a substantial likelihood of propagation to other fuel bundles that have been discharged within the last one or two years. Subsequent propagation to low power bundles by thermal radiation is highly unlikely, but with a substantial amount of fuel and

cladding debris on the pool floor, the coolability of even low power bundles is uncertain.

4.2.1 Estimated Releases for Self-Sustaining Cladding Oxidation Cases (Cases 1 and 2)

As discussed in Section 3.1 there are a broad range of spent fuel storage conditions for which self-sustaining oxidation of the cladding will occur if the water in the pool is lost. For Ginna with high density racks the conditional probability of a cladding "fire" is predicted to be nearly 100% while for Millstone 1 the probability is about 25%. If self-sustaining oxidation occurs the fuel rods are predicted to reach 1500 to 2100°C over a substantial portion of their length. At these temperatures, the release fraction is predicted to be substantial.

Rough estimates of the fractional release of various isotopes have been presented in an attachment to Ref. 4. Included in the estimates were noble gases (100%), halogens (100%), alkali metals (100%), tellurium (2 to 100%), barium (0.2%), strontium (0.2%) and ruthenium (0.002%).

Estimated release fractions of other isotopes are given in Table 4.2. These estimates are based on empirical fission product release correlations used in the CORSOR code.[5] The uncertainty range included in Table 4.2 is based upon the CORSOR coefficient for the reduced fuel rod temperatures predicted by the modified SFUEL1W code. Comments on the estimates listed in Table 4.2 follow:

Cesium: The uncertainty range in the cesium releases include a decontamination factor of 2 to 10.

Tellurium: The releases shown assume the lower limit of Ref. 4 based on the tellurium release model recently proposed by Lorenz, et al.[6] The low release value assumes that a fraction of the Zircaloy cladding relocates (melts and flows downward) before oxidation is complete.[6]

Alkali Earths: Because of the high boiling points of the oxides of Sr and Ba, it is estimated that only a very small fraction (2×10^{-3}) of these elements of fission product origin in the fuel pellets escape. It is estimated that 100% of the activation product Sr-89 and Y-91 contained in the Zircaloy cladding are released as aerosols.

Transition Elements: It is estimated that 100% of the transition element activation products contained in the cladding are levitated as aerosols of the oxides (smoke). Note that the small release fraction of Zr-95 (0.01) takes into account the large inventory of fission product Zr-95 trapped in the fuel pellets.

It is assumed that only 10% of the activation products in the assembly hardware escapes (see Table 4.2, Fe-55, Co-58, Co-60 and Y-91). The Co-60 fraction is corrected for its small content in the cladding.

64

Antimony: It is estimated that 100% of the Sb-125 is roasted out of the fuel pellets, because of its high mobility.

Lanthanides and Actinides: A negligible release of the oxides of the lanthanides and actinides is estimated because of their chemical stability, low vapor pressures and ceramic characteristics.

Case 1: Case 1, the "worst" case, assumes an accident that results in a Zircaloy fire that propagates throughout the entire spent fuel inventory in the pool, and that the accident occurs 30 days after the reactor was shut down for discharge of the last fuel batch. The estimated releases of radionuclides are listed in Table 4.3. These were obtained by combining the "30-day" inventory given in Column 3 of Table 4.1 with the release fractions listed in Table 4.2.

Case 2: Case 2 assumes an accident that results in a Zircaloy fire that involves only the last fuel batch to be discharged, and that the accident occurs 90 days after the reactor was shut down for fuel discharge. The estimated releases of radionuclides are listed in Table 4.4. These were obtained by combining the inventory in the last fuel batch (data tabulated in Table A.6 of Appendix A) with the release fractions in Table 4.2.

4.2.2 Estimated Release for Low-Temperature Cladding Failure (Cases 3 and 4)

For a less severe accident in which fuel is exposed to air but does not reach temperatures at which a Zircaloy fire ignites, it is assumed that the cladding on many fuel rods will fail (i.e., develop leaks) resulting in a release limited to the noble gases and halogens. Two limiting cases have been considered:

Case 3: in which the entire pool is drained but the decay time since the last discharge is one year, and 50% of the fuel rods suffer clad rupture.

Case 4: in which the pool drains to a level that exposes the upper portion of the fuel assemblies, the decay time for the last discharged fuel batch is 30 days, no Zircaloy fire occurs but all of the fuel rods in the last discharged batch rupture.

The estimated releases for Cases 3 and 4 are given in Table 4.5.

4.3 Off-Site Radiological Consequences

4.3.1 Scenarios for Consequences Calculations

The off-site radiological consequences have been calculated using the CRAC2 computer code.[7] The scenario used in the CRAC2 calculations consisted of the following conditions:

- a generalized site surrounded by a constant population density of 100 persons per square mile;

- generalized meteorology (a uniform wind rose, average weather conditions); and

- the population in affected zones was relocated after 24 hours.

The radiological effects were calculated out to distances of both 50 and 500 miles.

CRAC2 calculations were made for a range of possible releases as described in Section 4.2. While CRAC2 has been used extensively at BNL and elsewhere to calculate consequences for core melt accidents, its use for spent fuel accidents is subject to considerable interpretations. A sample input file is provided in Appendix C for the purpose of documentation of the present usage. The consequence calculations are summarized in Table 4.7.

4.3.2 Consequence Results

There are several unusual characteristics of a spent fuel accident that cause anomalous results with respect to the radiation dose calculations. Specifically, the calculated radiation exposure is insensitive to fairly large variations in the estimated release. This is due principally to the health physics assumptions within CRAC. For the long lived isotopes (predominantly cesium), the exposure is due mainly to exposure after the area is decontaminated and people return to their homes. The CRAC code assumes that decontamination will limit the exposure of each person to 25 rem. Thus, for this type of release the long term whole body dose is limited by the population in the affected sectors (about 0.8 million people in the 16 sectors for a 50 mile radius) to about 3×10^6 person-rem (only 3 of the 16 sectors are downwind). The extreme cases (1A; immediately after refueling and 1B and 1C; with the total fuel pool inventory involved) result in much higher releases but no significant change in population dose.

A more sensitive indication of the severity of a spent fuel accident is the interdiction area (the area with such a high level of radiation that it is assumed that it cannot ever be decontaminated). For these long lived isotopes the interdicted area increases directly with the release fraction and provides a convenient measure of the societal consequences. As indicated in Table 4.7 the worst spent fuel accident is calculated to result in an interdiction area of 224 sq. miles.

For the nominal cases (2A and 2B) in which propagation is assumed not to occur, the person-rem exposure is still high even with an assumed decontamination factor of 10 (Case 2B). The interdiction area is seen to be reduced substantially for Case 2B.

For cases in which the air cooling is sufficient to prevent clad fires (Case 3), the bulk of the releases are noble gases and the consequences are very small.

66

4.4 References for Section 4

1. Internal Memorandum, Brookhaven National Laboratory, V.L. Sailor and K.R. Perkins to W.T. Pratt, "Study of Beyond Design Basis Accidents in Spent Fuel Pools," May 8 1985.

2. A.G. Croff, "ORIGEN2: A Versatile Computer Code for Calculating the Nuclide Compositions and Characteristics of Nuclear Materials," Nuclear Technology, Vol. 62, pp. 335-352, September 1983.

3. Internal Memorandum, Brookhaven National Laboratory, from V.L. Sailor to R.A. Bari, "Comparison of BNL ORIGEN2 Calculations with ORNL," May 27, 1986.

4. Memorandum of J.T. Han to M. Silberberg, "Response to a NRR Request to Review SNL Studies Regarding Spent Fuel Heatup and Burning Following Loss of Water in Storage Pool," U.S. Nuclear Regulatory Commission, (May 21, 1984).

5. M.R. Kuhlman, D.J. Lehmicke and R.O. Meyer, "CORSOR Users' Manual," Battelle Columbus Laboratories, NUREG/CR-4173, BMI-2122, March 1985.

6. R.A. Lorenz, E.C. Beahm and R.P Wichner, "Review of Telliurium Release Rates from LWR Fuel Elements Under Accident Conditions," Proceedings of the International Meeting on Light Water Reactor Severe Accident Evaluation, August 28-September 1, 1983, pg. 4.4-1, American Nuclear Society Order 700085, ISBN 0-89448-1112-6.

7. L.T. Ritchie, J.D. Johnson and R.M. Blond, Calculations of Reactor Accident Consequences Version 2, CRAC2: Computer Code, User's Guide, prepared by Sandia National Laboratories for the U.S. Nuclear Regulatory Commission, NUREG/CR-2326 (SAND81-1994), February 1983.

Table 4.1 Comparison of Radioactive Inventories of Equilibrium Core with Spent Fuel Assemblies for Selected Isotopes (Millstone 1)

Isotope	Equilibrium Core	Spent Fuel Pool[a] (time after last discharge)		
		30-days	90-days	1 year
(Total Radioactivity, Curies)				
Co 58	8.81E+4	2.29E+4	1.26E+4	8.54E+2
Co 60	1.64E+5	3.72E+5	3.15E+5	2.85E+5
Kr 85	5.35E+5	1.41E+6	1.39E+6	1.33E+6
Rb 86	6.22E+4	1.01E+4	1.05E+3	3.84E-2
Sr 89	4.71E+7	8.39E+6	3.63E+6	8.33E+4
Sr 90	4.25E+6	1.42E+7	1.42E+7	1.39E+7
Y 90	4.37E+6	1.43E+7	1.42E+7	1.39E+7
Y 91	6.06E+7	1.18E+7	5.75E+6	2.21E+5
Zr 95	8.70E+7	1.94E+7	1.00E+7	5.10E+5
Nb 95	8.91E+7	2.54E+7	1.70E+7	1.11E+6
Mo 99	8.78E+7	1.49E+4	3.12E-3	neg.[b]
Tc 99m	7.69E+7	1.43E+4	3.01E-3	neg.[b]
Ru 103	7.23E+7	1.53E+7	5.21E+6	4.07E+4
Ru 106	2.48E+7	1.72E+7	1.53E+7	9.13E+6
Rh 106	2.63E+7	1.72E+7	1.53E+7	9.13E+6
Sb 125	9.07E+5	1.19E+6	1.14E+6	9.48E+5
Sb 127	4.97E+6	8.21E+3	1.39E-1	neg.[b]
Te 125m	1.93E+5	2.84E+5	2.76E+5	2.31E+5
Te 127	4.92E+6	2.21E+5	1.45E+5	2.52E+4
Te 127m	6.61E+5	2.18E+5	1.48E+5	2.57E+4
Te 129	1.49E+7	2.74E+5	7.79E+4	2.68E+2
Te 129m	2.24E+6	4.21E+5	1.20E+5	4.12E+2
Te 132	6.72E+7	3.74E+4	8.64E-2	neg.[b]
I 129	1.75E+0	7.15E+0	7.15E+0	7.15E+0
I 131	4.74E+7	1.22E+6	6.35E+3	neg.[b]
I 132	6.83E+7	3.85E+4	8.90E-2	neg.[b]
Xe 133	9.72E+7	7.29E+5	2.30E+2	neg.[b]
Cs 134	6.10E+6	7.90E+6	7.47E+6	5.80E+6
Cs 136	2.10E+6	2.05E+5	8.13E+3	3.91E-3
Cs 137	5.84E+6	2.02E+7	2.01E+7	1.97E+7
Ba 137m	5.53E+6	1.91E+7	1.90E+7	1.87E+7
Ba 140	8.36E+7	5.19E+6	1.90E+5	6.41E-2
La 140	8.54E+7	5.97E+6	2.19E+5	7.37E-2
Ce 141	7.94E+7	1.32E+7	3.61E+6	1.03E+4
Ce 144	6.05E+7	2.64E+7	2.27E+7	1.16E+7
Pr 143	7.37E+7	5.44E+6	2.41E+5	1.90E-1
Pr 144	6.08E+7	2.64E+7	2.27E+7	1.16E+7
Nd 147	3.16E+7	1.54E+6	3.36E+4	1.10E-3
Sm 151	2.44E+4	8.22E+4	8.21E+4	8.16E+4
Eu 154	4.61E+5	1.34E+6	1.32E+6	1.25E+6
Eu 156	5.61E+6	8.26E+5	5.10E+4	1.80E-1
Np 239	9.98E+8	5.59E+4	2.88E+3	2.88E+3
Pu 238	9.33E+4	4.51E+5	4.53E+5	4.54E+5
Pu 239	2.49E+4	8.89E+4	8.89E+4	8.89E+4
Pu 240	3.14E+4	1.30E+5	1.30E+5	1.30E+5
Pu 241	7.19E+6	2.29E+7	2.27E+7	2.19E+7
Am 241	8.86E+3	2.88E+5	2.94E+5	3.21E+5
Cm 242	2.09E+6	1.45E+6	1.12E+6	3.50E+5
Cm 244	6.72E+4	2.27E+5	2.25E+5	2.19E+5

[a]Spent fuel pool inventory includes discharges from 11 refuelings covering the period from August 1972 through the projected refueling of April 1987.
[b]neg. = less than 10^{-3} Curies.

68

Table 4.2 Estimated Radionuclide Release Fraction
During a Spent Fuel Pool Accident Resulting
in Complete Destruction of Cladding (Cases
1 and 2)

Chemical Family	Element or Isotope	Release Fraction[a] Value Used	Release Fraction[a] Uncertainty Range
Noble gases	Kr, Xe	1.00	0
Halogens	I-129, I-131	1.00	0.5-1.0
Alkali Metals	Cs, (Ba-137m) Rb	1.00	0.1-1.0
Chalcogens	Te, (I-132)	0.02	.002-.02
Alkali Earths	Sr, (Y-90), Ba (in fuel)	2×10^{-3}	$10^{-4}-10^{-2}$
	Sr, Y-91 (in clad)	1.00	0.5-1.0
Transition Elements	Co-58 (assembly hardware)	0.10	0.1-1.0
	Co-60 (assembly hardware)[b]	0.12	0.1-1.0
	Y-91 (assembly hardware)	0.10	0.1-1.0
	Nb-95, Zr-95 (in fuel)	0.01	$10^{-3}-10^{-1}$
	Nb-95, Zr-95 (in clad)	1.00	0.5-1.0
Miscellaneous	Mo-99	1×10^{-6}	$10^{-8}-10^{-5}$
	Ru-106	2×10^{-5}	$10^{-6}-10^{-4}$
	Sb-125	1.00	0.5-1.0
Lanthanides	La, Ce, Pr, Nd, Sm, Eu	1×10^{-6}	$10^{-8}-10^{-5}$
Transuranics	Np, Pu, Am, Cm	1×10^{-6}	$10^{-8}-10^{-5}$

[a]Release fractions of several daughter isotopes are determined by their precursors, e.g., Y-90 by Sr-90, Tc-99m by Mo-99, Rh-106 by Ru-106, I-132 by Te-132, Ba-137m by Cs-137, and La-140 by Ba-140.

[b]Release fraction adjusted to account for a 100% release of the small amount of Co-60 contained in the Zircaloy cladding.

Table 4.3 Estimated Releases of Radionuclides for Case 1 in Which a Zircaloy Fire Propagates Throughout the Entire Pool Inventory (Worst Case)

Isotope	Time after Last Discharge		
	30-days	90-days	1 year
	(Radioactivity, Curies)		
Co 58	2.74E+3	1.51E+3	1.02E+2
Co 60	4.46E+4	3.78E+4	3.42E+4
Kr 85	1.41E+6	1.39E+6	1.33E+6
Rb 86	1.01E+4	1.05E+5	3.84E-2
Sr 89	1.68E+4	7.26E+3	1.67E+2
Sr 90	2.84E+4	2.84E+4	2.78E+4
Y 90	2.84E+4	2.84E+4	2.78E+4
Y 91	1.18E+6	5.75E+5	2.21E+4
Zr 95	1.63E+6	8.39E+5	4.26E+4
Nb 95	2.13E+6	1.42E+6	9.27E+4
Mo 99	1.49E-2	neg.[a]	neg.[a]
Tc 99m	1.43E-2	neg.[a]	neg.[a]
Ru 103	3.06E+2	1.04E+2	8.14E-1
Ru 106	3.44E+2	3.06E+2	1.83E+2
Rh 106	3.44E+2	3.06E+2	1.83E+2
Sb 125	1.19E+6	1.14E+6	9.48E+5
Sb 127	8.21E+3	1.39E-1	neg.[a]
Te 125m	5.68E+3	5.52E+3	4.62E+3
Te 127	4.42E+3	2.90E+3	5.04E+2
Te 127m	4.36E+3	2.96E+3	5.14E+2
Te 129	5.48E+3	1.56E+3	5.36E+0
Te 129m	8.42E+3	2.40E+3	8.24E+0
Te 132	7.48E+2	1.72E-3	neg.[a]
I 129	7.15E+0	7.15E+0	7.15E+0
I 131	1.22E+6	6.35E+3	neg.[a]
I 132	7.70E+2	1.78E-3	neg.[a]
Xe 133	7.29E+5	2.30E+2	neg.[a]
Cs 134	7.90E+6	7.47E+6	5.80E+6
Cs 136	2.05E+5	8.13E+3	3.91E-3
Cs 137	2.02E+7	2.01E+7	1.97E+7
Ba 137m	1.91E+7	1.90E+7	1.87E+7
Ba 140	1.04E+4	3.80E+2	neg.[a]
La 140	1.19E+4	4.38E+2	neg.[a]
Ce 141	1.32E+4	3.61E+0	1.03E-2
Ce 144	2.64E+4	2.27E+4	1.16E+4
Pr 143	5.44E+0	2.41E-1	neg.[a]
Pr 144	2.64E+4	2.27E+4	1.16E+4
Nd 147	1.54E+0	3.36E-2	neg.[a]
Sm 151	8.22E-2	8.21E-2	8.16E-2
Eu 154	1.34E+0	1.32E+0	1.25E+0
Eu 156	8.26E-1	5.10E-2	neg.[a]
Np 239	5.59E-2	2.88E-3	2.88E-3
Pu 238	4.51E-1	4.53E-1	4.54E-1
Pu 239	8.89E-2	8.89E-2	8.89E-2
Pu 240	1.30E-1	1.30E-1	1.30E-1
Pu 241	2.29E+1	2.27E+1	2.19E+1
Am 241	2.28E-1	2.94E-1	3.21E-1
Cm 242	1.45E+0	1.12E+0	3.50E-1
Cm 244	2.27E-1	2.25E-1	2.19E-1

[a]neg. = less than 10^{-3} Curies.

70

Table 4.4 Estimated Releases of Radionuclides for Case 2 in Which Only the Last Discharged Fuel Batch Suffers a Zircaloy Fire

Isotope	Time after Last Discharge		
	30-days	90-days	1 year
	(Radioactivity, Curies)		
Co 58	2.28E+3	1.26E+3	8.49E+1
Co 60	9.17E+3	8.68E+3	8.12E+3
Kr 85	2.39E+5	2.36E+5	2.25E+5
Rb 86	1.01E+4	1.05E+3	3.84E-2
Sr 89	1.79E+4	7.75E+3	1.78E+2
Sr 90	3.84E+3	3.82E+3	3.78E+3
Y 90	3.86E+3	3.84E+3	3.78E+3
Y 91	2.66E+4	1.30E+4	4.99E+2
Zr 95	1.62E+6	8.37E+5	4.25E+4
Nb 95	2.11E+6	1.41E+6	9.24E+4
Mo 99	1.49E-2	neg.[a]	neg.[a]
Tc 99m	1.43E-2	neg.[a]	neg.[a]
Ru 103	3.06E+2	1.04E+2	8.14E-1
Ru 106	2.24E+2	1.99E+2	1.19E+2
Rh 106	2.24E+2	1.99E+2	1.19E+2
Sb 125	4.17E+5	4.00E+5	3.31E+5
Sb 127	8.21E+3	1.39E-1	neg.[a]
Te 125m	1.88E+3	1.88E+3	1.61E+3
Te 127	4.28E+3	2.80E+3	4.86E+2
Te 127m	4.20E+3	2.86E+3	4.96E+2
Te 129	5.48E+3	1.56E+3	5.36E+0
Te 129m	8.42E+3	2.40E+3	8.24E+0
Te 132	7.48E+2	1.73E-3	neg.[a]
I 129	8.84E-1	8.86E-1	8.86E-1
I 131	1.22E+6	6.35E+3	neg.[a]
I 132	7.70E+2	1.78E-3	neg.[a]
Xe 133	7.29E+5	2.30E+2	neg.
Cs 134	3.53E+6	3.34E+6	2.59E+6
Cs 136	2.05E+5	8.13E+3	3.91E-3
Cs 137	2.83E+6	2.81E+6	2.77E+6
Ba 137m	2.67E+6	2.66E+6	2.62E+6
Ba 140	1.04E+5	3.80E+3	1.28E-3
La 140	1.19E+4	4.38E+2	neg.[a]
Ce 141	1.32E+1	3.61E+0	1.03E-2
Ce 144	1.91E+1	1.65E+1	8.43E+0
Pr 143	5.44E+0	2.41E-1	neg.[a]
Pr 144	1.91E+1	1.65E+1	8.43E+0
Nd 147	1.54E+0	3.36E-2	neg.[a]
Sm 151	9.31E-3	9.30E-3	9.25E-3
Eu 154	2.89E-1	2.85E-1	2.69E-1
Eu 156	8.37E-1	5.82E-2	neg.[a]
Np 239	5.36E-2	neg.[a]	neg.[a]
Pu 238	6.73E-2	6.87E-2	7.18E-2
Pu 239	9.28E-3	9.28E-3	9.28E-3
Pu 240	1.55E-2	1.55E-2	1.55E-2
Pu 241	3.73E+0	3.70E+0	3.56E+0
Am 241	6.01E-3	7.00E-3	1.14E-2
Cm 242	1.31E+0	1.01E+0	3.16E-1
Cm 244	5.88E-2	5.84E-2	5.68E-2

[a]neg. = less than 10^{-3} Curies.

71

Table 4.5 Estimated Releases of Radionuclides for Cases 3
and 4 in Which Low-Temperature Cladding Failures
Occur

Isotope	Case 3[a]	Case 4[b]
	(Radioactivity, Curies)	
Kr 85	6.65E+5	2.39E+5
I 129	3.58E+0	8.84E-1
I 131	neg.[c]	1.22E+6
I 132	neg.[c]	7.70E+2
Xe 133	neg.[c]	7.29E+5

[a]Case 3 assumes:
1. last fuel discharge has decayed for 1 year.
2. no Zircaloy fire occurs.
3. 50% of the fuel rods develop leaks.
4. 100% release of noble gases and halogens from leaking fuel rods.

[b]Case 4 assumes:
1. last fuel batch discharged has decayed for 30 days.
2. no Zircaloy fire occurs.
3. 100% of fuel rods in last discharge develop leaks.
4. 100% release of noble gases and halogens from leaking fuel rods.

[c]neg. = less than 10^{-3} Curies.

Table 4.6 Comparison of Radioactive Inventories of Equilibrium Core with Spent Fuel Assemblies for Selected Isotopes (Ginna)

Isotope	Equilibrium Core	Spent Fuel Pool[a] (time after last discharge)		
		30-days	90-days	1 year
(Total Radioactivity, Curies)				
Co 58	3.57E+5	5.93E+4	3.26E+4	2.21E+3
Co 60	3.20E+5	5.97E+5	5.84E+5	5.29E+5
Kr 85	3.73E+5	9.84E+5	9.74E+5	9.27E+5
Rb 86	6.53E+5	7.22E+3	7.48E+2	2.74E-2
Sr 89	3.55E+7	3.53E+6	1.53E+6	3.50E+4
Sr 90	2.95E+6	1.02E+7	1.01E+7	9.95E+6
Y 90	3.15E+6	1.02E+7	1.01E+7	9.95E+6
Y 91	4.57E+7	5.11E+6	2.48E+6	9.54E+4
Zr 95	6.41E+7	8.64E+6	4.46E+6	2.27E+5
Nb 95	6.34E+7	1.12E+7	7.51E+6	4.93E+5
Mo 99	6.83E+7	7.03E+3	1.48E-3	neg.[b]
Tc 99m	5.89E+7	6.77E+3	1.42E-3	neg.[b]
Ru 103	5.85E+7	7.86E+6	2.88E+6	2.09E+4
Ru 106	1.95E+7	1.09E+7	9.71E+6	5.78E+6
Rh 106	2.15E+7	1.09E+7	9.71E+6	5.78E+6
Sb 125	6.04E+5	7.11E+5	6.82E+5	5.65E+5
Sb 127	4.12E+6	4.33E+3	7.35E-2	neg.[b]
Te 125m	1.27E+5	1.70E+5	1.65E+5	1.37E+5
Te 127	4.05E+6	1.19E+5	7.79E+4	1.36E+4
Te 127m	5.19E+5	1.17E+5	7.95E+4	1.38E+4
Te 129	1.21E+7	1.38E+5	3.93E+4	1.35E+2
Te 129m	1.80E+6	2.12E+5	6.03E+4	2.07E+2
Te 132	5.33E+7	1.83E+4	4.23E-2	neg.[b]
I 129	1.27E+0	5.32E+0	5.32E+0	5.32E+0
I 131	3.76E+7	6.00E+5	3.12E+3	neg.[b]
I 132	5.42E+7	1.89E+4	4.36E-2	neg.[b]
Xe 133	7.64E+7	3.52E+5	1.11E+2	neg.[b]
Cs 134	5.82E+6	6.35E+6	6.00E+6	4.66E+6
Cs 136	1.87E+6	1.26E+5	4.99E+3	2.40E-3
Cs 137	4.21E+6	1.48E+7	1.47E+7	1.44E+7
Ba 137m	4.00E+6	1.40E+7	1.39E+7	1.37E+7
Ba 140	6.55E+7	2.47E+6	9.07E+4	3.05E-2
La 140	6.74E+7	2.85E+6	1.04E+5	3.51E-2
Ce 141	6.28E+7	6.34E+6	1.72E+6	4.91E+3
Ce 144	4.24E+7	1.38E+7	1.19E+7	6.09E+6
Pr 143	5.71E+7	2.54E+6	1.12E+5	8.86E-2
Pr 144	4.27E+7	1.38E+7	1.19E+7	6.09E+6
Nd 147	2.48E+7	7.42E+5	1.62E+4	neg.[b]
Sm 151	1.42E+4	5.14E+4	5.13E+4	5.10E+4
Eu 154	4.09E+5	1.09E+6	1.07E+6	1.01E+6
Eu 156	7.22E+6	7.58E+5	4.68E+4	1.66E-1
Np 239	7.81E+8	3.02E+4	3.26E+3	3.26E+3
Pu 238	1.01E+5	4.46E+5	4.46E+5	4.46E+5
Pu 239	1.35E+4	5.25E+4	5.25E+4	5.25E+4
Pu 240	2.02E+4	8.60E+4	8.60E+4	8.61E+4
Pu 241	4.85E+6	1.52E+7	1.51E+7	1.46E+7
Am 241	4.99E+3	2.10E+5	2.14E+5	2.32E+5
Cm 242	1.91E+6	9.33E+5	7.20E+5	2.25E+5
Cm 244	1.25E+5	3.59E+5	3.56E+5	3.46E+5

[a]Spent fuel pool inventory includes discharges from 15 refuelings covering the period from April 1983 through the projected refueling of April 1987.
[b]neg. = less than 10^{-3} Curies.

73

Table 4.7   CRAC2 Results for Various Releases Corresponding to
            Postulated Spent Fuel Pool Accidents with Total Loss
            of Pool Water

	Case Description	Whole Body Dose (Man-rem)	Interdiction Area (sq. miles)
1A.	Total inventory 30 days after discharge 50 mile radial zone	2.6×10^6	224
1B.	Total inventory 90 days after discharge 50 mile radial zone	2.6×10^6	215
1C.*	Total inventory 30days after discharge 500 mile radial zone	7.1×10^7	224
2A.	Last fuel discharge 90 days after discharge 50 mile radial zone (maximum release fraction)	2.3×10^6	44
2B.	Last fuel discharge 90 days after discharge 50 mile radial zone (mimimum release fraction)	1.1×10^6	4
3.	50% of all fuel rods leak 1 year after discharge 50 mile radial zone	4.0	0.0

*Note that the consequence calculations in NUREG-1150 are based on
a 50 mile radial zone. Case 1C is given as a sensitivity result.

5. RISK PROFILE

The likelihood and consequences of various spent fuel pool accidents has been estimated in the previous sections. The risk is summarized in Table 5.1. As previously mentioned, the exposure results are tied to the health physics assumptions regarding decontamination and maximum allowable exposure. Thus the land interdiction area is included in Table 5.1 as a more meaningful representation of severity. The uncertainty in each of these risk indices is quite large and is due principally to the uncertainty in the fragility of the pools and the uncertainty in the seismic hazard, but there is also a significant uncertainty in the human error contribution to the cask drop frequency and the fission product release estimates.

Note that the risk results are calculated for two older plants with full fuel pools which were identified as being potentially vulnerable to spent fuel pool accidents. The present risk estimates are not expected to be applicable to more recent plants for which the fuel pools have been designed to more stringent seismic criteria (and can therefore be expected to be less susceptible to seismic failure). There is a potential for larger fission product inventories when some of the newer dual unit plants begin to fill up the pools. However, the seismic margin in the newer designs appears to contribute to an overall risk reduction.

5.1 Failure Frequency Estimates

5.1.1 Spent Fuel Pool Failure Probability

The likelihood of the various postulated spent fuel pool accidents was developed in Section 2 and summarized in Table 2.9. The major contributors to the estimated accident frequency are:

1. Cask drop accidents,
2. Seismic induced pool failure,
3. Loss of pool cooling, and
4. Pneumatic seal failure.

Note that all of these potential accidents are plant specific and their frequency will vary widely from plant to plant. In particular, most BWR's do not have pneumatic seals so their failure frequency is zero. At least one dual unit BWR (Hatch) has its fuel pool outside the reactor building and uses pneumatic seals during refueling operations.

5.1.2 Spent Fuel Failure Likelihood

Previous investigations[1,2] of spent fuel behavior after a loss of pool integrity accident focused on the conditions necessary to initiate cladding "fires" after a spent fuel pool has drained. The present project has reevaluated these conditions using the SFUEL code[2] developed by SNL. The likelihood of such cladding fires has been assessed in Section 3. For a PWR with high density storage racks, the conditional probability of a clad fire given a pool drainage event, was found to be about 1.0 while for a BWR with low density storage racks the probability of a clad fire was found to be about 0.25. The improved air circulation and the lower power density contribute to the improved cooling (and reduced likelihood of fire) for the BWR storage racks.

5.2 Conclusions Regarding Risk

The overall risk due to beyond design basis accidents in spent fuel pools for the PWR and BWR plants is shown in Table 5.1. The unique character of such an accident (substantial releases of long lived isotopes) makes it difficult to compare to reactor core melt accidents. The exposure calculations are driven by assumptions in the CRAC modeling and the results are not sensitive to the severity of the accident.

The uncertainty in risk in terms of person-rem/Ry is driven principally by the uncertainty in the calculation of initiating event frequency for events which completely drain the spent fuel pool. The uncertainty in event frequency is, in turn, driven by the uncertainty in the seismic hazard and fragility along with the uncertainty in human error for cask drop accidents.

5.3 References for Section 5

1. A.S. Benjamin, D.J. McCloskey, D.A. Powers, S.A. Dupree, "Spent Fuel Heat-up Following Loss of Water During Storage," NUREG/CR-0649, March 1979.

2. N.A. Pisano, F. Best, A.S. Benjamin, K.T. Stalker, "The Potential for Propagation of a Self-Sustaining Zirconium Oxidation Following Loss of Water in a Spent Fuel Storage Pool," Draft Report, January 1984.

Table 5.1   Estimated Risk for the Two Spent Fuel Pools from the Two Dominant Contributors

Accident Initiator	Spent Fuel Pool Fire Probability/Ry	Health Risk[1] (Man-rem/Ry)	Interdiction[1] Risk (Sq. Mi./Ry)
Seismic induced PWR pool failure	2.6×10^{-4}-1.6×10^{-10}	600-Neg.*	.011-Neg.
Seismic induced BWR pool failure	6.5×10^{-5}-4×10^{-11}	156-Neg.	.003-Neg.
Cask drop[2] induced PWR pool failure	3×10^{-5}-3×10^{-12}	70-Neg.	.001-Neg.
Cask drop[2] induced BWR pool failure	8×10^{-6}-8×10^{-13}	20-Neg.	4×10^{-4}-Neg.

*Neg. - Negligible.

[1]The upper end of the risk ranges assumes no fire propagation from the last fuel discharge to older fuel. However, the fission products in the last fuel discharge were assumed to be released during the fire with no fission product decontamination on structures (Case 2A).

[2]After removal of accumulated inventory resumes. Presently, most plants are accumulating spent fuel in the pool without shipping to permanent storage. (Note that many new plants have pool configurations and administrative procedures which would preclude this failure mode.)

6. CONSIDERATION OF RISK REDUCTION MEASURES

Due to diversity in the nature of initiating events for beyond design basis accidents in spent fuel pools, there appear to be several possible ways to reduce the risks. It must be emphasized that each of the contributors to risk are plant specific and one or more of the risk significant sequences identified in Section 5 may not be important at other plant sites. The following sections discuss the advantage and disadvantages of a number of proposed risk reduction strategies. A cost benefit analysis has not been performed. Rather, the phenomenological insights, developed during the investigation, have been used to generate the lists of possible risk reduction measures provided below.

6.1 Risk Prevention

1. Reduction of Stored Radioactive Inventory - Most of the consequences of a release of radioactivity from a pool accident is associated with the large inventory of isotopes of intermediate halflives, e.g., Cs-137, Sr-90. The potential release increases approximately in proportion to the number of fuel assemblies in the storage inventory. One obvious measure for risk reduction is to transfer part of the inventory to alternative storage locations (e.g., see Ref. 1).

2. Air Circulation - The one universal prevention measure is to promote air cooling in the event of loss of water cooling of the spent fuel. The new high density fuel storage racks restrict air flow and make even old spent fuel (one to two years) susceptible to heat-up and self-sustaining oxidation. The older style fuel baskets with large inlet holes (3 inch diameter or more per assembly) allow much freer air circulation. If all recently discharged fuel (less than two years) is kept in low density fuel baskets and they are separated from the wall and the older fuel by a one foot gap then the likelihood of self-sustaining oxidation would be reduced by a factor of 5 or more compared to the high density storage configuration.

3. Additional Cooling Systems - Although loss-of-pool cooling appears to be risk significant, an additional cooling system is unlikely to be cost beneficial (unless the cooling system for a specific plant was substantially more unreliable than the two current systems). An additional cooling system would not affect the risk from pool failure events (seismic or cask drop accidents). Thus the net risk reduction would be minimal unless loss-of-cooling were the dominant event.

4. Improved Procedures and Equipment - The likelihood of cask drop accidents can be reduced by improving procedures, administrative controls and/or installing more reliable equipment as suggested in the heavy load drop investigation.[3] Improvements in operator training, heavy load procedures and equipment, which is recommended as part of the resolution for Generic Issue A-36, is estimated to reduce this failure mode by at least a factor of 1000. However, none of these improvements would reduce the risk from the other dominant sequences. Thus the net risk reduction would have to be quantified on a plant specific basis.

5. <u>Plant-Specific Risk Evaluation</u> - This option provides for a limited risk evaluation before spent fuel shipment is begun at each site. A key piece of such an evaluation would be a structural analysis of the pool response to the loading from a dropped cask or a seismic event.

6.2 <u>Accident Mitigation</u>

1. <u>Post-Accident Spray</u> - Water spray has the potential to terminate the progression of a spent fuel pool accident whether or not the pool is intact. However, large quantities of water must be available (it would be necessary to continue spraying until the pool could be repaired and reflooded) and the equipment would have to be seismically qualified to a higher ground motion (g) level than the pool structure (in order for the sprays to have a high likelihood of surviving). Some pools may have fire sprays available in the spent fuel pool building. For those plants without sprays available, it seems unlikely that the expense of a new safety grade spray system could be justified considering the large uncertainty in the risk. Temporary fire hoses were suggested by Benjamin et al.,[2] but the radiation levels would make such ad hoc measures extremely difficult. Furthermore, if the spray is not initiated before the rods reach 900 C or there is insufficient flow, the water may aggravate the reaction by providing additional oxidation potential. (The steam/Zircaloy reaction is also highly exothermic.)

2. <u>Filtering</u> - For those plants with a standby gas treatment system available, operation of the system has the potential to substantially reduce the fission product release from the building. However, the high temperatures and large aerosol production rate would tend to rapidly degrade the effectiveness of the system. The performance of such a filtering system would be difficult to characterize under fuel pool accident conditions. It is unlikely to be cost effective to install a new system large enough to handle the worst case spent fuel pool accident scenarios.

3. <u>Fuel Fire Retardation Modules</u> - Certain materials are known to retard fuel fires, as was demonstrated during the 1986 Chernobyl accident (sand, boron, etc.). Such materials stored in large quantities on site, with a special emergency transport system (helicopter, robots, etc.) could allow for a viable spent fuel pool fire mitigation system.

6.3 <u>Conclusions Regarding Preventive and Mitigative Measures</u>

For those plants which have a significant spent fuel pool risk, the one preventive measure which appears to have a substantial effect on risk (a risk reduction of 5 or more) is to maintain recently discharged fuel in low density storage racks that are isolated from the rest of the fuel racks by a foot or more of space (to provide free air circulation). However, there may be plant specific features which make a substantial difference in the order of the dominant contributors to risk. Therefore plant specific risk evaluations should be performed before any changes are implemented at a given plant.

6.4 References for Section 6

1. D.D. Orvis, C. Johnson, and R. Jones, "Review of Proposed Dry-Storage Concepts Using Probabilistic Risk Assessment," prepared for the Electric Power Research Institute by the NUS Corporation, EPRI NP-3365, February 1984.

2. A.S. Benjamin, D.J. McCloskey, D.A. Powers, S.A. Dupree, "Spent Fuel Heat-up Following Loss of Water During Storage," NUREG/CR-0649, March 1979.

3. H. George, "Control of Heavy Loads at Nuclear Power Plants," U.S. Nuclear Regulatory Commission, NUREG-0612, January 1980.

APPENDIX A

RADIOACTIVE INVENTORIES

A.1 INTRODUCTION

The radionuclide inventories contained in various spent fuel batches has been calculated for two older plants, Millstone-1 (BWR) and Ginna (PWR). The purpose of this appendix is to describe the methods used to simulate the operating history of the two plants and to summarize the calculated radioactive inventories contained in the fuel assemblies stored in the spent fuel basins.

A.2 SIMULATION OF OPERATING HISTORIES

A.2.1 Thermal Energy Production vs Time

The operating history of each plant was reconstructed from several sources. The early history, prior to December 1, 1975 was reconstructed from monthly summaries contained in Refs. 1-3. Data for the period December 1, 1975 through April 30, 1986 were taken from Ref. 4. Data from May 1, 1986 to April 1, 1987 were extrapolated, based on recent average capacity factors and scheduled shutdowns.

During each operating cycle (the period between successive refuelings), the average thermal power was calculated from the total thermal energy produced during the cycle. No attempt was made to model variations in power levels during an operating period. (Fluctuations in the monthly energy production are illustrated in Fig. A.1.)

A.2.2 Fuel Burnup Calculations

The number of fuel assemblies discharged at each refueling and their specific burnup was obtained from a data base maintained by R.A. Libby of Pacific Northwest Laboratories (PNL) for the U.S. Department of Energy.[5] It should be noted that the inventory of spent fuel assemblies stored in the spent fuel basins at various points in time listed in the Libby data base differ from the data listed in Ref. 4. It is apparent from the operating histories that the data in the earlier volumes of Ref. 4 are less accurate.

In general, the burnups listed in the Libby data base differ by a few percent from the burnups calculated by the methods described in the following paragraphs. These discrepancies do not have significant effects on the overall inventories of radionuclides, but only on the distribution of the inventories among the older fuel batches.

In order to model the burnup of the various discharged batches of spent fuel, the following method was used. It was assumed that all fuel assemblies in the core during a given operating cycle provided the average specific power, i.e.,

$$(MW_{th}/MT)_i = (MW_{th}D)_i/D_i(MT)_{core} ,$$

where for operating cycle, i, MW_{th}/MT is the average specific power per metric tonne of initial heavy metal, $(MW_{th}D)_i$ is the total thermal energy produced in D_i days of the cycle, i, and MT_{core} is the metric tonnes of initial heavy metal in the core.

The average specific burnup for each fuel batch, j, at discharge was calculated from the formula,

$$(MW_{th}D/MT)_j = \sum_i (MW_{th}/MT)_i D_i ,$$

where $\sum_i$ is the summation over the several operating cycles, i, that the fuel was in the reactor. (As noted below, ORIGEN2 also calculates the specific burnup which provides a check on internal consistency of the data).

The total burnup in the discharged fuel plus the burnup of assemblies remaining in the core at the time of the April 1, 1987 refueling equaled the total thermal energy production over the preceding history of the plant (e.g., see Table A.4).

A.2.3 Calculation of Radioactive Inventories

The average radionuclide content in each metric tonne of discharged fuel was calculated using the ORIGEN2 Computer Code.[6] The calculations treated the reactor core as a homogeneous body operating at an average specific power. Account is taken of radionuclide decay during and following irradiation, decay chains, and successive neutron captures.

The BNL version of ORIGEN2 was benchmarked against the version in use at Oak Ridge National Laboratory by calculating an identical case, which yielded identical results.[7]

The results obtained from an ORIGEN2 calculation are slightly sensitive to the size of the time steps used in the irradiation calculation. Several preliminary calculations were made to select an appropriate set of time steps for which the sensitivity was negligible. (Shorter time steps give higher precision results, but at the expense of increased computer time. The criterion adopted was that the time-step sensitivity be less than 0.1% in the calculated concentration of several key nuclides.)

In a mature operating nuclear power plant fuel management strategies are complicated (e.g., see Ref. 8). Most fuel assemblies remain in the core for several operating cycles and are often shifted in location during refueling so as to optimize burnup. Also, U-235 enrichment is varied. ORIGEN2 as used at BNL did not take account of such detail, nor of the axial and radial distribution of the power density. Thus, the radioactivity calculated for a particular assembly would not correspond exactly to an actual assembly. Nevertheless, the total calculated radioactivity in a discharged batch closely approximates the total in a real batch (in so far as the precision of ORIGEN2 allows).

The calculations do take account of the irradiation times in each operating cycle and the decay that occurs during shutdowns for refueling or prolonged shutdowns for maintenance and repair.

As used at BNL, the input for each irradiation cycle is the average specific power and the length of the cycle. ORIGEN2 calculates the total average burnup of each fuel batch over the irradiation cycles during which it was in the core. This calculated burnup was cross checked against "hand" calculations for each batch, the "hand" calculations being based on the operating history (see Section A.2.2).

The input for ORIGEN2 requires the specification of the elements contained in the fuel including trace impurities, the U-235 enrichment and the composition and amount of alloys used in the fuel cladding and assembly hardware. For each plant, BWR and PWR, only a single fuel and assembly composition was modeled which is typical of fuel of recent vintage for the respective reactors. Data for the fuel models were taken from Reference 9.

The output of ORIGEN2 includes isotopic concentrations (of stable as well as radioactive isotopes), activity of radionuclides, and thermal power production of each radionuclide. These are given at specified decay times for activation products (in cladding, hardware and trace elements in the fuel pellets), fission products and actinides.

The BNL calculations were made for each fuel batch from the date of the end of irradiation to the projected dates of May 1, 1987, July 1, 1987, October 1, 1987 and April 1, 1988.

A.3 DATA FOR MILLSTONE 1

A.3.1 Reactor and Fuel Cycle Parameters

Table A.1 summarizes several of the major reactor characteristics and fuel cycle parameters for Millstone 1.

A.3.2 History of Operations

Several milestones in the operation of Millstone-1 are summarized in Table A.2. Monthly gross thermal energy production from 1976 through 1984 is plotted in Fig. A.1. During the first 10 years of operation the plant experienced two prolonged outages, i.e. Sept. 1972 to March 1973 (198 days) and October 1980 to June 1981 (254 days). Otherwise the refueling/maintenance outages have ranged from 35 to 76 days in duration averaging about 57 days.

A more detailed narrative of the plant operating history from 1970 through 1981 appears in Ref. 10, Appendix F, pp. F-31 through F-70. The only unusual experience with fuel cladding failures that has been noted occurred in 1974 when some 25 assemblies were found to have leaking fuel elements which forced a temporary power derating to stay within off-gas release limits.[11] Since mid-1981, the plant has operated with nearly 100% unit service factor except for scheduled refueling outages.[4]

There have been 10 refueling campaigns since beginning of commercial operations on March 1, 1971 (see Table A.3). The next scheduled refueling will

be about April 1987. During the first 10 years, refueling occurred at somewhat irregular intervals, being dictated by unscheduled forced outages. Since 1981, refueling has been scheduled for approximately 18 month intervals, occurring in April or September. During the lifetime of the plant the average fuel burnup has generally increased from about 20,000 MWD/MT in 1972 to about 28,000 MWD/MT at present.

A.3.3 BWR Fuel Assembly Model Used in ORIGEN2 Calculations

A nominal BWR fuel element has been modeled, based on data presented in Ref. 9. This is an 8x8 element assembly of 2.75% U-235 enrichment, containing 1.5873 kg of gadolinium burnable poison per metric tonne of uranium. The fuel cladding is Zircaloy-2. Other alloys present in the fuel assembly hardware include Zircaloy-4, Inconel X-750, SS302 and SS304. The alloy contents of the assembly hardware are included with weighting factors to take account of the axial variation of neutron flux which results in lower neutron activation at the ends of the assemblies. In addition to the fuel, the cladding and the assembly hardware, an allowance was made for the presence of "crud" composed of Fe, Co, and Ni on the outer surfaces of the cladding and assembly hardware.

A.3.4 Calculated Radioactive Inventories

The calculated inventories of selected radionuclides* are listed in Table A.5 for the reactor core at the end of operating cycle number 11 projected to be on April 1, 1987. Also listed are the inventories in the spent fuel basin on May 1 and July 1, 1987 and April 1, 1988 assuming that 167 assemblies will be discharged in the April 1987 refueling.

It should be noted that many of the isotopes that are of considerable importance in a core melt accident are those of short half-lives which are no longer present in the spent fuel after a few days of decay, e.g., Rb-91, Rb-93, Sr-93, Sr-95, Y-94, Y-95, Tc-104, I-134, I-135, I-136, Cs-138, Cs-140. On the other hand, the spent fuel inventory contains much larger quantities of several long-lived isotopes than does the equilibrium core. Noteworthy among these are H-3, C-14, Sr-90 (Y-90), I-129, Cs-137, Ba-137m, Eu-154, Pu-239, Pu-240, Pu-241, Am-241, and Cm-244.

Table A.6 gives a comparison of the radionuclide inventories in the last fuel batch to be discharged with the summation of the inventories contained in the ten batches discharged in the period from 1972 through 1985.

A.3.5 Decay Heat

Table A.7 summarizes the decay thermal production in the various discharged batches. The data shown is for the whole batch, i.e., the specific thermal power (kilowatts per metric tonne) multiplied by the metric tonnes in the batch.

Table A.8 summarizes the fraction of the decay heat contributed by various isotopes. The main contributors change with decay time, e.g., in the

---

*The selection of radionuclides was based on several criteria including potential for biological concern, thermal power, and total curies of activity.

oldest fuel (batches 1, 2, etc.) the largest contributors are Y-90 and Ba-137m, whereas the last discharged batch 11 is dominated by Cs-134, Rh-106, and Pr-144. The actinides are relatively small contributors.

A.4 DATA FOR GINNA

A.4.1 Reactor and Fuel Cycle Parameters

Table A.9 summarizes several of the major reactor characteristics and fuel cycle parameters for Ginna.

A.4.2 History of Operations

Several milestones in the operation of Ginna are summarized in Table A.10. A narrative of the operating history from 1969 through 1979 can be found in Ref. 12, Appendix F.

Reconstruction of the refueling history during the early years of operation has been difficult using data readily accessible to BNL Staff (direct access to the Licensee for information was precluded). Table A.11 lists the refueling data used by BNL for the ORIGEN2 calculations, which were carried out in 1985.

Subsequently, additional information has been located that would permit a revision of the data in Table A.11, but repeating the ORIGEN2 calculations did not seem worthwhile since only minor changes in the spent fuel radioactive inventories would have resulted. At the time Table A.11 was constructed, no data on the first refueling in February, 1971 was available. Also, some 84 fuel assemblies from early refuelings could not be accounted for. Later, it was learned that 81 assemblies had been shipped for reprocessing at the West Valley facility. These apparently were returned in 1985 to Ginna for storage in the spent fuel pool.[13]

At the time of the April 1972 refueling, cladding distortions due to fuel densification was discovered and 61 assemblies were replaced (Ref. 12, pg. F-56). Thus, the entry in Table A.11 for the second discharge is incorrect.

The total burnup not accounted for in the ORIGEN2 calculations amounts to 4.2% of the total thermal energy production from 1969 through April 1, 1987. The missing 4.2% burnup is for fuel discharged on or before April 1972.

A.4.3 PWR Fuel Assembly Model Used in ORIGEN2 Calculations

A nominal PWR fuel element has been modeled based on data presented in Ref. 9. This is a 17x17 element assembly (264 fuel elements per assembly) of 3.2% U-235 enrichment containing 461.4 kg of uranium. The cladding is Zircaloy-4. Other alloys present in the fuel assembly hardware include Inconel-718, Nicrobraze 50, SS-302 and SS-304. The alloy contents of the assembly hardware are included with weighting factors to take account of the axial variation of the neutron flux which results in lower neutron flux which results in lower neutron activation at the ends of the assemblies. In addition to the fuel, the cladding and the assembly hardware, an allowance was made for the presence of "crud," composed of Cr, Fe, Co and Ni, on the outer surfaces of the cladding and hardware.

No corrections were made in the ORIGEN2 calculations to account for stainless steel clad fuel that was used in the early history of the plant.

A.4.4 Calculated Radioactive Inventories

The calculated inventories of selected radionuclides* are listed in Table A.12 for the end of operating cycle number 16 projected to be on April 1, 1987. Also listed are the inventories in the spent fuel basin on May 1 and July 1, 1987 and April 1, 1988, assuming that 24 assemblies will be discharged in the April 1987 refueling.

It should be noted that many of the isotopes that are of considerable importance in a core melt accident are those of short half-lives which are no longer present in the spent fuel after a few days of decay, e.g., Rb-91, Rb-93, Sr-93, Sr-95, Y-94, Y-95, Tc-104, I-134, I-135, I-136, Cs-138, Cs-140. On the other hand, the spent fuel inventory contains much larger quantities of several long-lived isotopes than does the equilibrium core. Noteworthy among these are H-3, C-14, Sr-90 (Y-90), I-129, Cs-137, Ba-137m, Eu-154, Pu-239, Pu-240, Pu-241, Am-241, and Cm-244.

Table A.13 gives a comparison of the radionuclide inventories in the last fuel batch to be discharged with the summation of the inventories contained in batches 2-15 discharged between 1976 and 1986.

A.4.5 Decay Heat

Table A.14 summarizes the decay heat production in the various discharged batches. The data shown is for the whole batch, i.e., the specific thermal power (kilowatts per metric tonne) multiplied by the metric tonnes in the batch.

Table A.15 summarizes the fraction of the decay heat contributed by various isotopes. The main contributors change with decay time, e.g., in the oldest fuel (batches 2, 3, etc.) the largest contributors are Y-90 and Ba-137m, whereas the last discharged batch 16 is dominated by Cs-134, Rh-106 and Pr-144. The actinides are relatively small contributors.

---

*The selection of radionuclides was based on several criteria including potential for biological concern, thermal power and total curies of activity.

A.5 REFERENCES FOR APPENDIX A

1. Nucleonics Week, a weekly newsletter published by McGraw-Hill Publishing Co., New York, NY.

2. Nuclear Safety, published bimonthly by the Nuclear Safety Information Center, Oak Ridge National Laboratory.

3. Nuclear Engineering International, published monthly by IPC Business Press, Ltd., Sussex, England.

4. U.S. Nuclear Regulatory Commission, Licensed Operating Reactors, NUREG-0020, Vols. 1-10, published monthly.

5. U.S. Department of Energy, Richland Operations Office, Program Office, Commercial Spent Fuel Management, (private communication from P.A. Craig, Director, June 11, 1985).

6. A.G. Croff, "ORIGEN2: A Versatile Computer Code for Calculating the Nuclide Compositions and Characteristics of Nuclear Materials," Nuclear Technology, Vol. 62, pp. 335-352, September 1983.

7. Internal Memorandum, Brookhaven National Laboratory from V.L. Sailor to R.A. Bari, "Comparison of BNL ORIGEN2 Calculations with ORNL, May 27, 1986.

8. T.G. Piascik, L.E. Fennern, S.R. Specker, K.L. Stark, R.E. Brown, J.P. Rea, and K.T. Schaefer, "BWR Operating Experience at Millstone-1 with Control Cell Improved Design," Transactions of the American Nuclear Society, Vol. 32, pg. 706, June 1979.

9. A.G. Croff, M.A. Bjerke, G.W. Morrison, and L.M. Petrie, Revised Uranium-Plutonium Cycle PWR and BWR Models for the ORIGEN Computer Code, Oak Ridge National Laboratory, ORNL/TM-6051, September 1978.

10. U.S. Nuclear Regulatory Commission, Integrated Plant Safety Assessment Systematic Evaluation Program, Millstone Nuclear Power Station, Unit 1, NUREG-0824, February 1983.

11. U.S. Nuclear Regulatory Commission, Nuclear Power Plant Operating Experience, 1974-1975, NUREG-0227, April 1977, pg. 65.

12. U.S. Nuclear Regulatory Commission, Integrated Plant Safety Assessment Systematic Evaluation Program, R.E. Ginna Nuclear Power Plant, NUREG-0821, December 1982.

13. Rochester Gas and Electric Corporation, "Application for Amendment to Operating License to Amend Appendix A to Increase Spent Fuel Pool Storage Capacity," submitted to NRC April 2, 1984, Docket No.50-244.

Table A.1 Reactor and Fuel Cycle Parameters for Millstone 1
         (Sources: Refs. 1-4)

Assemblies in core: 580

Licensed thermal power: 2011 MW_{th} (gross)

Thermal power corresponding to maximum dependable capacity:
  2006.5 MW_{th} (gross)

Nominal initial metric tonnes of heavy metal (IMTHM) per
  assembly: 0.1833 MT

Average refueling cycle interval (since initial commercial
  operation): 21 to 22 months

Recent refueling cycle interval (since April, 1979):
  about 18 months

Average number of assemblies per discharge: about 173

Average IMTHM per discharge: about 31.7 MT

Average number of fuel cycles per assembly: about 3.35

Average period of irradiation (including downtime): about 72 months

Authorized Storage Pool Capacity (as of 1985): 2184 assemblies

---

Table A.2   Summary of Operational Milestones for Millstone 1
            (Source: Ref. 4)

Date of Initial Criticality: October 26, 1970

Date of First Electricity Generation: November 29, 1970

Date of Commercial Operation: March 1, 1971

Lifetime Cumulative Data: (January 1, 1971 - March 31, 1986)

    Hours, Generator on Line: 100,307.9 hours

    Gross Thermal Energy: 184.83×10^6 MWh

    Capacity Factor (MDC net):   67.4%

Table A.3 Summary of Spent Fuel Batches in Millstone 1 Storage Basin
(With Projections to 1987)

Spent Fuel Batch No.	Date of End of Irradiation	Number of Assemblies	Weight H.M. (MT)	Avg. Burnup (MWD/MT)	Decay[a] Days to 5/1/87 (days)	Cumulative Assemblies in Pool	Cumulative[b] Gross Weight of Spent Fuel in Pool (MT)
1	08/31/72	28	5.132	12686	5356	28	8.95
2	08/31/74	204	38.126	19695	4626	236	75.47
3	09/11/75	144	26.395	26581	4250	380	121.52
4	09/30/76	124	22.729	21290	3865	504	161.18
5	03/10/78	124	22.729	24090	3339	628	200.83
6	04/27/79	148	27.128	24354	2926	776	248.16
7	10/03/80	168	30.794	24998	2394	944	301.89
8	09/11/82	192	35.194	23670	1693	1136	363.29
9	04/12/84	172	31.528	26763	1114	1308	418.30
10[c]	10/01/85	178	32.627	28052	577	1486	475.22
11[c]	04/01/87	167	30.611	29963	30	1653[d]	528.63

[a]Decay days from end of irradiation to 5/1/87.
[b]Gross fuel tonnage in pool includes heavy metal plus cladding and hardware but not including fuel racks. Each assembly contains approximately 0.1833 metric tonnes of heavy metal, 0.0246 tonnes of oxygen (in UO_2) and 0.1119 tonnes of hardware, totaling 0.3198 metric tonnes gross.
[c]Projected data.
[d]The present authorized storage capacity is 2184 assemblies. After the 04/01/87 refueling, the accumulated assemblies plus the 580 assemblies in the core would exceed the authorized storage capacity should a full core discharge be required.

Table A.4 Comparison of Cumulative Gross Thermal Energy Production
with Calculated Fuel Burnup from Start of Operations in
1970 to April 1, 1987 (Millstone 1)

Total Cumulative Gross Thermal Energy (MWD x 10^{-3})	Spent Fuel Batch No.	Total Burnup in Batch (MWD x 10^{-3})
	1	65.10
	2	750.88
	3	701.61
	4	483.91
	5	547.54
	6	660.68
	7	769.78
	8	833.05
	9	843.78
	10	915.25
	11	917.21
	12*	612.74
	13*	329.55
Total 8440.25		8440.01

*Burnup in fuel remaining in the core.

Table A.5 Comparison of Radioactive Inventories in Reactor Core and Spent Fuel Basin (Millstone 1). The Assumed Refueling Scenario is Described in Section A.3.4

Isotope	Reactor Core	Spent Fuel Storage Basin[a]			
		5/1/87	7/1/87	10/1/87	4/1/88
		(Radioactivity, Curies)			
H 3	4.95E+4	1.38E+5	1.37E+5	1.35E+5	1.31E+5
C 14	1.02E+2	4.12E+2	4.12E+2	4.12E+2	4.12E+2
Co 58	8.81E+4	2.29E+4	1.26E+4	5.12E+3	8.54E+2
Co 60	1.64E+5	3.72E+5	3.15E+5	3.04E+5	2.85E+5
Kr 85	5.35E+5	1.41E+6	1.39E+6	1.37E+6	1.33E+6
Rb 86	6.22E+4	1.01E+4	1.05E+3	3.44E+1	3.84E-2
Sr 89	4.71E+7	8.39E+6	3.63E+6	1.03E+6	8.33E+4
Sr 90	4.25E+6	1.42E+7	1.42E+7	1.41E+7	1.39E+7
Y 90	4.37E+6	1.43E+7	1.42E+7	1.41E+7	1.39E+7
Y 91	6.06E+7	1.18E+7	5.75E+6	1.98E+6	2.21E+5
Zr 95	8.70E+7	1.94E+7	1.00E+7	3.70E+6	5.10E+5
Nb 95	8.91E+7	2.54E+7	1.70E+7	7.35E+6	1.11E+6
Mo 99	8.78E+7	1.49E+4	3.12E-3	neg.[b]	neg.[b]
Tc 99m	7.69E+7	1.43E+4	3.01E-3	neg.[b]	neg.[b]
Ru 103	7.23E+7	1.53E+7	5.21E+6	1.03E+6	4.07E+4
Ru 106	2.48E+7	1.72E+7	1.53E+7	1.29E+7	9.13E+6
Rh 106	2.63E+7	1.72E+7	1.53E+7	1.29E+7	9.13E+6
Sb 125	9.07E+5	1.19E+6	1.14E+6	1.07E+6	9.48E+5
Sb 127	4.97E+6	8.21E+3	1.39E-1	neg.[b]	neg.[b]
Te 125m	1.93E+5	2.84E+5	2.76E+5	2.61E+5	2.31E+5
Te 127	4.92E+6	2.21E+5	1.45E+5	8.06E+4	2.52E+4
Te 127m	6.61E+5	2.18E+5	1.48E+5	8.23E+4	2.57E+4
Te 129	1.49E+7	2.74E+5	7.79E+4	1.17E+4	2.68E+2
Te 129m	2.24E+6	4.21E+5	1.20E+5	1.79E+4	4.12E+2
Te 132	6.72E+7	3.74E+4	8.64E-2	neg.[b]	neg.[b]
I 129	1.75E+0	7.15E+0	7.15E+0	7.15E+0	7.15E+0
I 131	4.74E+7	1.22E+6	6.35E+3	2.28E+0	neg.[b]
I 132	6.83E+7	3.85E+4	8.90E-2	neg.[b]	neg.[b]
Xe 133	9.72E+7	7.29E+5	2.30E+2	1.21E-3	neg.[b]
Cs 134	6.10E+6	7.90E+6	7.47E+6	6.86E+6	5.80E+6
Cs 136	2.10E+6	2.05E+5	8.13E+3	6.26E+1	3.91E-3
Cs 137	5.84E+6	2.02E+7	2.01E+7	2.00E+7	1.97E+7
Ba 137m	5.53E+6	1.91E+7	1.90E+7	1.89E+7	1.87E+7
Ba 140	8.36E+7	5.19E+6	1.90E+5	1.30E+3	6.41E-2
La 140	8.54E+7	5.97E+6	2.19E+5	1.50E+3	7.37E-2
Ce 141	7.94E+7	1.32E+7	3.61E+6	5.07E+5	1.03E+4
Ce 144	6.05E+7	2.64E+7	2.27E+7	1.81E+7	1.16E+7
Pr 143	7.37E+7	5.44E+6	2.41E+5	2.19E+3	1.90E-1
Pr 144	6.08E+7	2.64E+7	2.27E+7	1.81E+7	1.16E+7
Nd 147	3.16E+7	1.54E+6	3.36E+4	1.05E+2	1.10E-3
Sm 151	2.44E+4	8.22E+4	8.21E+4	8.19E+4	8.16E+4
Eu 154	4.61E+5	1.34E+6	1.32E+6	1.29E+6	1.25E+6
Eu 156	5.61E+6	8.26E+5	5.10E+4	7.76E+2	1.80E-1
Np 239	9.98E+8	5.59E+4	2.88E+3	2.88E+3	2.88E+3
Pu 238	9.33E+4	4.51E+5	4.53E+5	4.54E+5	4.54E+5
Pu 239	2.49E+4	8.89E+4	8.89E+4	8.89E+4	8.89E+4
Pu 240	3.14E+4	1.30E+5	1.30E+5	1.30E+5	1.30E+5
Pu 241	7.19E+6	2.29E+7	2.27E+7	2.25E+7	2.19E+7
Am 241	8.86E+3	2.88E+5	2.94E+5	3.03E+5	3.21E+5
Cm 242	2.09E+6	1.45E+6	1.12E+6	7.60E+5	3.50E+5
Cm 244	6.72E+4	2.27E+5	2.25E+5	2.23E+5	2.19E+5

[a]Spent fuel pool inventory includes discharges from 11 refuelings covering the period from August 1972 through the projected refueling of April 1987.
[b]neg. = less than 10^{-3} Curies.

94

Table A.6 Comparison of Radioactive Inventories of Most Recently Discharged Fuel Batch (Batch 11) with Longer Aged Discharged Batches (Batches 1-10) (Millstone 1)

Isotope	Spent Fuel Batch 11[a]				Spent Fuel Batch 1-10[b]			
	5/1/87	7/1/87	10/1/87	4/1/88	5/1/87	7/1/87	10/1/87	4/1/88
	(Radioactivity, Curies)							
H 3	2.27E+4	2.24E+4	2.21E+4	2.15E+4	1.16E+5	1.15E+5	1.13E+5	1.10E+5
C 14	5.18E+1	5.18E+1	5.18E+1	5.18E+1	3.61E+2	3.61E+2	3.61E+2	3.61E+2
Co 58	2.28E+4	1.26E+4	5.10E+3	8.49E+2	1.18E+2	6.48E+1	2.63E+1	4.39E+0
Co 60	7.64E+4	7.48E+4	7.24E+4	6.77E+4	2.45E+5	2.40E+5	2.32E+5	2.17E+5
Kr 85	2.39E+5	2.36E+5	2.32E+5	2.25E+5	1.17E+6	1.16E+6	1.14E+6	1.10E+6
Rb 86	1.01E+4	1.05E+3	3.44E+1	3.84E-2	neg.[c]	neg.	neg.	neg.
Sr 89	8.39E+6	3.63E+6	1.03E+6	8.33E+4	5.39E+3	2.33E+3	6.60E+2	5.35E+1
Sr 90	1.93E+6	1.92E+6	1.91E+6	1.89E+6	1.23E+7	1.23E+7	1.22E+7	1.21E+7
Y 90	1.93E+6	1.92E+6	1.91E+6	1.89E+6	1.23E+7	1.23E+7	1.22E+7	1.21E+7
Y 91	1.18E+7	5.74E+6	1.93E+6	2.21E+5	2.11E+4	1.02E+4	3.44E+3	3.94E+2
Zr 95	1.94E+7	1.00E+7	3.69E+6	5.09E+5	5.90E+4	3.05E+4	1.12E+4	1.55E+3
Nb 95	2.53E+7	1.69E+7	7.33E+6	1.11E+6	1.31E+5	6.76E+4	2.49E+4	3.44E+3
Mo 99	1.49E+4	3.12E-3	neg.	neg.	neg.	neg.	neg.	neg.
Tc 99m	1.43E+4	3.01E-3	neg.	neg.	neg.	neg.	neg.	neg.
Ru 103	1.53E+7	5.21E+6	1.03E+6	4.07E+4	1.09E+3	3.73E+2	7.35E+1	2.91E+0
Ru 106	1.12E+7	9.98E+6	8.40E+6	5.95E+6	5.98E+6	5.30E+6	4.48E+6	3.18E+6
Rh 106	1.12E+7	9.98E+6	8.40E+6	5.95E+6	5.98E+6	5.30E+6	4.48E+6	3.18E+6
Sb 125	4.17E+5	4.00E+5	3.76E+5	3.31E+5	7.76E+5	7.44E+5	6.99E+5	6.16E+5
Sb 127	8.21E+3	1.39E-1	neg.	neg.	neg.	neg.	neg.	neg.
Te 125m	9.42E+4	9.39E+4	9.04E+4	8.07E+4	1.89E+5	1.82E+5	1.70E+5	1.50E+5
Te 127	2.14E+5	1.40E+5	7.79E+4	2.43E+4	7.15E+3	4.85E+3	2.70E+3	8.44E+2
Te 127m	2.10E+5	1.43E+5	7.95E+4	2.48E+4	7.30E+3	4.95E+3	2.76E+3	8.62E+2
Te 129	2.74E+5	7.79E+4	1.17E+4	2.68E+2	3.85E+0	1.09E+0	1.64E-1	3.76E-3
Te 129m	4.21E+5	1.20E+5	1.79E+4	4.12E+2	5.91E+0	1.68E+0	2.52E-1	5.77E-3
Te 132	3.74E+4	8.64E-2	neg.	neg.	neg.	neg.	neg.	neg.
I 129	8.84E-1	8.86E-1	8.86E-1	8.86E-1	6.26E+0	6.26E+0	6.26E+0	6.26E+0
I 131	1.22E+6	6.35E+3	2.28E+0	neg.	neg.	neg.	neg.	neg.
I 132	3.85E+4	8.90E-2	neg.	neg.	neg.	neg.	neg.	neg.
Xe 133	7.29E+5	2.30E+2	1.21E-3	neg.	neg.	neg.	neg.	neg.
Cs 134	3.53E+6	3.34E+6	3.07E+6	2.59E+6	4.37E+6	4.13E+6	3.80E+6	3.21E+6
Cs 136	2.05E+5	8.13E+3	6.26E+1	3.91E-3	neg.	neg.	neg.	neg.
Cs 137	2.83E+6	2.82E+6	2.80E+6	2.77E+6	1.73E+7	1.73E+7	1.72E+7	1.70E+7
Ba 137m	2.67E+6	2.66E+6	2.65E+6	2.62E+6	1.64E+7	1.63E+7	1.63E+7	1.61E+7
Ba 140	5.19E+6	1.90E+5	1.30E+3	6.41E-2	neg.	neg.	neg.	neg.
La 140	5.97E+6	2.19E+5	1.50E+3	7.37E-2	neg.	neg.	neg.	neg.
Ce 141	1.32E+7	3.61E+6	5.07E+5	1.03E+4	1.31E+2	3.57E+1	5.02E+0	1.01E-1
Ce 144	1.91E+7	1.65E+7	1.32E+7	8.43E+6	7.23E+6	6.23E+6	4.98E+6	3.19E+6
Pr 143	5.44E+6	2.41E+5	2.19E+3	1.90E-1	neg.	neg.	neg.	neg.
Pr 144	1.91E+7	1.65E+7	1.32E+7	8.43E+6	7.23E+6	6.23E+6	4.98E+6	3.19E+6
Nd 147	1.54E+6	3.36E+4	1.05E+2	1.10E-3	neg.	neg.	neg.	neg.
Sm 151	9.31E+3	9.30E+3	9.28E+3	9.25E+3	7.29E+4	7.28E+4	7.26E+4	7.24E+4
Eu 154	2.89E+5	2.85E+5	2.79E+5	2.68E+5	1.05E+6	1.04E+6	1.02E+6	9.75E+5
Eu 156	8.38E+5	5.18E+4	7.76E+2	1.83E-1	neg.	neg.	neg.	neg.
Np 239	5.36E+4	5.26E+2	5.26E+2	5.26E+2	2.35E+3	2.35E+3	2.35E+3	2.35E+3
Pu 238	6.73E+4	6.87E+4	7.02E+4	7.18E+4	3.84E+5	3.84E+5	3.83E+5	3.82E+5
Pu 239	9.28E+3	9.28E+3	9.28E+3	9.28E+3	7.96E+4	7.96E+4	7.96E+4	7.96E+4
Pu 240	1.55E+4	1.55E+4	1.55E+4	1.55E+4	1.15E+5	1.15E+5	1.15E+5	1.15E+5
Pu 241	3.73E+6	3.70E+6	3.65E+6	3.56E+6	1.92E+7	1.91E+7	1.88E+7	1.84E+7
Am 241	6.01E+3	7.00E+3	8.48E+3	1.14E+4	2.82E+5	2.87E+5	2.95E+5	3.09E+5
Cm 242	1.31E+6	1.01E+6	6.86E+5	3.16E+5	1.39E+5	1.08E+5	7.33E+4	3.47E+4
Cm 244	5.88E+4	5.84E+4	5.79E+4	5.68E+4	1.68E+5	1.67E+5	1.65E+5	1.62E+5

[a]Fuel batch 11 is projected discharge during April 1987.
[b]Fuel batches 1-10 were discharged between August 1972 and October 1985.
[c]neg. = less than 10^{-3} Curies.

95

Table A.7 Decay Heat Released from Spent Fuel Inventory for
Various Discharged Fuel Batches (Millstone 1)

	Date, End of Irradiation[a]	Batch Size[a] (Metric Tonnes)	Decay Heat Released by Batch		
			May 1, 1987	July 1, 1987	April 1, 1988
			(Kilowatts, Thermal)		
1	08/31/72	5.13	1.8	1.8	1.8
2	08/31/74	38.13	22.0	21.9	21.5
3	09/11/75	26.40	21.8	21.7	21.2
4	09/30/76	22.73	15.2	15.1	14.8
5	03/10/78	22.73	18.4	18.3	17.7
6	04/27/79	27.13	23.5	23.3	22.4
7	10/03/80	30.79	30.3	29.9	28.2
8	09/11/82	35.19	41.5	40.3	35.9
9	04/12/84	31.53	67.4	63.6	50.9
10	10/01/85[b]	32.63	146.0	132.7	91.8
11	04/01/87[b]	30.61	909.0	537.7	210.5
Total[c] 1-10		272.38	387.9	368.5	306.3
Total[c] 1-11		302.99	1297.0	906.3	516.8

[a]See Table A.3.
[b]Projected dates.
[c]Totals may not equal sum of the entries due to rounding of decimals.

Table A.8 Radionuclide Contributions to Decay Heat for Various Spent Fuel Batches. The Percentage Contributions Depend on the Total Burnup of Each Batch, as well as Decay Time After End of Irradiation (Millstone 1)

Isotope	Spent Fuel Batch Number										
	1	2	3	4	5	6	7	8	9	10	11
	(PERCENT OF TOTAL DECAY HEAT)										
Sr 90	7.48	6.79	6.14	6.61	6.32	6.18	5.85	5.23	3.78	2.34	1.39
Y 90	35.73	32.44	29.33	31.82	30.21	29.52	27.92	24.97	18.06	11.17	4.96
Zr 95	---[a]	---	---	---	---	---	---	---	---	0.01	1.13
Nb 95	---	---	---	---	---	---	---	---	---	0.02	2.33
Rh 106	---	---	---	---	---	0.81	1.89	5.75	13.49	22.53	27.10
Cs 134	0.43	0.98	1.76	2.24	3.74	5.15	7.65	11.63	16.26	16.66	12.53
Cs 137	9.02	8.77	8.43	8.70	8.45	8.28	7.87	6.95	5.16	3.22	1.45
Ba 137m	30.29	29.44	28.30	29.22	28.29	27.80	26.43	23.34	17.34	10.82	4.88
Ce 144	---	---	---	---	---	---	0.06	0.26	0.79	1.73	2.66
Pr 144	---	---	---	---	---	---	0.64	2.93	8.80	19.20	29.42
Eu 154	1.22	2.15	3.03	2.63	3.15	3.32	3.52	3.30	3.03	2.15	1.12
Pu 238	2.14	4.85	7.33	4.66	5.38	5.31	5.33	4.49	3.72	2.37	1.13
Pu 239	2.16	1.54	1.14	1.36	1.16	1.10	0.99	0.88	0.57	0.33	0.14
Pu 240	1.84	1.90	1.79	1.78	1.68	1.61	1.49	1.27	0.90	0.53	0.23
Pu 241	0.19	0.22	0.23	0.24	0.24	0.24	0.24	0.22	0.17	0.11	0.05
Am 241	7.57	7.96	7.34	6.70	5.84	5.12	4.22	2.92	1.61	0.70	0.18
Cm 242	0.01	0.04	0.05	0.02	0.03	0.03	0.03	0.05	0.21	1.21	5.52
Totals[b]	98.08	97.08	94.87	95.98	94.59	94.47	94.13	94.19	93.89	95.10	96.22

[a]Dashes indicate less than 0.01%.
[b]Total percentage of isotopes listed. The balance of the decay heat is distributed among many other less important contributors.

Table A.9   Reactor and Fuel Cycle Parameters for Ginna
(Sources: Refs. 1-4)

Assemblies in core: 121

Licensed thermal power: 1520 MW$_{th}$ (gross)[a]

Thermal power corresponding to maximum dependable capacity:
  1499 MW$_{th}$ (gross)

Nominal initial metric tonnes of heave metal (IMTHM) per
  assembly: 0.375 MT

Average refueling cycle interval (since initial commercial
  operation): 12.6 months

Average number of assemblies per discharge: 1975-1980:   37
                                              1981-1987:   24

Average IMTHM per discharge: 1975-1908:   15.3 MT
                               1981-1987:   9.0

Average number of fuel cycles per assembly: 1975-1980:   3.27
                                              1981-1987:   5.04

Average period of irradiation (including down time):   1976-1980:   3.3 years
                                                       1981-1987:   5.0 years

Authorized storage pool capacity: 1016

---

[a]On March 1, 1972 the Atomic Energy Commission authorized an increase in
  gross thermal power from 1300 to 1520 MW.

Table A.10 Summary of Operational Milestone for Ginna
(Source: Ref. 4)

Date of Initial Criticality: November 8, 1969

Date of First Electricity Generation: December 2, 1969

Date of Commercial Operation: July 1, 1970

Lifetime Cumulative Data: (January 1, 1968-March 31, 1986)

  Hours, Generator on Line: 107,134.3 hours

  Gross Thermal Energy: 149.26×10^6 MWh

  Capacity Factor (MDC net): 70.3%

Table A.11 Summary of Spent Fuel Batches in Ginna Storage Basin
(With Projections to 1987)

Spent Fuel Batch No.	Date of End of Irradiation	Number of Assemblies	Weight H.M. (MT)	Avg. Burnup (MWD/MT)	Decay[a] Days to 5/1/87 (days)	Cumulative Assemblies in Pool	Cumulative[b] Gross Weight of Spent Fuel in Pool (MT)
1	02/27/71	(37)[c]	14.778	6933	--	0	0
2	04/13/72	(47)[c]	18.772	16695	5832	28	18.4
3	12/31/73	8	3.195	30039	4869	36	23.7
4	03/08/75	29	11.583	38043	4437	65	42.8
5	01/28/76	37	14.778	36958	4111	102	67.1
6	04/14/77	41	16.375	36022	3669	143	94.1
7	03/23/78	41	16.375	27921	3326	184	121.1
8	02/09/79	40	15.976	25451	3003	224	147.4
9	03/28/80	36	14.378	26088	2590	260	171.1
10	04/17/81	28	11.183	27884	2205	288	189.5
11	01/25/82	24	9.586	31054	1891	312	205.3
12	03/25/83	20	7.988	33772	1467	332	218.4
13	03/01/84	23	9.186	37532	1156	355	223.6
14	02/28/85	25	9.985	40533	792	380	250.0
15	03/30/86	24	9.586	42360	397	404	265.8
16[d]	04/01/87	24	9.586	45673	30	428[e]	281.6

[a]Decay days from end of irradiation to 5/1/87.

[b]Gross weight of fuel stored in pool includes heavy metal plus cladding and hardware but not the fuel racks. Each assembly contains approximately 0.4614 tonnes of heavy metal, 0.0620 tonnes of oxygen, 0.1345 tonnes of hardware, totaling 0.6579 tonnes gross.

[c]At the time of the ORIGEN2 calculations some 56 assemblies could not be accounted for using available data.

[d]Projected data.

[e]Authorized capacity is 1016 assemblies.

Table A.12 Comparison of Radioactive Inventories in Reactor Core and Spent Fuel Basin (Ginna)

Isotope	Reactor Core	Spent Fuel Storage Basin[a]		
		5/1/87	7/1/87	4/1/88
		(Radioactivity, Curies)		
H 3	3.32E+4	9.29E+4	9.20E+4	8.82E+4
C 14	6.42E+1	2.64E+2	2.64E+2	2.64E+2
Co 58	3.57E+5	5.93E+4	3.26E+4	2.21E+3
Co 60	3.20E+5	5.97E+5	5.84E+5	5.29E+5
Kr 85	3.73E+5	9.84E+5	9.74E+5	9.27E+5
Rb 86	6.53E+5	7.22E+3	7.48E+2	2.74E-2
Sr 89	3.55E+7	3.53E+6	1.53E+6	3.50E+4
Sr 90	2.95E+6	1.02E+7	1.01E+7	9.95E+6
Y 90	3.15E+6	1.02E+7	1.01E+7	9.95E+6
Y 91	4.57E+7	5.11E+6	2.48E+6	9.54E+4
Zr 95	6.41E+7	8.64E+6	4.46E+6	2.27E+5
Nb 95	6.34E+7	1.12E+7	7.51E+6	4.93E+5
Mo 99	6.83E+7	7.03E+3	1.48E-3	neg.[b]
Tc 99m	5.89E+7	6.77E+3	1.42E-3	neg.[b]
Ru 103	5.85E+7	7.86E+6	2.88E+6	2.09E+4
Ru 106	1.95E+7	1.09E+7	9.71E+6	5.78E+6
Rh 106	2.15E+7	1.09E+7	9.71E+6	5.78E+6
Sb 125	6.04E+5	7.11E+5	6.82E+5	5.65E+5
Sb 127	4.12E+6	4.33E+3	7.35E-2	neg.[b]
Te 125m	1.27E+5	1.70E+5	1.65E+5	1.37E+5
Te 127	4.05E+6	1.19E+5	7.79E+4	1.36E+4
Te 127m	5.19E+5	1.17E+5	7.95E+4	1.38E+4
Te 129	1.21E+7	1.38E+5	3.93E+4	1.35E+2
Te 129m	1.80E+6	2.12E+5	6.03E+4	2.07E+2
Te 132	5.33E+7	1.83E+4	4.23E-2	neg.[b]
I 129	1.27E+0	5.32E+0	5.32E+0	5.32E+0
I 131	3.76E+7	6.00E+5	3.12E+3	neg.[b]
I 132	5.42E+7	1.89E+4	4.36E-2	neg.[b]
Xe 133	7.64E+7	3.52E+5	1.11E+2	neg.[b]
Cs 134	5.82E+6	6.35E+6	6.00E+6	4.66E+6
Cs 136	1.87E+6	1.26E+5	4.99E+3	2.40E-3
Cs 137	4.21E+6	1.48E+7	1.47E+7	1.44E+7
Ba 137m	4.00E+6	1.40E+7	1.39E+7	1.37E+7
Ba 140	6.55E+7	2.47E+6	9.07E+4	3.05E-2
La 140	6.74E+7	2.85E+6	1.04E+5	3.51E-2
Ce 141	6.28E+7	6.34E+6	1.72E+6	4.91E+3
Ce 144	4.24E+7	1.38E+7	1.19E+7	6.09E+6
Pr 143	5.71E+7	2.54E+6	1.12E+5	8.86E-2
Pr 144	4.27E+7	1.38E+7	1.19E+7	6.09E+6
Nd 147	2.48E+7	7.42E+5	1.62E+4	neg.[b]
Sm 151	1.42E+4	5.14E+4	5.13E+4	5.10E+4
Eu 154	4.09E+5	1.09E+6	1.07E+6	1.01E+6
Eu 156	7.22E+6	7.58E+5	4.68E+4	1.66E-1
Np 239	7.81E+8	3.02E+4	3.26E+3	3.26E+3
Pu 238	1.01E+5	4.46E+5	4.46E+5	4.46E+5
Pu 239	1.35E+4	5.25E+4	5.25E+4	5.25E+4
Pu 240	2.02E+4	8.60E+4	8.60E+4	8.61E+4
Pu 241	4.85E+6	1.52E+7	1.51E+7	1.46E+7
Am 241	4.99E+3	2.10E+5	2.14E+5	2.32E+5
Cm 242	1.91E+6	9.33E+5	7.20E+5	2.25E+5
Cm 244	1.25E+5	3.59E+5	3.56E+5	3.46E+5

[a]Spent fuel pool Inventory Includes discharges from 15 refuelings covering the period from April 1983 through the projected refueling of April 1987.
[b]neg. = less than 10^{-3} Curies.

101

Table A.13   Comparison of Radioactive Inventories of Most Recently Discharged Fuel Batch (Batch 16) with Longer Aged Discharged Batches (Batches 2-15) (Ginna)

Isotope	Spent Fuel Batch 16[a]				Spent Fuel Batch 2-15[b]			
	5/1/87	7/1/87	10/1/87	4/1/88	5/1/87	7/1/87	10/1/87	4/1/88
	(Radioactivity, Curies)							
H 3	9.89E+3	9.80E+3	9.66E+3	9.39E+3	8.29E+4	8.22E+4	8.10E+4	7.88E+4
C 14	2.20E+1	2.20E+1	2.20E+1	2.20E+1	2.42E+2	2.42E+2	2.42E+2	2.42E+2
Co 58	5.77E+4	3.18E+4	1.29E+4	2.15E+3	1.60E+3	8.78E+2	3.57E+2	5.94E+1
Co 60	9.92E+4	9.70E+4	9.39E+4	8.79E+4	4.98E+5	4.87E+5	4.71E+5	4.41E+5
Kr 85	1.07E+5	1.05E+5	1.04E+5	1.00E+5	8.78E+5	8.68E+5	8.54E+5	8.27E+5
Rb 86	7.22E+3	7.48E+2	2.45E+1	2.73E-2	neg.	neg.	neg.	neg.
Sr 89	3.50E+6	1.52E+6	4.29E+5	3.48E+6	2.39E+4	1.04E+4	2.93E+3	2.38E+2
Sr 90	8.56E+5	8.53E+5	8.48E+5	8.38E+5	9.32E+6	9.28E+6	9.23E+6	9.12E+6
Y 90	8.57E+5	8.53E+5	8.48E+5	8.38E+5	9.32E+6	9.28E+6	9.23E+6	9.12E+6
Y 91	5.04E+6	2.45E+6	8.23E+5	9.41E+4	6.86E+4	3.33E+4	1.12E+4	1.28E+3
Zr 95	8.47E+6	4.37E+6	1.62E+6	2.23E+5	1.64E+5	8.48E+4	3.13E+4	5.60E+4
Nb 95	1.09E+7	7.33E+6	3.19E+6	4.83E+5	3.68E+5	1.89E+5	6.96E+4	9.57E+3
Mo 99	7.03E+3	1.48E-3	neg.[c]	neg.	neg.	neg.	neg.	neg.
Tc 99m	6.77E+3	1.42E-3	neg.	neg.	neg.	neg.	neg.	neg.
Ru 103	7.86E+6	2.68E+6	5.28E+5	2.09E+4	1.18E+4	4.02E+3	7.93E+2	3.14E+1
Ru 106	5.82E+6	5.19E+6	4.37E+6	3.09E+6	5.06E+6	4.51E+6	3.80E+6	2.69E+6
Rh 106	5.82E+6	5.19E+6	4.37E+5	3.09E+6	5.06E+6	4.51E+6	3.80E+6	2.69E+6
Sb 125	1.84E+5	1.76E+5	1.65E+5	1.46E+5	5.28E+5	5.06E+5	4.75E+5	4.19E+5
Sb 127	4.33E+3	7.35E-2	neg.	neg.	neg.	neg.	neg.	neg.
Te 125m	4.13E+4	4.12E+4	3.97E+4	3.55E+4	1.78E+5	1.24E+5	1.16E+5	1.02E+4
Te 127	1.08E+5	7.05E+4	3.93E+4	1.23E+4	1.09E+4	7.42E+3	4.14E+3	1.29E+4
Te 127m	1.06E+5	7.19E+4	4.01E+4	1.25E+4	1.12E+4	7.58E+3	4.22E+3	1.32E+3
Te 129	1.38E+5	3.93E+4	5.88E+3	1.35E+2	6.98E+1	1.98E+1	2.97E+0	6.82E-2
Te 129m	2.12E+5	6.03E+4	9.04E+3	2.07E+2	1.07E+2	3.05E+1	4.57E+0	1.05E-1
Te 132	1.83E+4	4.23E-2	neg.	neg.	neg.	neg.	neg.	neg.
I 129	4.22E-1	4.23E-1	4.23E-1	4.23E-1	4.89E+0	4.89E+0	4.89E+0	4.89E+0
I 131	6.00E+5	3.12E+3	1.12E+0	neg.	neg.	neg.	neg.	neg.
I 132	1.89E+4	4.36E-2	neg.	neg.	neg.	neg.	neg.	neg.
Xe 133	3.52E+5	1.11E+2	neg.	neg.	neg.	neg.	neg.	neg.
Cs 134	2.26E+6	2.13E+6	1.96E+6	1.66E+6	4.09E+6	3.87E+6	3.55E+6	3.01E+6
Cs 136	1.26E+5	4.99E+3	3.84E+1	2.40E-3	neg.	neg.	neg.	neg.
Cs 137	1.34E+6	1.34E+6	1.33E+6	1.31E+6	1.34E+7	1.34E+7	1.33E+7	1.31E+7
Ba 137m	1.27E+6	1.26E+6	1.26E+6	1.24E+6	1.27E+7	1.26E+7	1.26E+7	1.24E+7
Ba 140	2.47E+6	9.07E+4	6.19E+2	3.05E-2	neg.	neg.	neg.	neg.
La 140	2.85E+6	1.04E+5	7.13E+2	3.51E-2	neg.	neg.	neg.	neg.
Ce 141	6.34E+6	1.73E+6	2.43E+5	4.91E+3	2.53E+3	6.89E+2	9.69E+1	1.96E+0
Ce 144	8.25E+6	7.11E+6	5.68E+6	3.64E+6	5.58E+6	4.81E+6	3.84E+6	2.46E+6
Pr 143	2.54E+6	1.12E+5	1.02E+3	8.86E-2	neg.	neg.	neg.	neg.
Pr 144	8.25E+6	7.11E+6	5.68E+6	3.64E+6	5.58E+6	4.81E+6	3.84E+6	2.46E+6
Nd 147	7.42E+5	1.62E+4	5.08E+1	neg.	neg.	neg.	neg.	neg.
Sm 151	3.47E+3	3.47E+3	3.46E+3	3.45E+3	4.79E+4	4.79E+4	4.78E+4	4.76E+4
Eu 154	1.67E+5	1.65E+5	1.61E+5	1.55E+5	9.19E+5	9.06E+5	8.88E+5	8.53E+5
Eu 156	7.58E+5	4.68E+4	7.02E+2	1.66E-1	neg.	neg.	neg.	neg.
Np 239	2.74E+4	4.59E+2	4.59E+2	4.59E+2	2.80E+3	2.80E+3	2.80E+3	2.80E+3
Pu 238	4.87E+4	4.95E+4	5.04E+4	5.13E+4	3.97E+5	3.97E+5	3.96E+5	3.95E+5
Pu 239	3.05E+3	3.05E+3	3.05E+3	3.05E+3	4.95E+4	4.95E+4	4.95E+4	4.95E+4
Pu 240	6.01E+3	6.01E+3	6.01E+3	6.02E+3	8.00E+4	8.00E+4	8.00E+4	8.00E+4
Pu 241	1.58E+6	1.57E+6	1.55E+6	1.51E+6	1.37E+7	1.35E+7	1.34E+7	1.31E+7
Am 241	2.05E+3	2.47E+3	3.10E+3	4.33E+3	2.08E+5	2.12E+5	2.17E+5	2.28E+5
Cm 242	7.57E+5	5.85E+5	3.96E+5	1.82E+5	1.75E+5	1.36E+5	9.21E+4	4.30E+4
Cm 244	8.06E+4	8.00E+4	7.93E+4	7.78E+4	2.78E+5	2.76E+5	2.74E+5	2.68E+5

[a]Fuel batch 16 is projected discharge during April 1987.
[b]Fuel batches 2-15 were discharged between April 1972 and April 1986.
[c]neg. = less than 10^{-3} Curies.

Table A.14 Decay Heat Released from Spent Fuel Inventory for
Various Discharged Fuel Batches (Ginna)

Date, End of Irradiation[a]		Batch Size[a] (Metric Tonnes)	Decay Heat Released by Batch		
			May 1, 1987	July 1, 1987	April 1, 1988
			(Kilowatts, Thermal)		
2	04/13/72	18.772	8.5	8.5	8.4
3	12/31/73	3.195	2.9	2.9	2.8
4	03/08/75	11.583	14.3	14.2	13.9
5	01/28/76	14.778	18.1	18.0	17.6
6	04/14/77	16.375	20.5	20.4	19.8
7	03/23/78	16.375	15.8	15.7	15.1
8	02/09/79	15.976	14.7	14.5	14.0
9	03/28/80	14.378	14.7	14.5	13.7
10	04/17/81	11.183	13.7	13.4	12.4
11	01/25/82	9.586	15.0	14.6	13.2
12	03/25/83	7.988	17.2	16.5	14.2
13	03/01/84	9.186	28.6	27.1	22.0
14	02/28/85	9.985	50.9	47.2	35.3
15	03/30/86	9.586	96.1	85.8	56.5
16	04/01/87[b]	9.586	437.2	260.4	107.7
Total[c] 2-15			331.0	313.3	259.0
Total[c] 2-16			768.3	573.7	366.8

[a]See Table A.11.
[b]Projected dates.
[c]Totals may not equal sum of entries due to rounding of decimals.

Table A.15 Radionuclide Contributions to Decay Heat for Various Spent Fuel Batches. The Percentage Contributions Depend on the Total Burnup of Each Batch, as well as Decay Time After End of Irradiation (Ginna)

Isotope	Spent Fuel Batch Number														
	2	3	4	5	6	7	8	9	10	11	12	13	14	15	16
	(PERCENT OF TOTAL DECAY HEAT)														
Sr 90	7.32	6.26	5.56	5.61	5.61	6.23	6.32	6.07	5.61	5.01	4.23	3.43	2.51	1.60	0.90
Y 90	34.95	29.89	26.57	26.82	26.79	29.77	30.20	29.01	26.79	23.95	20.19	16.37	12.01	7.64	4.31
Zr 95	---[a]	---	---	---	---	---	---	---	---	---	---	---	---	0.04	1.01
Nb 95	---	---	---	---	---	---	---	---	---	---	---	---	---	0.08	2.08
Rh 106	---	0.02	0.05	0.08	0.19	0.41	0.76	1.46	2.86	4.65	8.19	12.24	18.16	24.96	27.54
Cs 134	0.33	1.12	1.77	2.26	3.29	4.01	4.95	6.72	9.38	12.21	15.67	18.46	20.18	19.07	15.65
Cs 137	8.89	8.42	7.93	7.94	7.89	8.23	8.19	7.89	7.38	6.75	5.81	4.83	3.63	2.33	1.35
Ba 137m	29.85	28.26	26.64	26.67	26.48	27.65	27.50	26.51	24.79	22.68	19.51	16.22	12.18	7.84	4.52
Ce 144	---	---	---	---	---	0.01	0.02	0.05	0.11	0.19	0.39	0.63	1.07	1.78	2.24
Pr 144	---	---	---	0.01	0.03	0.09	0.23	0.52	1.21	2.13	4.31	6.99	11.84	19.75	24.80
Eu 154	1.33	2.73	3.37	3.48	3.66	3.21	3.05	3.20	3.41	3.64	3.60	3.41	2.88	2.02	1.29
Pu 238	2.90	6.98	9.46	9.12	8.67	5.77	4.76	4.71	4.83	5.18	5.06	4.82	3.95	2.58	1.58
Pu 239	1.84	1.07	0.81	0.82	0.80	1.01	1.05	0.97	0.84	0.69	0.54	0.41	0.28	0.17	0.09
Pu 240	1.80	1.69	1.49	1.49	1.45	1.53	1.47	1.38	1.27	1.13	0.94	0.74	0.53	0.32	0.17
Pu 241	0.17	0.21	0.20	0.20	0.21	0.22	0.22	0.22	0.21	0.20	0.18	0.15	0.11	0.08	0.04
Am 241	7.88	7.68	6.60	6.20	5.56	5.19	4.67	4.07	3.31	2.69	1.97	1.39	0.82	0.37	0.13
Cm 242	0.01	0.03	0.03	0.03	0.03	0.02	0.02	0.02	0.02	0.03	0.07	0.21	0.70	2.20	6.22
Cm244	0.25	2.74	6.45	5.94	5.63	2.18	1.52	1.64	2.03	2.87	3.47	4.25	4.35	3.32	2.52
Totals[b]	97.52	97.10	96.93	96.67	96.29	95.53	94.93	94.44	94.05	94.00	94.13	94.55	95.20	96.15	96.44

[a]Dashes indicate less than 0.01%.
[b]Total percentage of isotopes listed. The balance of the decay heat is distributed among many other less important contributors.

104

Figure A.1 Millstone 1: Operating history 1976-1984 (Source: Ref. 4).

APPENDIX B

IMPACT OF REVISED REACTION RATE EQUATION ON THE LIKELIHOOD OF
ZIRCONIUM FIRES IN A DRAINED SPENT FUEL POOL

The SNL investigation[1] of the potential for cladding oxidation during loss of fuel pool inventory accidents has been controversial due to many unique features of the postulated "beyond design basis accident." The purpose of the BNL investigation has been two-fold:

1. Provide an independent assessment of several important areas of the phenomenological treatment of the SFUEL code.[1]

2. Provide an estimate of the likelihood and consequences of the postulated accidents so that the risk can be compared to the risk of severe reactor accidents evaluated in typical PRAs.

The purpose of this appendix is to re-evaluate the oxidation rate equation used in the SFUEL code and to perform a sensitivity study to demonstrate the influence of the reaction rate on the results of the SFUEL analysis.

The oxidation rate equation is also a key factor which affects the possible propagation of Zircaloy fires to low power (i.e., older) spent fuel bundles. Based on the information available to date it appears impossible to justify any major changes to the Sandia equation; in particular, the curve from the work of White at temperatures above 1150°C appears to be all we have. However, this was obtained on unalloyed Zr, not Zircaloy, and the higher rates for Zircaloy-4 over those for unalloyed Zr observed by Pawel and Campbell in steam may also exist in air. For temperatures from 800-1150°C, the new German data fit in well with the previous data. However, if the exposure is for periods greater than 30 minutes, this curve may not be conservative, as shown in the new German data plotted in Figure B.3.

After an extensive review of the zirconium/Zircaloy reaction rate data and recent unpublished data, BNL has concluded that the reaction rate in Equation (1) is representative of the existing data.

$$w^2/t = 3.09 \times 10^8 \exp(-56600/RT) \tag{1}$$

where: w is the oxygen consumption (mg/cm^2)
        t is time (sec)
        T is the clad temperature (K)
        R is the gas constant (1.987 cal/K)

This equation is equivalent to that suggested by Benjamin et al.[1] except that it provides a smooth transition to the self-sustaining oxidation regime (above 800°C) and does not put undue emphasis on the threshold effect of a shift in oxidation rate due to metallic phase change.

The reaction rate has been varied by a factor of four based on the data scatter in the temperature range of 800 to 900°C (where self-sustaining oxidation is initiated). Only a slight change (±50°C) in the initiation temperature occurs for this broad range of uncertainty in the oxidation rate. This translates into an uncertainty of ±25% in the critical decay power. This

insensitivity to the oxidation rate equation basically confirms the SNL analysis[1] for zirconium fire initiation in a dry spent fuel pool.

As Benjamin et al.[1] pointed out, the most sensitive parameters for clad fire initiation are the decay heat level and the fuel rack geometry (related to natural circulation flow resistance). Thus, for BWRs with low power density and relatively open fuel storage racks, the critical cooling time (to ensure that air cooling will keep the fuel rods below 800°C) is about 1 to 5 months. Whereas PWRs with higher power density and tighter storage racks require 2 months to 2 years (the longer time is required for the new high density storage racks).

Note that even temperatures as low as 650°C can be expected to cause clad failure and release of some fission products if the temperatures are sustained over a long period (several hours). However, below 800°C the energy from oxidation is insufficient to significantly increase the fuel rod temperature.

The results indicate that the SNL code (SFUEL) and the clad oxidation rate equation used therein accurately represents the potential for self-sustaining oxidation in a drained fuel pool. The largest uncertainty appears to be due to uncertainties in natural convection flows in the transition flow regime. Changes in the storage rack configuration result in large changes in the calculated flow rate and correspondingly large changes in the "critical power level" (above which self-sustaining oxidation is predicted to occur).

Based on the review of the cladding oxidation rate model and the sensitivity study, it is concluded that the conditional probability of self-sustaining clad oxidation and resultant fission product release, given a loss of pool integrity event, is about 10% to 40% for BWRs and 16% to 100% for PWRs, depending on the storage rack configuration.

In terms of power level, our sensitivity studies indicate that the critical power level (above which self-sustaining oxidation will occur) varies from about 50 kW/MTU (for cylindrical racks with large openings) to 6 kW/MTU for the new high density PWR fuel storage racks.

In order to ensure that self-sustaining oxidation in the current high density racks will not occur, it is recommended that spent fuel not be stored in high density racks until it has been stored for 2 or more years in the old style cylindrical racks with adequate coolant openings (3 or more inch diameter holes).

It is also recommended that a test program be initiated to confirm the capability of natural air convection cooling capability for high density storage racks. Such tests could be performed with old low power spent fuel (2 to 4 kw/MTU) and minimal instrumentation (such as thermocouples placed near the top of the fuel bundle).

Two Sandia reports[1,2] deal with the question of rapid zirconium oxidation in a spent fuel pool following loss of water. Both the computer modeling and the experimental simulation, as described in these reports, suggested that in certain fuel racking configurations (a) a self-sustaining zirconium-air oxidation reaction can be initiated, and (b) this self-sustaining reaction can propagate from one region of a pool to another. There are large uncertainties

associated with the phenomenology of Zircaloy oxidation and its propagation in spent fuel assemblies. This review addresses some of these uncertainties and their effects on the initiation and propagation of a self-sustaining Zircaloy-air oxidation reaction.

1. The propagation rates of rapid Zircaloy clad oxidation in air from the hottest section of the pool (after a loss of water incident) to adjacent sections were estimated (in Ref. 2) under the conditions that the spent fuel in the hottest section of the pool was generating 30 kw/MTU in a room maintained at constant temperature. As pointed out by Han,[3] this estimate should be re-calculated under inadequate room ventilation conditions, to simulate properly the conditions at many licensed facilities. Similarly, additional calculations should be performed in which the hot spent fuel decay power is varied from 20 to 90 kw/MTU for both the adequate and inadequate room ventilation conditions. These studies would determine how sensitive the oxidation propagation is to the decay power of the spent fuel stored adjacent to hot fuel, assuming the input oxidation rate data are known with sufficient accuracy.

2. The above assumes the Zircaloy-air reaction rate equation used in the Sandia work is sufficiently accurate. There are a number of uncertainties associated with this equation. We discuss each of these uncertainties in turn.

    A. Experimental Data: A literature search[4-147] has revealed that there is a great deal of data for zirconium oxidation; most of it, however, is concerned with oxidation in steam or oxygen. The data for zirconium (Zircaloy)-air oxidation presented in Refs. 1 and 2 appear to be the best available. These are shown in Figure B.1. The authors (of the SNL reports) fit the data with three separate Arrhenius plots over the temperature range 500-1500°C; one break occurs at the α-β transformation temperature for zirconium, the other at the temperature at which the oxide undergoes a monoclinic-tetragonal transformation. (N.B. two of the sets of data are for zirconium, the other for Zircaloy-4). These assumptions are reasonable. It should be noted, however, that there is no a priori reason to expect that the data would be fit by an Arrhenius expression, particularly above the α-β transformation temperature where a number of different processes are occurring simultaneously (discussed further below); therefore the use of the Arrhenius expression should be viewed in this case only as a computational tool. It is difficult to assess the validity of the data employed. What are really required are new experiments to determine the oxidation rate of Zircaloy in air over the temperature range of interest, for both isothermal and non-isothermal conditions.

    B. Kinetics: The questions was raised[2] as to whether the assumption of parabolic kinetics was valid. Data were presented (from Refs. 86 and 126) which show examples of linear as well as cubic kinetics. However, they all apply at temperatures below the α-β transformation temperature. Since almost all rapid oxidation occurs above the α-β transformation temperature, where the oxidation rate is controlled by

one or more diffusion processes, the assumption of parabolic kinetics appears to be reasonable.

C. Zirconium vs. Zircaloy: It is assumed in the Sandia work that the oxidation rates of zirconium and Zircaloy are essentially the same. Recent work by Pawel and Campbell[136] has shown that this is not the case. Oxidation in steam of both pure zirconium and Zircaloy-4 was studied in the temperature range of rapid oxidation (1000°C-1500°C). It was found that at all temperatures the oxidation rate of Zircaloy-4 was higher than that of zirconium; the ratio of the two rates is approximately 3 at 1000°C and decreases with increasing temperature to a value of approximately 1.5 at 1500°C (cf. Figure B.2). The higher oxidation rate of Zircaloy-4 is attributed to increased oxygen diffusivity in the oxide phase; a lower activation energy was observed, implying that some mechanistic differences exist. Analogous results are expected to apply for oxidation in air.

D. Oxidation Model: The oxidation in steam of both zirconium and Zircaloy-4 (in the temperature range 1000-1500°C) is a multi-phase layer process.[136] Not only is an oxide layer formed, but also (beneath it) a layer of oxygen-stabilized α-phase (zirconium or Zircaloy). The multi-phase model is only significant above the α-β transformation temperature (approximately 900°C), but this is exactly where rapid oxidation occurs. The parabolic rate constants for oxide layer growth, α-layer growth, and oxygen consumption were determined in Ref. 136 from experimental data and computer modeling. The rate of oxygen consumption is significantly higher at all temperatures than the rate of oxide formation for both zirconium and Zircaloy-4. For zirconium the ration of oxygen consumption rate to oxidation rate is approximately 4 at 1000°C and increases with increasing temperature to a value of approximately 5.4 at 1500°C; for Zircaloy-4 the corresponding values are approximately 3.0 and 4.5 at 1000°C and 1500°C, respectively (cf. Figure B.2). Although these results were obtained for oxidation in steam, analogous results are again expected for oxidation in air.

E. Effect of Nitrogen: Before discussing the reaction of zirconium with air, let us consider the reaction with nitrogen alone.[148-151] The rate of reaction of nitrogen with zirconium is much less than the corresponding reaction rate with oxygen; weight gain data[151] after one hour (800°C<T<1200°C) indicate that zirconium reacts with nitrogen about 20 times slower than with oxygen. The overall process is very similar to oxidation in view of the high solubility of nitrogen in zirconium, and involves a large amount of dissolution along with film formation. In the case of nitriding in the α-region, a two phase diffusion process describes the behavior whereas β-phase nitriding involves three phases (nitrogen, like oxygen, stabilizes the α-phase, leading to a wide range of α between the nitride and the β-matrix). The reaction product is zirconium nitride (ZrN); the reaction is exothermic, releasing approximately 82 kcal/mole. (The energy released in forming the oxide is approximately 262 kcal/mole.) The thickness of the zirconium nitride layer has been found[149] to be much smaller than that of the dissolution zone (in the temperature range 750°C-1000°C) which indicates that the rate constant for film

109

formation is considerably smaller than the rate constant for nitrogen dissolution. In fact, at 1000°C, 84% of the total nitrogen uptake was due to dissolution in the metal.

The role of nitrogen in the high temperature reaction of zirconium with air has been investigated.[151] The reaction process is multi-phase in nature. Adjacent to the β-phase of the zirconium is a layer of α-phase (stabilized by both oxygen and nitrogen) and a surface layer of ZrO_2. In general, a certain amount of nitride (ZrN) is formed. For temperatures up to approximately 1050°C the nitride is found as a layer between the stabilized α-phase and the oxide layer; above 1050°C the nitride occurs as discrete particles dispersed in the oxide.

It is doubtful whether any appreciable amount of nitride is formed in the problem currently being considered. At the lower temperatures (during heat up) the reaction rate is very slow. Once rapid oxidation is initiated (approximately 900°C) the self-sustaining reaction proceeds very quickly, and there may not be sufficient time for ZrN to be formed. Any nitride that does form, however, will contribute to the chemical energy release for the self-sustaining reaction.

The reaction rate of zirconium is higher with air than with oxygen alone. The explanation advanced is that nitrogen dissolves in ZrO_2. By replacing oxygen ions in the oxide structure, the higher valency nitrogen can increase the anion vacancy concentration, thus permitting a higher rate of diffusion of oxygen through the anion-deficient zirconia.

There are a number of uncertainties associated with the Zircaloy-air reaction equation. These are particularly important above 900°C where rapid oxidation occurs. The most significant appear to be (i) the difference in the oxidation rates of zirconium and Zircaloy, and (ii) the multi-phase nature of the oxidation process itself at these temperatures. The results given above in Section C and D (i.e., for zirconium vs. Zircaloy-4, and oxygen consumption rate vs. oxidation rate, respectively) apply to oxidation in steam only. Analogous results are expected for oxidation in air, i.e., it is expected that the oxidation rate in Zircaloy will be greater than that in zirconium, and the rate of oxygen consumption will be greater than the rate of oxide formation in both materials. The relative magnitude of these effects cannot be deduced from the steam oxidation data. What are required are new experiments and computer modeling (similar to those carried out by Pawel and Campbell[136] for oxidation in steam) for the high temperature reaction of zirconium and Zircaloy with air. In lieu of these, we suggest that additional calculations be performed for two other zirconium-air reaction correlations which will serve as bounds for those presented in Figure B.1. (a) The high temperature correlation for zirconium (above the phase change of ZrO_2) should be multiplied by a factor m_1 to account for the higher reaction rate in Zircaloy. (b) The correlations above the α-β transformation temperature should be divided by a factor m_2 to account for

the difference in oxygen consumption rate and rate of oxide formation. Values of m_1 and m_2 as large as five should be considered.

F. New Data: The Pawel and Campbell data are compared with the Sandia curve in Figure B.3. It is immediately apparent that the Pawel and Campbell[152] parabolic rate constants are considerably lower than the curve used by Sandia. While the rate controlling step in the high temperature oxidation of zirconium or Zircaloys is the diffusion of oxygen through the oxide and/or though the solid solution of oxygen in Zircaloy that underlies it in both steam and air oxidation, there is a significant decrease in the oxidation rate observed in a steam environment due to an effect of the hydrogen produced during this oxidation on these diffusion constants. This effect has been observed by several workers, but it is not sufficiently quantified to permit the use of high temperature steam data (such as those of Prater and Courtright[153] and those of Pawel and Campbell[152]) to estimate oxidation rates under the fuel pool accident scenario. This leaves only the White[124] data in the high temperature range.

Some new unpublished data from Leistikow show roughly a parabolic corrosion rate behavior (slope of 1/2 on the log log plot) for the first 30-60 minutes in both air and steam. They also show that the difference between the air and the steam rates increases with temperature. After 30-60 minutes, however, the rate at all but the highest temperature increased dramatically, especially in air. This may be due either to difficulty in controlling the temperature of the highly exothermic zirconium/air oxidation, or to some "breakaway" type phenomenon in the surface oxides exposing the bare metal underneath.

At lower temperatures, zirconium and Zircaloy are known to oxidize according to the cubic law, which would mean a slope of 1/3 on a log log plot. The high temperature data used by Benjamin et al.[1] were all approximated using parabolic growth, which is more typical of diffusion controlled phenomenon such as are believed to occur at high temperatures. The new German data show a slope somewhere between 1/3 and 1/2 for the first 30 minutes or so. In an attempt to compare these data with the Sandia curve, a parabolic rate constant was calculated for Leistikow's data and compared with the Sandia curves and the Pawel and Campbell data in steam in Figure B.3. It is apparent that the German steam data and those of Pawel and Campbell for Zircaloy-4 in steam are consistent in the temperature range in which they overlap. The new German air data are consistent with some of their own work (at short exposure times) published some years earlier.[125] The new German data can be approximated by the rate equation:

$$\frac{(w)^2}{t} = 3.09 \times 10^8 \exp\left(-\frac{56,600}{RT}\right) \qquad (2)$$

where w is in mg O_2 reacted per square cm, t is in seconds, and T is in °K.

111

The instantaneous rate, dw/dt at time t and temperature T is given by

$$\frac{dw}{dt} = \frac{1}{2w}\ 3.09 \times 10^8\ \exp\ (-\frac{56,600}{RT}) \tag{3}$$

The Sandia[1] curve shows an abrupt increase in oxidation rate at $10^4/T$ = 7, which was attributed to the mono-tetragonal phase change of ZrO_2. As can be seen in Figure B.3, the Pawel and Campbell data do not show such an abrupt change at this temperature; however, these data were obtained in steam. The recent results of Prater and Courtright[153] (which were presented at the 1985 Symposium on Zirconium) show that for reactions in steam they find a similar jump at temperatures as high as 1500°C (1/T is 5.5 x 10^{-4}). This may be due to effects of the hydrogen produced by steam reaction on the oxide structure on the Zircaloy. Unfortunately, Prater and Courtright plotted their data in terms of thickness of the ZrO_2 film, and thus these could not readily be transferred to Figure B.3 which is in wt. of O_2 reacted. Since a considerable amount of the oxygen that reacts either from air or steam exists in high concentration solid solutions in the Zircaloy, and since the heat generated by this reaction is the main concern, it is important that the total oxygen consumption be considered rather than just the thickness of the layer. It is anticipated that the free energy of formation per gram atom of oxygen reacted would be approximately the same for the zirconium oxygen solid solution as for ZrO_2 at these high temperatures.

References for Appendix B

1. A.S. Benjamin, D.J. McCloskey, D.A. Powers and S.A., Dupree, "Spent Fuel Heatup Following Loss of Water During Storage," NUREG/CR-0649, March 1979.

2. N.A. Pisano, F. Best, A.S. Benjamin and K.T. Stalker, "The Potential for Propagation of a Self-Sustaining Zirconium Oxidation Following Loss of Water in a Spent Fuel Storage Pool," Draft Report, January 1984.

3. J.T. Han, Memo to M. Silberberg, May 21, 1984.

4. D.L. Douglass, "The Physical Metallurgy of Zirconium," Atom. Energy Rev. 1 4(1963) 71.

5. B. Lustman and F. Kerze, "Metallurgy of Zirconium," McGraw-Hill, NY (1955).

6. G.L. Miller, "Zirconium," Butterworths Science Publications, London (1954).

7. D.L. Douglass, "The Metallurgy of Zirconium," International Atomic Energy Agency, Vienna, 1971.

8. J.P. Pemsler, "Diffusion of Oxygen in Zirconium and its Relation to Oxidation and Corrosion," J. Electrochem. Soc. 105 (1958) 315.

9. M.W. Mallett, W.M. Albrecht and P.R. Wilson, "The Diffusion of Oxygen in Alpha and Beta Zircaloy-2 and Zircaloy-3 at High Temperatures," J. Electrochem. Soc. 106 (1959) 181.

10. J. Debuigne and P. Lehr, "Sur la Determination des Coefficients de Diffusion de L'Oxygene Dans le Systeme Zirconium-Oxygene," C.R. Acad. Sci. Paris 256 (1963) 1113.

11. G. Sainforth, R. Jacquesson and P. Laurent, "Diffusion de L'Oxygene Dans le Zirconium," Proc. Colloque sur la Diffusion a l'Etat Solide," North Holland Publishing Co., Amsterdam (1959) 79.

12. M. Davis, K.R. Montgomery and J. Standring, "The Diffusion Coefficient for Oxygen in Alpha-Zirconium," J. Inst. Metal 89 (1961) 172.

13. N. Cabrera and N.F. Mott, "Theory of Oxidation of Metals," Rep. Prog. Phys. 12 (1948) 163.

14. W.E. Campbell and U.B. Thomas, "The Oxidation of Metals," Trans. Electrochem. Soc. 91 (1947) 623.

15. H.H. Uhlig, "Initial Oxidation Rate of Metals and the Logarithmic Equation," Acta Metall. 4 (1956) 541.

16. J.E. Draley, D.H. Bradhurst and C.J. Van Drunen, Argonne National Lab. Report, ANL-7000 (1964) 223.

17. J.K. Dawson, Una C. Baugh and J.F. White, "Observations on the Early Stages of Oxidation of Zirconium and Zircaloy-2," Electrochem. Technol. 4 (1966) 137.

18. B. Cox, "The Oxidation and Corrosion of Zirconium and Its Alloys - V. Mechanism of Oxide Film Growth and Breakdown on Zirconium and Zircaloy-2," J. Electrochem. Soc. 108 (1961) 24.

19. B. Cox, "Low Temperature (<300°C) Oxidation of Zircaloy-2 in Water," J. Nucl. Mater. 25 (968) 310.

20. E.A. Gulbransen and K.F. Andrew, "Oxidation of Zirconium Alloys in Water Vapor Atmospheres Containing Trace Amounts of Oxygen at 375 and 575°C," Electrochem. Technol. 4 (1966) 99.

21. C.F. Britton and J.N. Wanklyn, "Inhibition by Boric Acid of the Oxidation of Zirconium in High-Pressure Steam," J. Nucl. Mater. 5 (1962) 326.

22. C.F. Britton, J.V. Arthurs and J.N. Wanklyn, "Further Studies on the Inhibition by Boric Acid of the Oxidation of Zirconium in High-Pressure Steam," J. Nucl. Mater. 15 (1965) 263.

23. J.T. Demant and J.N. Wanklyn, "Effects of Contamination on Oxidation of Zirconium in Steam," Corrosion 22 (1966) 60.

24. B. Cox and J.A. Reed, "Oxidation of a Zr-2, 5Nb Alloy in Steam and Air," Report AERE-R-4459 (1963).

113

25. A.B. Johnson, Jr., "Effects of Nuclear Radiation on the Corrosion, Hydriding and Oxide Properties of Six Zirconium Alloys," ASTM STP 458 (1969) 301.

26. D.L. Douglass, "Corrosion Mechanism of Zirconium and Its Alloys - III. Solute Distribution Between Corrosion Films and Zirconium Alloy Substrates," Corr. Sci. 5 (1965) 347.

27. S. Kass, J.D. Grozier and F.L. Shubert, "Effects of Silicon, Nitrogen, and Oxygen on the Corrosion and Hydrogen Absorption of Zircaloy-2," Corrosion 20 (1964) 350t.

28. E.A. Gulbransen and K.F. Andrew, "Oxidation of Zirconium Between 400 and 800°C," J. Metals (1957) 394.

29. B. Cox, "Rate-Controlling Processes During the Pre-Transition Oxidation of Zirconium Alloys," J. Nucl. Mater. 31 (1969) 48.

30. O. Flint and J.H.O. Varley, "On the Mechanism of Oxide-Film Formation on Zirconium," J. Phys. Chem. Solids 6 (1958) 213.

31. B. Cox, "Effects of Irradiation on the Oxidation of Zirconium Alloys in High Temperature Aqueous Environments," J. Nucl. Mater. 28 (1968) 1.

32. B. Cox, K. Alcock and F.W. Derrick, "The Oxidation and Corrosion of Zirconium and Its Alloys," J. Electrochem. Soc. 108 (1961) 129.

33. B. Cox, "The Effect of Fission Fragments and Neutron Irradiation on the Kinetics of Zirconium Oxidation," Reactivity of Solids (J.H. De Boer, Ed.) Proc. Fourth International Symposium on the Reactivity of Solids, Amsterdam (1960) 425.

34. R.C. Asher, D. Davis, A. Hall, B.A. Kirstein, J.W. Marriott and P.J. White, "Effects of Radiation on the Oxidation and Hydrogen Absorption of Zirconium Alloys in Steam," Electrochem. Technol. 4 (1966) 231.

35. C.J. Rosa, "Oxidation of Zirconium, A Critical Review of Literature," J. Less-Common Metals 16 (1968) 173.

36. P. Kofstad, "High Temperature Oxidation of Metals," Wiley and Sons, New York (1966).

37. J. Belle and M.W. Mallett, "Kinetics of the High Temperature Oxidation of Zirconium, J. Electrochem. Soc. 101 (1954) 339.

38. G.R. Wallwork, W.W. Smeltzer and C.J. Rosa, "The Parabolic Oxidation Kinetics of Alpha-Zirconium at 850°C," Acta Metall. 12 (1964) 409.

39. D.H. Bradhurst, J.E. Draley and C.J. Van Drunen, "An Electrochemical Model for the Oxidation of Zirconium," J. Electrochem. Soc. 112 (1965) 1171.

40. R.G. Charles, S. Barnartt and E.A. Gulbransen, "Prolonged Oxidation of Zirconium at 350 and 450°C," Trans. AIME 212 (1958) 101.

41. H.A. Porte, J.G. Schnizlein, R.C. Vogel and D.F. Fischer, "Oxidation of Zirconium and Zirconium Alloys," J. Electrochem. Soc. 107 (1960) 506.

42. K. Osthagen and P. Kofstad, "Oxidation of Zirconium and Zirconium-Oxygen Alloys at 800°C," J. Electrochem. Soc. 109 (1962) 204.

43. R.E. Westerman, "High-Temperature Oxidation of Zirconium and Zircaloy-2 in Oxygen and Water Vapor," J. Electrochem. Soc. 111 (1964) 140.

44. G. Beranger and P. Lacombe, "Contribution a l'etude de la cinetique de l'oxydation du zirconium-α et de la diffusion de l'oxygene dans le metal sous-jacent a l'oxyde," J. Nucl. Mater. 16 (1965) 190.

45. E. Hillner, "The High-Temperature Oxidation Kinetics of Zirconium in Dry Oxygen," Electrochem. Technol. 4 (1966) 132.

46. D. Cubicciotti, "The Oxidation of Zirconium at High Temperatures," J. Am. Chem. Soc. 72 (1950) 4138.

47. R.J. Hussey and W.W. Smeltzer, "The Mechanism of Oxidation of Zirconium in the Temperature Range of 400 to 850°C," J. Electrochem. Soc. 111 (1964) 1222.

48. J. Debuigne and P. Lehr, "Corrosion seche du zirconium non allie," Corrosion of Reactor Materials (Proc. Conf. Salzburg, 1962) 2 IAEA, Vienna (1962) 105.

49. B. De Gelas, G. Beranger and P. Lacombe, "L'oxydation a haute temperature du zirconium et de ses alliages binaires a faible teneur en element d'addition," J. Nucl. Mater. 29 (1969) 1.

50. I.I. Korobkov, D.V. Ignatov, A.I. Yevstyukhin and V.S. Yemel Yanov, "Electronographic and Kinetic Investigations of the Process of Oxidation of Zirconium and Certain Alloys of its Base," Metallurgiya i Metallovedenie chistykh Metallov 1 (1959) 144.

51. T.L. Mackay, "Oxidation of Single Crystal and Polycrystalline Zirconium," Trans. AIME 227 (1963) 1184.

52. G. Saur, H.J. Laue and H. Borchers, "Untersuchungen uber die Oxydation von Reactor-Grade-Zirkon," Metallurgie 15 (1961) 9.

53. A. Madeyski, D.J. Poulton and W.W. Smeltzer, "Parabolic Oxidation Kinetics of Alpha-Zirconium," Acta Metall. 17 (1969) 579.

54. K.A. Sense, "On the Oxidation of Zirconium," J. Electrochem. Soc. 109 (1962) 377.

55. C.A. Phalnikar and W.M. Baldwin, "Scaling of Zirconium in Air," Am. Soc. Testing Mater. Proc. 51 (1951) 1038.

56. D.J. Garibotti, H.M. Green and W.M. Baldwin, Jr., Report AECU-3013 (1955).

57. G. Beranger and P. Lacombe, "Contribution a l'etude de la cinetique d'oxydation du zirconium," C. r. Acad. Sci., Paris 258 (1964) 6147.

58. S. Nomura and C. Akutsu, "Oxidation Kinetics and Oxide Film Breakaway of Zirconium and its Alloys at High Temperatures," Electrochem. Technol. 4 (1966) 93.

59. J. Debuigne and P. Lehr, "Sur l'oxydation du zirconium," C. r. Acad. Sci., Paris 254 (1962) 3710.

60. P. Kofstad, "Effect of Impurities on the Defects in Oxides and their Relationship to Oxidation of Metals," Corrosion 24 (1968) 379.

61. W.M. Fassel, Jr., "The High-Temperature Oxidation of Metals," University of Utah Progress Report for the Period June 1 to September 26 (1952) NP-4246.

62. J. Takamura and Y. Sasaki, "Study on the Oxidation Resistance of Zirconium," Technical Reports of the Engineering Research Institute, Kyoto University, Vol. IX, No. 6, Report No. 58 (1959).

63. R.D. Misch and C. Van Drunen, "The Oxidation of Zirconium Binary Alloys in 700°C Oxygen for Times up to 200 Days," Proceedings of the USAEC Symposium on Zirconium Alloy Development, GEAP-4089, Vol. II (1962).

64. M. Perdereau and J. Bardolle, "Etude cinetique de l'oxydation de zirconium aux temperatures elevees," C. r. Acad. Sci., Paris 256 (1963) 4665.

65. A. Ronnquist and S. Shiels, "Reaction of Zirconium with Oxygen, Nitrogen, and Air, a Review of Published Data," Forsvarets Forskiningsanstalt Institution M, Stockholm Report A 14 (1966).

66. W.W. Smeltzer, R.R. Haering and J.S. Kirkaldy, "Oxidation of Metals by Short Circuit and Lattice Diffusion of Oxygen," Acta Metall. 9 (1961) 880.

67. J. Levitan, J.E. Draley and C.J. Van Drunen, "Low-Pressure Oxidation of Zirconium," J. Electrochem. Soc. 114 (1967) 1086.

68. J. Nierlich and J. Paidassi, "Sur la Cinetique de la Reaction du Zirconium avec l'oxygene sous basses pressions aux temperatures elevees, C. r. Acad. Sci., Paris 267 (1968) 1429.

69. J. Paidassi and J. Nierlich, "Sur les phenomenes de germination et de croissance de la zircone, ainsi que de striation du zirconium, au cours de la reaction de ce metal avec l'oxygene sous basses pressions, aux temperatures elevees," C. r. Acad. Sci., Paris 267 (1968) 1085.

70. G. Beranger and P. Lacombe, "Phenomenes de germination et de croissance au cours de l'oxydation superficielle du zirconium," Proc. IXe Colloque de Metallurgie, Presses Universitaires de France (1966) 181.

71. L. Rennuci and J.P. Langeron, "Oxydation du zirconium en phase β sous tres basses pressions, aspect superficiel presente par les alliages zirconium-oxygene," J. Nucl. Mater. 23 (1967) 79.

72. M. Perdereau and J. Bardolle, "Etude micrographique de l'oxydation menagee du zirconium," C. r. Acad. de Sci., Paris 257 (1963) 2477.

73. J.P. Pemsler, "Studies on the Oxygen Gradients in Oxidizing Metals," J. Electrochem. Soc. 113 (1966) 1242.

74. R.J. Hussey and W.W. Smeltzer, "The Oxidation Kinetics of Zirconium in the Temperature Range 400-600°C," J. Electrochem. Soc. 111 (1968) 564.

75. W.C. Hagel and C.J. Rosa, "Oxygen Diffusion in Hypostoichiometric Zirconium Oxide in the Temperature Range of 875 to 1050°C, Trans. AIME 242 (1968) 1293.

76. C.J. Rosa and W.C. Hagel, "Oxygen-ion Diffusivity in Hypostoichiometric Zirconium Dioxide," J. Nucl. Mater. 27 (1968) 12.

77. C.J. Rosa, "Evaluation of Oxidation Rates for Alpha-Zirconium," J. Less-Commons Metals 15 (1968) 35.

78. C.J. Rosa and W.W. Smeltzer, "The Parabolic Oxidation Kinetics of Beta-Zirconium," Acta Metall. 13 (1965) 55.

79. D.L. Douglass, "Corrosion Mechanism of Columbium, Zirconium, and Their Alloys: I. Diffusion of Oxygen in Columbium Pentoxide and Zirconium Dioxide," Corrosion of Reactor Materials (Proc. Conf. Salzburg, 1962) 2, IAEA, Vienna (1962) 223.

80. D.L. Douglass and G. Wagner, "The Oxidation of Oxygen-Deficient Zirconia and its Relationship to the Oxidation of Zirconium," J. Electrochem. Soc. 113 (1966) 671.

81. T. Smith, "Diffusion Coefficients and Anion Vacancy Concentrations for the Zirconium-Zirconium Dioxide System," J. Electrochem. Soc. 112 (1965) 560.

82. S. Aronson, "Oxidation and Equilibrium in Nonstoichiometric Zirconium Dioxide Powder," J. Electrochem. Soc. 108 (1961) 312.

83. B. Cox and J.P. Pemsler, "Diffusion of Oxygen in Growing Zirconia Films," J. Nucl. Mater. 28 (1968) 73.

84. A. Madeyski and W.W. Smeltzer, "Oxygen Diffusion in Monoclinic Zirconia," Mater. Res. Bull. 3 (1968) 369.

85. F.J. Keneshea and D.L. Douglass, "The Diffusion of Oxygen in Zirconia as a Function of Oxygen Pressure," Oxidation of Metals 3 (1970) 1.

86. M.W. Mallett and W.M. Albrecht, "High Temperature Oxidation of Two Zirconium-Tin Alloys," J. Electrochem. Soc. 102 (1955) 407.

87. D.J. Poulton and W.W. Smeltzer, "Oxygen Diffusion in Monoclinic Zirconia," J. Electrochem. Soc. 117 (1970) 378.

88. D.L. Douglass and J. Van Landuyt, "The Oxidation of Zirconium: An Electron Microscopy Study of Zirconia Formed in the Thin-Film Region," Acta Metall. 13 (1965) 1069.

89. G. Beranger, F. Duffaut, B. De Gelas and P. Lacombe, "Observations en microscopie electronique de films minces de zircone obtenus par oxydation du zirconium," J. Nucl. Mater. 19 (1966) 290.

90. G.F. Missiroli, "Electron Microscopic Observation of Oxidized Zirconium Films," J. Nucl. Mater. 25 (1968) 93.

91. D.L. Douglass and J. Van Landuyt, "Transmission Electron Microscopy of Zirconium and Zircaloy-2 Corrosion Films Formed in Air and Water," Proc. IXe Colloque de Metallurgie, Presses Universitaires de France (1966) 155.

92. B. De Gelas, G. Beranger and P. Lacombe, "Etude par microscopie electronique en transmission de films minces d'oxyde obtenus par oxydation d'alliages de zirconium a teneur en element d'addition inferieore a 4% en poids," J. Nucl. Mater. 28 (1968) 185.

93. J.E. Bailey, "On the Oxidation of Thin Films of Zirconium," J. Nucl. Mater. 8 (1963) 259.

94. J.E. Bailey, "The Oxidation of Thin Films of Zirconium," Electron Microscopy, 1964, Vol. A, Non-Biology, (Titlbach, M., Ed.) Publ. House Czech. Sci., Prague (1964) 395.

95. M. Denoux and J.J. Trillat, "Sur l'obtention de couches minces orientees de zirconium et leur oxydation," C. r. Acad. Sci., Paris 258 (1964) 4683.

96. M. Denoux, "Sur l'oxydation de couches minces orientees de zirconium," C. r. Acad. Sci., Paris 260 (1965) 5003.

97. M. Denoux and I.J. Trillat, "Etude de l'oxydation de couches minces orientees de zirconium; relation d'epitaxie oxyde-metal," Proc. IXe Colloque de Metallurgie, Presses Universitaires de France (1966) 173.

98. F.W. Vahldiek, "Epitaxial Oxidation of Zirconium at Various Temperatures," J. Less-Common Metals, 12 (1967) 19.

99. E.A. Gulbransen and K.F. Andrew, "Oxidation of Zircaloy-2 and -3A at 300 to 850°C," Trans. AIME 212 (1958) 281.

100. J.C. Greenbank and S. Harper, "Solute Distribution in Oxidized Zirconium Alloys," Electrochem. Technol. 4 (1966) 142.

101. B. Cox, "Oxidation and Corrosion of Zirconium and its Alloys" Corrosion 16 (1960) 380t.

102. B. Cox, "Causes of a Second Transition Point Occurring During Oxidation of Zirconium Alloys," Corrosion 18 (1962) 33t.

103. J.P. Pemsler, "The Kinetics and Mechanism of Oxide Film Growth on Zirconium," Electrochem. Technol. 4 (1966) 128.

104. J.C. Greenbank and S. Harper, "The Mechanism of Breakaway Oxidation in Zirconium Alloys," Electrochem. Technol. 4 (1966) 88.

105. D.L. Douglass, "Oxide Plasticity in the Oxidation Mechanism of Zirconium and its Alloys," Corrosion Sci. 5 (1965) 225.

106. L.H. Keys, G. Beranger, B. De Gelas and P. Lacombe, "Etude micrographique du processus de desquamation ("breakaway") au cours de l'oxydation du zirconium," J. Less-Common Metals 14 (1968) 181.

107. C. Roy and B. Burgess, "A Study of the Stresses Generated in Zirconia Films During the Oxidation of Zirconium Alloys," Oxidation of Metals 2 (1970) 235.

108. B. Cox, "Processes Occurring During the Breakdown of Oxide Films on Zirconium Alloys," J. Nucl. Mater. 29 (1969) 50.

109. E.A. Gulbransen and K.F. Andrew, "Breakaway Oxidation of Zirconium-Tin Alloys," Corrosion 14 (1958) 32t.

110. E.A. Gulbransen and K.F. Andrew, "Kinetics of the Reactions of Zirconium with O_2, N_2 and H_2," J. Metals 1 (1949) 515.

111. W.G. Guldner and L.A. Wooten, "Reactions of Zirconium with Gases at Low Pressure," Trans. Electrochem. Soc., 93: 223-235 (1948).

112. D. Cubicciotti, "The Oxidation of Zirconium at High Temperatures," J. Am. Chem. Soc., 72: 4138 (1950).

113. E.T. Hayes and A.H. Roberson, "Some Effects of Heating Zirconium in Air, Oxygen, and Nitrogen," Trans. Electrochem. Soc., 96: 142 (1949).

114. M.W. Mallett, H.R. Nelson and C.A. Papp, "The Reaction of Zirconium Metal Surfaces with Oxygen," Report BMI-727, 1952.

115. D.E. Thomas and J. Chirigos, "Oxidation of Zirconium and Relation to High-Temperature Corrosion in Water," Report WAPD-98, Oct. 15, 1953.

116. J. Chirigos and D.E. Thomas, "The Mechanism of Oxidation and Corrosion of Zirconium," Proc. AEC Metallurgy Conf. March 1952, p. 337, Report TID-5084; also Report WAPD-53.

117. H.A. Porte, J.G. Schnizlein, R.C. Vogel and D.F. Fischer, "Oxidation of Zirconium and Zirconium Alloys," Argonne National Laboratory, ANL-6046, September 1959.

118. R.R. Biederman, R.G. Ballinger and W.G. Dobson, "A Study of Zircaloy 4-Steam Oxidation Reaction Kinetics," EPRI NP-225, September 1976.

119. R.R.B. Biederman, R.D. Sisson, Jr., J.K. Jones and W.G. Dobson, "A Study of Zircaloy 4-Steam Oxidation Reaction Kinetics," EPRI NP-734, April 1978.

120. L.A. Charlot and A.B. Johnson, Jr., "Reaction of Zircaloy-2 with Water Vapor at 900 to 1200°C," on BNWL 120, July 15, 1965.

121. W.A. Bostrom, "The High Temperature Oxidation of Zircaloy in Water," WAPD-104, Westinghouse Electric Corporation, March 1954.

122. J.P. Pemsler, "Studies of the Oxygen Gradients in Oxidizing Metals, III. Kinetics of the Oxidation of Zirconium at High Temperatures," J. Electrochem. Soc. Vol. 112, pp. 447-484, 1965.

123. G.R. Wallwork, C.J. Rosa and W.W. Smeltzer, "Breakaway Phenomena in the Oxidation of Zirconium at 850 and 950°C," Corrosion Sci., Vol. 5, pp. 113-119, 1965.

124. J.H. White, Reported in AEC Fuels and Materials Development Program, Progress Report No. 67, GEMP-67, General Electric Co., 151, 1967.

125. S. Leistikow et al., "Study on High Temperature Steam Oxidation of Zircaloy-4 Cladding Tubes," Nuclear Safety Project Second Semiannual Report, 1975, KFK-2262, Karlsruhe, 233, 1976.

126. L.F. Kendall, "Reaction Kinetics of Zirconium and Zircaloy-2 in Dry Air at Elevated Temperatures," Hanford Atomic Products Operation, Washington, Contract No. W-31-109-Eng.-52, September 1955.

127. A.W. Urquhart and D.A. Vermilyea, "Characterization of Zircaloy Oxidation Films," Zirconium in Nuclear Applications, ASTM STP 551, American Society for Testing and Materials, 1974, pp. 463-478.

128. G.P. Sabol, S.G. McDonald and G.P. Airey, "Microstructure of the Oxide Films Formed on Zirconium-Based Alloys," Zirconium in Nuclear Applications, ASTM STP 551, American Society for Testing and Materials, 1974, pp. 435-448.

129. E. Hillner, "Corrosion of Zirconium-Base Alloys-An Overview," Zirconium in the Nuclear Industry, ASTM STP 633, A.L. Lowe, Jr. and G.W. Parry, Eds., American Society for Testing and Materials, 1977, pp. 211-235.

130. V.F. Urbanic, "Oxidation of Zirconium Alloys in Steam at 1000 to 1850°C," Zirconium in the Nuclear Industry, ASTM STP 633, A.L. Lowe, Jr. and G.W. Parry, Eds., American Society for Testing and Materials, 1977, pp. 168-181.

131. W.G. Dobson, R.R. Biederman and R.G. Ballinger, "Zircaloy-4 Oxidation in Steam Under Transient Oxidizing Conditions," Zirconium in the Nuclear Industry, ASTM STP 633, A.L. Lowe, Jr. and G.W. Parry, Eds., American Society for Testing and Materials, 1977, pp. 150-167.

132. A. Sawatzky, G.A. Ledoux and S. Jones, "Oxidation of Zirconium During a High-Temperature Transient," Zirconium in the Nuclear Industry, ASTM STP

633, A.L. Lowe, Jr. and G.W. Parry, Eds., American Society for Testing and Materials, 1977, pp. 134-149.

133. R.E. Pawel, R.A. Perkins, R.A. McKee, J.V. Cathcart, G.J. Yurek and R.E. Druschel, "Diffusion of Oxygen in Beta-Zircaloy and the High Temperature Zircaloy-Steam Reaction," Zirconium in the Nuclear Industry, ASTM STP 633, A.L. Lowe, Jr. and G.W. Parry, Eds., American Society for Testing and Materials, 1977, pp. 119-133.

134. P. Hofmann and C. Politis, "Chemical Interaction Between Uranium Oxide and Zircaloy-4 in the Temperature Range Between 900 and 1500°C," Zirconium in the Nuclear Industry (Fourth Conference), ASTM STP 681, American Society for Testing and Materials, 1979, pp. 537-560.

135. H. Ocken, R.R. Biederman, C.R. Hann and R.E. Westerman, "Evaluation Models of Zircaloy Oxidation in Light of Recent Experiments," Zirconium in the Nuclear Industry (Fourth Conference), ASTM STP 681, American Society for Testing and Materials, 1979, pp. 514-536.

136. R.E. Pawel and J.J. Campbell, "A Comparison of the High Temperature Oxidation Behavior of Zircaloy-4 and Pure Zirconium," Zirconium in the Nuclear Industry (Fifth Conference), ASTM STP 754, D.G. Franklin, Ed., American Society for Testing and Materials, 1982, pp. 370-389.

137. P. Hofmann, D. Kerwin-Peck and P. Nikolopoulos, "Physical and Chemical Phenomena Associated with the Dissolution of Solid UO_2 by Molten Zircaloy-4," Zirconium in the Nuclear Industry (Sixth Conference), ASTM STP 824, D.G. Franklin and R.B. Adamson, Eds., American Society for Testing and Materials, 1984, pp. 810-834.

138. H.M. Chung and G.R. Thomas, "High-Temperature Oxidation of Zircaloy in Hydrogen-Steam Mixtures," Zirconium in the Nuclear Industry (Sixth Conference), ASTM STP 824, D.G. Franklin and R.B. Adamson, Eds., American Society for Testing and Materials, 1984, pp. 793-809.

139. S. Leistikow, "Comparison of High-Temperature Steam Oxidation Kinetics Under LWR Accident Conditions: Zircaloy-4 Versus Austenitia Stainless Steel No. 1.4970," Zirconium in the Nuclear Industry (Sixth Conference), ASTM STP 824, D.G. Franklin and R.B. Adamson, Eds., American Society for Testing and Materials, 1984, pp. 763-779.

140. G.J. Yurek, J.V. Cathcart and R.E. Pawel, "Microstructures of the Scales Formed on Zircaloy-4 in Steam at Elevated Temperatures," Oxidation of Metals 10, 255 (1976).

141. R.E. Pawel, J.V. Cathcart and R.A. McKee, "The Kinetics of Oxidation of Zircaloy-4 in Steam at High Temperatures," J. Electrochem. Soc. 126, 1105 (1979).

142. R.E. Pawel, J.V. Cathcart and J.J. Campbell, "The Oxidation of Zircaloy-4 at 900 and 1100°C in High Pressure Steam," J. Nucl. Mater. 82, 129 (1979).

143. R.E. Pawel, "Oxygen Diffusion in the Oxide and Alpha Phases During Reaction of Zircaloy-4 with Steam from 1000°C to 1500°C," J. Electrochem. Soc. 126, 1111 (1979).

144. R.E. Pawel, J.V. Cathcart and R.A. McKee, "Anomalous, Oxide Growth During Transient-Temperature Oxidation of Zircaloy-4," Oxidation of Metals 14, 1 (1980).

145. R.E. Pawel and J.J. Campbell, "The Observation of Effects of Finite Specimen Geometry on the Oxidation Kinetics of Zircaloy-4," J. Electrochem. Soc. 127, 2188 (1980).

146. R.E. Pawel and J.J. Campbell, "The Oxidation of Pure Zirconium in Steam from 1000° to 1416°C," J. Electrochem. Soc. 128, 1999 (1981).

147. R.E. Pawel and J.J. Campbell, "The Effect of Structural Changes in the Oxide on the Oxidation Kinetics of Zirconium in High Temperatures Corrosion," NACE-6, 1983, p. 162.

148. A. Dravnieks, "The Kinetics of the Zirconium-Nitrogen Reaction at High Temperatures," J. Am. Chem. Soc. 72 (1950) 3568.

149. C.J. Rosa and W.W. Smeltzer, "The Nitriding Kinetics of Zirconium in the Temperature Range 750-1000°C," Electrochem. Technol. 4 (1966) 149.

150. M.W. Mallett, E.M. Baroody, H.R. Nelson and C.A. Papp, "The Surface Reaction of Nitrogen with Beta Zirconium and the Diffusion of Nitrogen in the Metal," Report BMI-709 (rev.), Dec. 12, 1951.

151. E.B. Evans, N. Tsangarakis, H.B. Probst and N.J. Garibotti, "Critical Role of Nitrogen During High Temperature Scaling of Zirconium," in High Temperature Gas-Metal Reactions in Mixed Environments; TMS-AIME, 1972, p. 248.

152. R.E. Pawel and J.J. Campbell, "Zirconium in the Nuclear Industry," ASTM STP 754, pg. 370, 1982.

153. J.T. Prater and E.L. Courtright, "Oxidation of Zircaloy-4 in Steam at 1300 to 2400°C," Presented at Seventh International Conference on Zirconium in the Nuclear Industry, June 24-27, 1985.
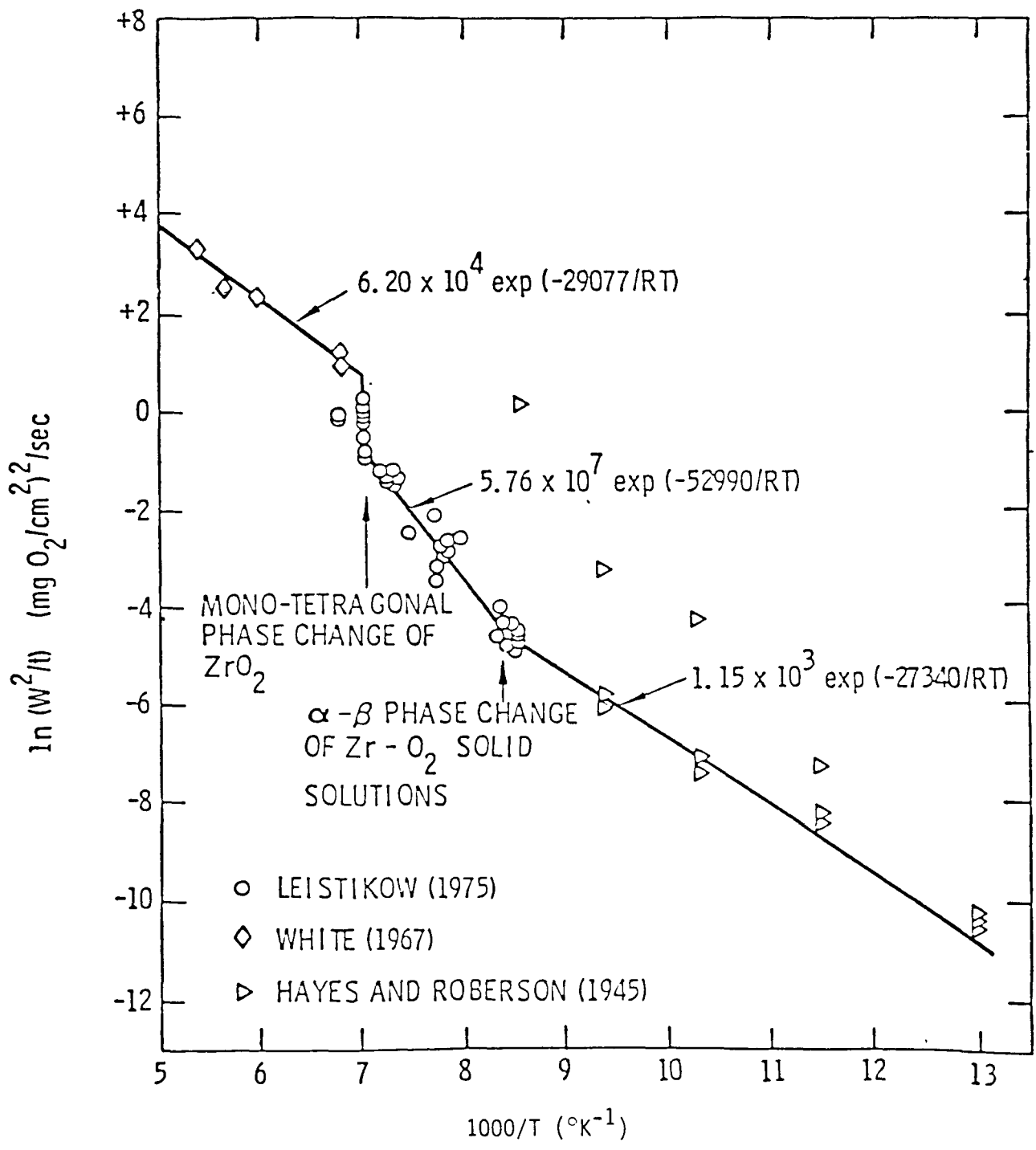
Figure B.1   Correlations for zirconium and Zr-4 oxidation
in air (from Ref. 1).

TEMP. (°C)

1600 1500 1400 1300 1200 1100 1000

10^{-5}

10^{-6}

Δ ALPHA LAYER,

$\dfrac{\delta_a^2}{2}$, cm²/s

OXIDATION OF Zr (———)

AND Zr-4 (— — —) IN STEAM

○ OXIDE LAYER, $\dfrac{\delta_b^2}{2}$, cm²/s

◇ OXYGEN CONSUMED, $\dfrac{\delta_T^2}{2}$, (g/cm²)²/s

$\dfrac{\delta^2}{2}$, PARABOLIC RATE CONSTANT

$1000/T(°K)$

50 55 60 65 70 75 80
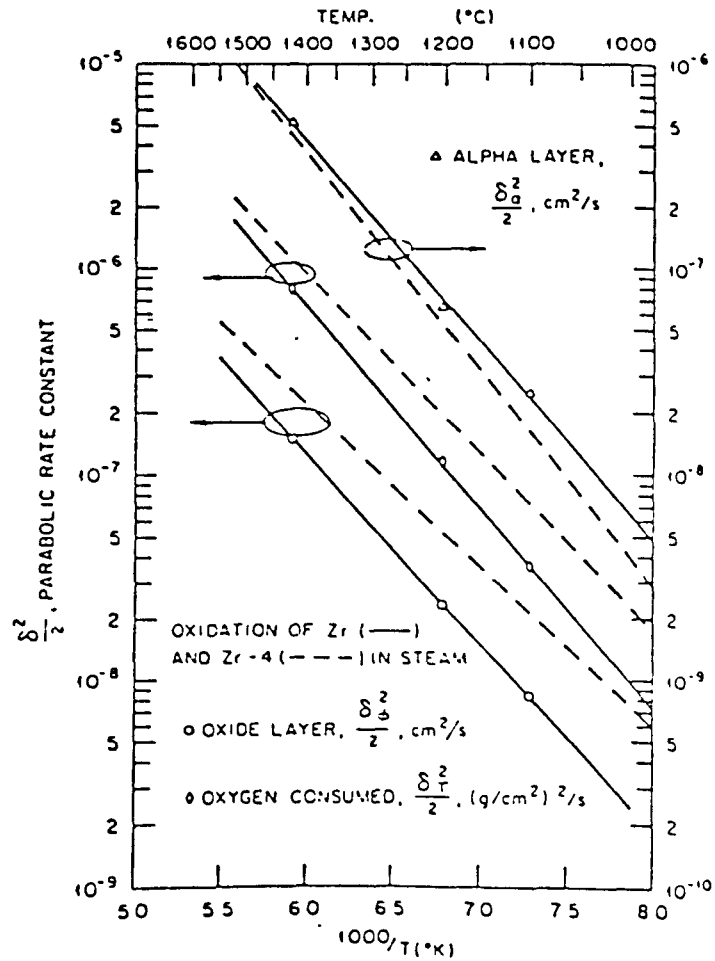
Figure B.2 Parabolic rate constants for oxide layer growth,
α-layer growth, and oxygen consumption for the
reaction of zirconium (solid lines) and Zircaloy-4
(dashed lines) with steam. The rate constants for
oxygen consumed (weight gain) were determined from
modeling analyses (from Ref. 136).

124
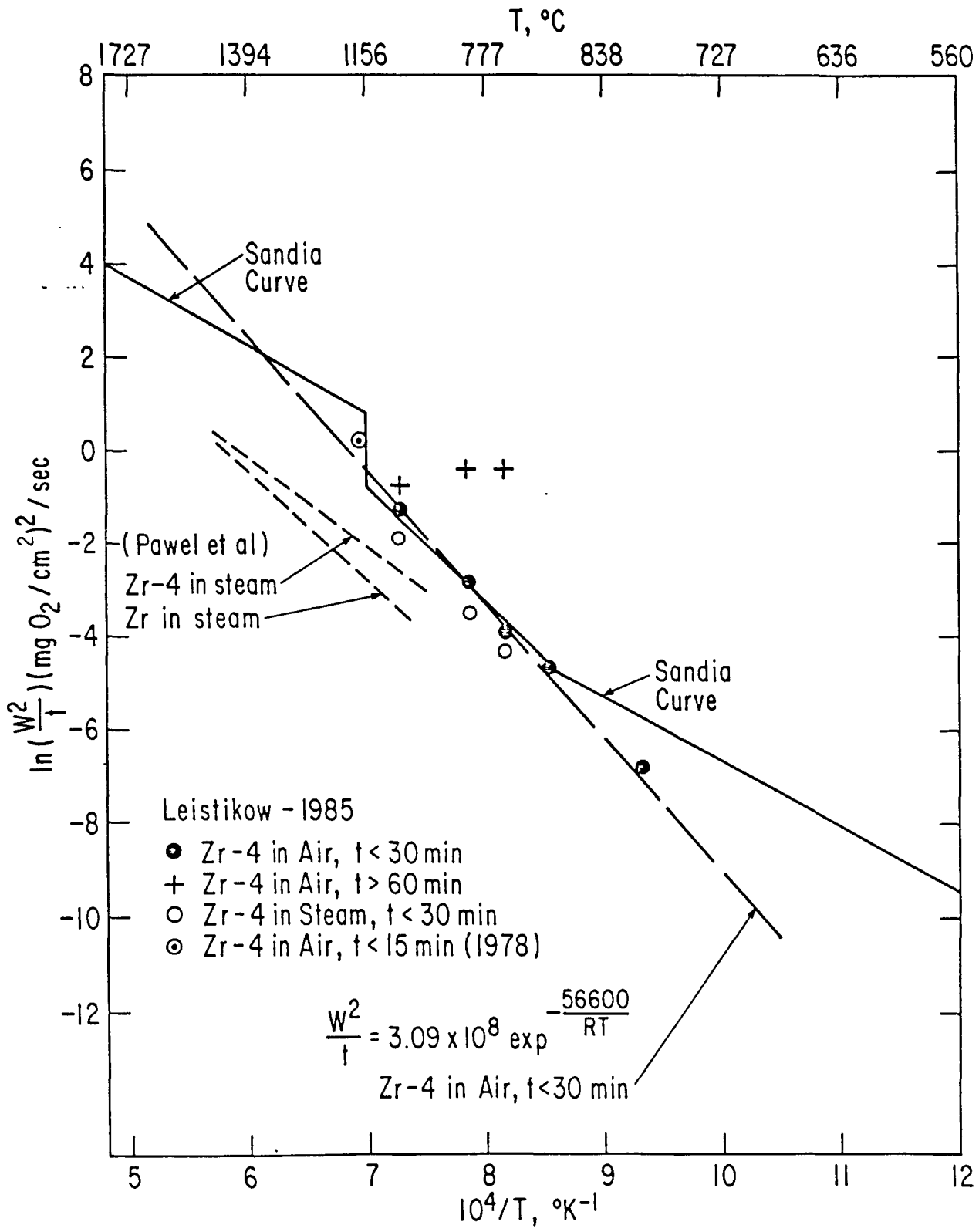
Figure B.3 Comparison of recent Zircaloy oxidation data with suggested correlations.

APPENDIX C

EXAMPLE IMPACT FOR SFUEL AND CRAC2 CALCULATIONS

C.1 INTRODUCTION

As discussed in the main report the uncertainty, in the risk estimates for spent fuel pool accidents is dominated by the uncertainty in the frequency estimate for loss of pool integrity events. However, the phenomenological progression and the resulting source terms for such accidents also have large uncertainties. In order to provide documentation of the methods used to analyze the phenomena, typical input files for SFUEL[1,2] and CRAC2[3] are provided in this appendix.

C.2 SFUEL INPUT

The SFUEL code[1,2] was developed at Sandia National Laboratories (SNL) to address the problem of spent fuel pool heating after a loss-of-coolant event. The code has been used extensively in the previous investigations to address the conditions (geometry and power level) which would result in self-sustaining oxidation of the fuel rod cladding. The purpose of the present investigation is to provide an independent assessment of the SFUEL code and its ability to predict cladding oxidation and failure propagation. A review of the oxidation data is given in Appendix B and a summary of the propagation results is given in Section 3 of the main report. In order to ensure repeatability of the results, an input deck is provided in Figure C.1. The input corresponds to a PWR high density storage rack.

C.3 CRAC2 INPUT

CRAC2[3] has been used extensively to calculate off-site consequences for hypothetical core melt accidents. While its input options provide a wide range of user features which are subject to individual interpretation, in practice the input has become standardized. Unfortunately, these standardized features become less useful for spent fuel pool releases which tend to be dominated by long lived isotopes (principally cesium). In order to facilitate further sensitivity studies or possible plant specific analyses, the input file for a typical run (Case 2A) is provided in Figure C.2. Note that the fission product inventory has been changed from the "normal" assumption of an equilibrium core after shutdown to the release estimates given in Section 4 of the main report.

REFERENCES FOR APPENDIX C

1. A.S. Benjamin, D.J. McClosksy, D.A. Powers, and S.A. Dupree, "Spent Fuel Heatup Following Loss of Water During Storage," prepared for the U.S. Nuclear Regulatory Commission by Sandia National Laboratories, NUREG/CR-0649 (SAND77-1371), May 1979.

2. N.A. Pisano, F. Best, A.S. Benjamin and K.T. Stalker, "The Potential for Propagation of a Self-Sustaining Zirconium Oxidation Following Loss of Water in a Spent Fuel Storage Pool," prepared for the U.S. Nuclear Regulatory Commission by Sandia Laboratories, (Draft Manuscript, January 1984) (Note: the project ran out of funds before the report was published.)

3. R.A. Lorenz, E.C. Beahm and R.P Wichner, "Review of Telliurium Release Rates from LWR Fuel Elements Under Accident Conditions," <u>Proceedings of the International Meeting on Light Water Reactor Severe Accident Evaluation</u>, August 28-September 1, 1983, pg. 4.4-1, American Nuclear Society Order 700085, ISBN 0-89448-1112-6.

```
                10 in,hd,1yr,vent

        ASINK=   0.000E+00
        CSINK =  0.000E+00
        DAMP=    0.000E+00
        DELT=    5.000E+01
        DLFACT=  5.000E+00
        DMWTR=   0.000E+00
                 0.000E+00
                 0.000E+00
        FL=      3.660E+02
        FSTR=    1.000E+00
        IBLOCK=      3
        ICHEM=       1
        IPLOT=       0
        N=          21
        NCEND=       1
        NPRINT=     36
        NPRNEW=     36
        NROD=      289
        NSECT=       3
        POWO=    4.614E-01
        PRMAX=   1.150E+06
        RCI=     4.180E-01
        RCO=     4.750E-01
        RF=      4.010E-01
        ROWS=    0.000E+00
        SMB=     2.500E-02
        TIMAX=   6.000E+04
        TIMWOF=  1.000E+09
        TIMWON=  0.000E+00
        TRDELT=  1.400E+03
        TRMAX=   6.000E+03
        TRPNT=   2.400E+03
        UL=      0.000E+00
        VENT=    0.000E+00
        VROOM=   4.250E+09
        WS=      2.160E+01
        WW=      2.160E+01
        XB=      6.350E-01
        XL=      6.350E-01
        XS=      0.000E+00
        XTB=     4.060E+01
        XW=      3.510E-01
        XWL=     4.060E+01
        XWW=     3.690E+00

          J  NASS         TIMEO

          1    4    0.000E+00
          2    4    0.000E+00
          3    4    0.000E+00

        CPCON=   1.047E+00
        CPL=     4.600E-01
        CPNI=    1.130E+00
        CPOX=    1.130E+00
        CPS=     3.640E-01
        CPW=     4.600E-01
        EPC=     7.000E-01
```

Figure C.1   Input data for the SFUEL1W code corresponding to
             a PWR high density rack.

```
EPL=      3.000E-01
EPS=      7.000E-01
EPT=      7.000E-01
EPW=      3.000E-01
FMULT= -1.000E+00
KMAX=       15
NDECAY=      3
RHOC=     6.500E+00
RHOCON= 2.340E+00
RHOF=     1.040E+01
RHOL=     7.820E+00
RHOS=     6.500E+00
RHOW=     7.820E+00
SMKCON= 1.200E-02
TO=       2.830E+02
XKBOT=   1.650E+02
XKTOP=   0.000E+00

  I       TCOOL       FDECAY

  1    1.000E-01   4.000E+00
  2    1.000E+00   5.900E+00
  3    1.000E+01   1.100E+01
```

Figure C.1 (Cont'd)

```
TWENTY FIVE REGIONS
SPATIAL                 25    NO
.5          1.0     1.5       2.        2.5       3.0       3.5       4.
4.5         5.      6.        7.        8.5       10.       12.5      15.
17.5        20.     25.       30.       35.       40.       45.       50.
55.
SITE                    1
INDPT WITH NYC MET           5 0 0 0 1
   29   04
ECONOMIC                1           NO
   499.0  3349.0        0.2    31527.0    4344.0    135.0         685.0
N.Y.        5      9 0.315    0.579     188.0     642.0
POPULATION             16
   2
UNIFORM POPULATION AND WIND ROSE
6.25E-02    4.91E+00  1.47E+01  2.46E+01  3.44E+01  4.42E+01  5.40E+01  6.38E+0
7.37E+01    8.35E+01  9.33E+01  2.16E+02  2.55E+02  4.57E+02  5.45E+02  1.10E+0
1.35E+03    1.60E+03  1.84E+03  4.42E+03  5.40E+03  6.38E+03  7.37E+03  8.35E+0
9.33E+03    1.03E+04
6.25E-02    4.91E+00  1.47E+01  2.46E+01  3.44E+01  4.42E+01  5.40E+01  6.38E+0
7.37E+01    8.35E+01  9.33E+01  2.16E+02  2.55E+02  4.57E+02  5.45E+02  1.10E+0
1.35E+03    1.60E+03  1.84E+03  4.42E+03  5.40E+03  6.38E+03  7.37E+03  8.35E+0
9.33E+03    1.03E+04
6.25E-02    4.91E+00  1.47E+01  2.46E+01  3.44E+01  4.42E+01  5.40E+01  6.38E+0
7.37E+01    8.35E+01  9.33E+01  2.16E+02  2.55E+02  4.57E+02  5.45E+02  1.10E+0
1.35E+03    1.60E+03  1.84E+03  4.42E+03  5.40E+03  6.38E+03  7.37E+03  8.35E+0
9.33E+03    1.03E+04
6.25E-02    4.91E+00  1.47E+01  2.46E+01  3.44E+01  4.42E+01  5.40E+01  6.38E+0
7.37E+01    8.35E+01  9.33E+01  2.16E+02  2.55E+02  4.57E+02  5.45E+02  1.10E+0
1.35E+03    1.60E+03  1.84E+03  4.42E+03  5.40E+03  6.38E+03  7.37E+03  8.35E+0
9.33E+03    1.03E+04
6.25E-02    4.91E+00  1.47E+01  2.46E+01  3.44E+01  4.42E+01  5.40E+01  6.38E+0
7.37E+01    8.35E+01  9.33E+01  2.16E+02  2.55E+02  4.57E+02  5.45E+02  1.10E+0
1.35E+03    1.60E+03  1.84E+03  4.42E+03  5.40E+03  6.38E+03  7.37E+03  8.35E+0
9.33E+03    1.03E+04
6.25E-02    4.91E+00  1.47E+01  2.46E+01  3.44E+01  4.42E+01  5.40E+01  6.38E+0
7.37E+01    8.35E+01  9.33E+01  2.16E+02  2.55E+02  4.57E+02  5.45E+02  1.10E+0
1.35E+03    1.60E+03  1.84E+03  4.42E+03  5.40E+03  6.38E+03  7.37E+03  8.35E+0
9.33E+03    1.03E+04
6.25E-02    4.91E+00  1.47E+01  2.46E+01  3.44E+01  4.42E+01  5.40E+01  6.38E+0
7.37E+01    8.35E+01  9.33E+01  2.16E+02  2.55E+02  4.57E+02  5.45E+02  1.10E+0
1.35E+03    1.60E+03  1.84E+03  4.42E+03  5.40E+03  6.38E+03  7.37E+03  8.35E+0
9.33E+03    1.03E+04
6.25E-02    4.91E+00  1.47E+01  2.46E+01  3.44E+01  4.42E+01  5.40E+01  6.38E+0
7.37E+01    8.35E+01  9.33E+01  2.16E+02  2.55E+02  4.57E+02  5.45E+02  1.10E+0
1.35E+03    1.60E+03  1.84E+03  4.42E+03  5.40E+03  6.38E+03  7.37E+03  8.35E+0
9.33E+03    1.03E+04
                      1.47E+01  2.46E+01  3.44E+01  4.42E+01  5.40E+01  6.38E+0
7.37E+01    8.35E+01  9.33E+01  2.16E+02  2.55E+02  4.57E+02  5.45E+02  1.10E+0
1.35E+03    1.60E+03  1.84E+03  4.42E+03  5.40E+03  6.38E+03  7.37E+03  8.35E+0
9.33E+03    1.03E+04
6.25E-02    4.91E+00  1.47E+01  2.46E+01  3.44E+01  4.42E+01  5.40E+01  6.38E+0
7.37E+01    8.35E+01  9.33E+01  2.16E+02  2.55E+02  4.57E+02  5.45E+02  1.10E+0
1.35E+03    1.60E+03  1.84E+03  4.42E+03  5.40E+03  6.38E+03  7.37E+03  8.35E+0
9.33E+03    1.03E+04
6.25E-02    4.91E+00  1.47E+01  2.46E+01  3.44E+01  4.42E+01  5.40E+01  6.38E+0
7.37E+01    8.35E+01  9.33E+01  2.16E+02  2.55E+02  4.57E+02  5.45E+02  1.10E+0
1.35E+03    1.60E+03  1.84E+03  4.42E+03  5.40E+03  6.38E+03  7.37E+03  8.35E+0
9.33E+03    1.03E+04
6.25E-02    4.91E+00  1.47E+01  2.46E+01  3.44E+01  4.42E+01  5.40E+01  6.38E+0
```

Figure C.2   Input data for the CRAC2 code for spent fuel release
             corresponding to 1/3 core after 90 days decay (Case
             2A in Table 4.7.

```
     7.37E+01    8.35E+01    9.33E+01    2.16E+02    2.55E+02    4.57E+02    5.45E+02    1.10E+0
     1.35E+03    1.60E+03    1.84E+03    4.42E+03    5.40E+03    6.38E+03    7.37E+03    8.35E+0
     9.33E+03    1.03E+04
     6.25E-02    4.91E+00    1.47E+01    2.46E+01    3.44E+01    4.42E+01    5.40E+01    6.38E+0
     7.37E+01    8.35E+01    9.33E+01    2.16E+02    2.55E+02    4.57E+02    5.45E+02    1.10E+0
     1.35E+03    1.60E+03    1.84E+03    4.42E+03    5.40E+03    6.38E+03    7.37E+03    8.35E+0
     9.33E+03    1.03E+04
     6.25E-02    4.91E+00    1.47E+01    2.46E+01    3.44E+01    4.42E+01    5.40E+01    6.38E+0
     7.37E+01    8.35E+01    9.33E+01    2.16E+02    2.55E+02    4.57E+02    5.45E+02    1.10E+0
     1.35E+03    1.60E+03    1.84E+03    4.42E+03    5.40E+03    6.38E+03    7.37E+03    8.35E+0
     9.33E+03    1.03E+04
     6.25E-02    4.91E+00    1.47E+01    2.46E+01    3.44E+01    4.42E+01    5.40E+01    6.38E+0
     7.37E+01    8.35E+01    9.33E+01    2.16E+02    2.55E+02    4.57E+02    5.45E+02    1.10E+0
     1.35E+03    1.60E+03    1.84E+03    4.42E+03    5.40E+03    6.38E+03    7.37E+03    8.35E+0
     9.33E+03    1.03E+04
     6.25E-02    4.91E+00    1.47E+01    2.46E+01    3.44E+01    4.42E+01    5.40E+01    6.38E+0
     7.37E+01    8.35E+01    9.33E+01    2.16E+02    2.55E+02    4.57E+02    5.45E+02    1.10E+0
     1.35E+03    1.60E+03    1.84E+03    4.42E+03    5.40E+03    6.38E+03    7.37E+03    8.35E+0
     9.33E+03    1.03E+04
TOPOG                         0
    110
ISOTOPE                      54    NO
CO-58    7           1.26 E+03 7.130E+01 1.000E-02 1.000E-00
CO-60    7           8.68 E+03 1.921E+03 1.000E-02 1.000E-00
KR-85    1           2.36 E+05 3.919E+03 0.        0.
KR-85M   1           0.00      1.867E-01 0.        0.
KR-87    1           0.00      5.278E-02 0.        0.
KR-88    1           0.00      1.167E-01 0.        0.
RB-86    4           1.05 E+03 1.865E+01 1.000E-02 1.000E-00
SR-89    6           7.75 E+03 5.200E+02 1.000E-02 1.000E-00
SR-90    6           3.82 E+03 1.026E+04 1.000E-02 1.000E-00
SR-91    6           0.00      3.950E-01 1.000E-02 1.000E-00
Y-90     8 SR-90     3.84 E+03 2.670E+00 1.000E-02 1.000E-00
Y-91     8 SR-91     1.30 E+04 5.880E+01 1.000E-02 1.000E-00
ZR-95    8           8.37 E+05 6.550E+01 1.000E-02 1.000E-00
ZR-97    8           0.00      7.000E-01 1.000E-02 1.000E-00
NB-95    8 ZR-95     1.41 E+06 3.510E+01 1.000E-02 1.000E-00
MO-99    7           0.00      2.751E+00 1.000E-02 1.000E-00
TC-99M   7 MO-99     0.00      2.508E-01 1.000E-02 1.000E-00
RU-103   7           1.04 E+02 3.959E+01 1.000E-02 1.000E-00
RU-105   7           0.00      1.850E-01 1.000E-02 1.000E-00
RU-106   7           1.99 E+02 3.690E+02 1.000E-02 1.000E-00
RH-105   7 RU-105    0.00      1.479E+00 1.000E-02 1.000E-00
SB-127   5           1.39 E-01 3.800E+00 1.000E-02 1.000E-00
SB-129   5           0.00      1.808E-01 1.000E-02 1.000E-00
TE-127   5 SB-127    2.80 E+03 3.896E-01 1.000E-02 1.000E-00
TE-127M  5           2.86 E+03 1.090E+02 1.000E-02 1.000E-00
TE-129   5 SB-129    1.56 E+03 4.861E-02 1.000E-02 1.000E-00
TE-129M  5           2.40 E+03 3.340E+01 1.000E-02 1.000E-00
TE-131M  5           0.00      1.250E+00 1.000E-02 1.000E-00
TE-132   5           1.73 E-03 3.250E+00 1.000E-02 1.000E-00
I-131    3 TE-131M   6.35 E+03 8.040E+00 1.000E-02 1.000E-00
I-132    3 TE-132    1.78 E-03 9.521E-02 1.000E-02 1.000E-00
I-133    3           0.00      8.667E-01 1.000E-02 1.000E-00
I-134    3           0.00      3.653E-02 1.000E-02 1.000E-00
I-135    3           0.00      2.744E-01 1.000E-02 1.000E-00
XE-133   1 I-133     2.30 E+02 5.290E+00 0.        0.
XE-135   1 I-135     0.00      3.821E-01 0.        0.
CS-134   4           3.34 E+06 7.524E+02 1.000E-02 1.000E-00
CS-136   4           8.13 E+03 1.300E+01 1.000E-02 1.000E-00
```

Figure C.2   (Cont'd)

```
CS-137    4              2.81 E+06 1.099E+04 1.000E-02 1.000E-00
BA-140    6              3.80 E+03 1.279E+01 1.000E-02 1.000E-00
LA-140    8 BA-140       4.38 E+02 1.676E+00 1.000E-02 1.000E-00
CE-141    8              3.61 E+00 3.253E+01 1.000E-02 1.000E-00
CE-143    8              0.00      1.375E+00 1.000E-02 1.000E-00
CE-144    8              1.65 E+01 2.844E+02 1.000E-02 1.000E-00
PR-143    8 CE-143       2.41 E-01 1.358E+01 1.000E-02 1.000E-00
ND-147    8              3.36 E-02 1.099E+01 1.000E-02 1.000E-00
NP-239    8              0.00      2.350E+00 1.000E-02 1.000E-00
PU-238    8 CM-242       6.87 E-02 3.251E+04 1.000E-02 1.000E-00
PU-239    8 NP-239       9.28 E-03 8.912E+06 1.000E-02 1.000E-00
PU-240    8 CM-244       1.55 E-02 2.469E+06 1.000E-02 1.000E-00
PU-241    8              3.70 E+00 5.333E+03 1.000E-02 1.000E-00
AM-241    8 PU-241       7.00 E-03 1.581E+05 1.000E-02 1.000E-00
CM-242    8              1.01 E+00 1.630E+02 1.000E-02 1.000E-00
CM-244    8              5.84 E-02 6.611E+03 1.000E-02 1.000E-00
LEAKAGE              1    NO
EARLY     1.0      0.0        5.0        0.0           1.4E05 30.0
1.0       0.0      1.0        1.0        1.0        1.0        1.0        1.0
DISPERSION
100.0     25.0          0    34    0
EVACUATE             1    NO          NO
     1.0                                                    2.         .2
        .75        1.         .5         .75        .33        .5         .08        .3
     2.66E-4    2.66E-4   1.33E-4    2.66E-4
        8045.         90.       165.         3.      1
ACUTE                     7
T MARROW  320.      400.       510.       615.       .03        .5         1.
LLI WALL  2000.     5000.      5000.      5000.      1.         1.         1.
LUNG      5000.     14800.     22400.     24000.     .24        .73        1.
W BODY    55.       150.       280.       370.       .30        .8         0.
LUNG      3000.     3000.1     6000.      6000.      .05        1.0        0.
LLI WALL  1000.     1000.1     2500.      2500.      .05        1.0        0.
THYROID        1.E10      1.E10      1.E10      1.E10       1.0        1.0        0.
LATENT                    8
     10CENT EST  30.         5.          300.        2.5
T MARROW  LEUKEMIA   2.836E-05 2.720E-05 1.872E-05 1.382E-05 9.720E-06 6.770E-0
  4.040E-06 1.700E-06 4.900E-07 0.0        1.0
LUNG      LUNG       2.749E-05 2.749E-05 2.749E-05 1.587E-05 8.130E-06 3.990E-0
  1.500E-06 2.200E-07 0.0        0.0        0.5
OTHER     BREAST     3.172E-05 3.172E-05 3.172E-05 1.831E-05 9.380E-06 4.600E-0
  1.730E-06 2.500E-07 0.0        0.0        1.000E+09
SKELETON  BONE       1.107E-05 1.064E-05 6.990E-06 3.020E-06 1.670E-06 9.100E-0
  4.200E-07 1.200E-07 1.000E-08 0.0        1.0
LLI WALL  GI TRK     1.688E-05 1.688E-05 1.688E-05 9.740E-06 4.990E-06 2.450E-0
  9.200E-07 1.300E-07 0.0        0.0        1.0
OTHER     OTHER      3.220E-05 3.050E-05 2.539E-05 1.466E-05 7.520E-06 3.690E-0
  1.390E-06 2.000E-07 0.0        0.0        1.0
W BODY    W BODY     1.579E-04 1.533E-04 1.274E-04 7.542E-05 4.141E-05 2.241E-0
  1.000E-05 2.620E-06 5.000E-07 0.0        1.0
THYROID   THYROID    3.34E-04
                                         1.00E 09
CHRONIC EXPOSURE          6
     10    1    1.000        365.       25550.                 3.0        15.0
SR-90          0.0525     0.0718
RU-106         0.0397     0.0533
CS-137         0.0525     0.105
PU-238         0.0529     0.107
PU-239         0.0530     0.108
PU-240         0.0530     0.108
```

Figure C.2 (Cont'd)

```
PU-241          0.0520      0.101
AM-241          0.0530      0.108
CM-242          0.0292      0.0327
CM-244          0.0522      0.102
    3    11      1.0         365.        365.      14.0      2.0       3.3
CS-134          8.44        4.22
LUNG            6.47E+4     7.31E+4
T MARROW        6.50E+4     7.34E+4
SKELETON        6.41E+4     7.24E+4
T E C L         6.41E+4     7.24E+4
ST WALL         7.40E+4     8.34E+4
SI+CONT         8.05E+4     9.09E+4
ULI WALL        7.95E+4     8.96E+4
LLI WALL        8.28E+4     9.33E+4
THYROID         6.49E+4     7.33E+4
OTHER           6.27E+4     7.08E+4
W BODY          6.32E+4     7.14E+4
TESTES          7.57E+4     8.55E+4
OVARIES         6.68E+4     7.55E+4
CS-136          2.84        1.42
LUNG            8.82E+3     8.82E+3
T MARROW        9.29E+3     9.29E+3
SKELETON        9.10E+3     9.10E+3
T E C L         9.10E+3     9.10E+3
ST WALL         1.15E+4     1.15E+4
SI+CONT         1.19E+4     1.19E+4
ULI WALL        1.20E+4     1.20E+4
LLI WALL        1.35E+4     1.35E+4
THYROID         9.23E+3     9.23E+3
OTHER           8.88E+3     8.88E+3
W BODY          8.96E+3     8.96E+3
TESTES          1.03E+4     1.03E+4
OVARIES         9.48E+3     9.48E+3
CS-137          8.44        4.22
LUNG            4.71E+4     5.59E+4
T MARROW        4.73E+4     5.61E+4
SKELETON        4.68E+4     5.56E+4
T E C L         4.68E+4     5.56E+4
ST WALL         5.18E+4     6.13E+4
SI+CONT         5.39E+4     6.39E+4
ULI WALL        5.40E+4     6.39E+4
LLI WALL        5.64E+4     6.64E+4
THYROID         4.68E+4     5.55E+4
OTHER           4.60E+4     5.45E+4
W BODY          4.62E+4     5.49E+4
TESTES          5.18E+4     6.15E+4
OVARIES         4.81E+4     5.70E+4
    2     2      1.0         365.        365.      14.0      2.0       3.3
SR-89           .397        0.402
LUNG            2.91E+3     5.81E+2
T MARROW        2.63E+4     5.26E+3
SKELETON        5.95E+4     1.19E+4
T E C L         6.00E+4     1.20E+4
ST WALL         1.56E+4     3.12E+3
SI+CONT         2.73E+4     5.45E+3
ULI WALL        1.46E+5     2.91E+4
LLL WALL        4.27E+5     8.53E+4
THYROID         2.91E+3     5.81E+2
OTHER           2.91E+3     5.81E+2
W BODY          9.55E+3     1.91E+3
```

Figure C.2 (Cont'd)

```
TESTES        2.91E+3   5.81E+2
OVARIES       2.91E+3   5.81E+2
SR-90          .505      .588
LUNG          1.59E+4   3.18E+3   5.50E+2   1.80E+1
T MARROW      1.04E+6   2.08E+5   5.25E+4   1.29E+4   1.00E+4   3.10E+3
SKELETON      3.08E+6   6.15E+5   2.57E+5   9.81E+4   1.09E+5   4.30E+4
T E C L       2.64E+6   5.27E+5   1.93E+5   6.77E+4   7.20E+4   2.76E+4
ST WALL       2.03E+4   4.05E+3   5.50E+1   1.80E+1
SI+CONT       2.64E+4   5.28E+3   5.50E+1   1.80E+1
ULI WALL      1.06E+5   2.11E+4   5.00E+1   2.00E+1
LLL WALL      4.06E+5   8.12E+4   5.00E+1
THYROID       1.59E+4   3.18E+3   5.50E+1   1.80E+1
OTHER         1.59E+4   3.18E+3   5.50E+1   1.30E+1
W BODY        2.76E+5   5.52E+4   2.03E+4   7.44E+3   8.08E+3   3.13E+3
TESTES        1.59E+4   3.18E+3   5.50E+1   1.80E+1
OVARIES       1.59E+4   3.18E+3   5.50E+1   1.80E+1
      2    9     1.0       0.0      365.      _ 14.0      0.0      10.0
I-133         1.00E-8   0.00486
LUNG          8.53E+2   1.58E+2
T MARROW      7.99E+2   1.48E+2
SKELETON      7.88E+2   1.46E+2
T E C L       7.88E+2   1.46E+2
ST WALL       1.11E+4   2.06E+3
SI+CONT       2.30E+3   4.25E+2
ULI WALL      6.16E+3   1.14E+3
LLI WALL      9.83E+3   1.82E+3
THYROID       1.73E+6   3.21E+5
OTHER         9.07E+2   1.68E+2
W BODY        1.46E+3   2.70E+2
TESTES        7.13E+2   1.32E+2
OVARIES       9.99E+2   1.85E+2
I-131         1.00E-8   0.692
LUNG          1.92E+3   3.56E+2
T MARROW      1.55E+3   2.87E+2
SKELETON      1.67E+3   3.10E+2
T E C L       1.67E+3   3.10E+2
ST WALL       6.16E+3   1.14E+3
SI+CONT       1.79E+3   3.32E+2
ULI WALL      4.49E+3   8.32E+2
LLI WALL      1.03E+4   1.91E+3
THYROID       9.07E+6   1.68E+6
OTHER         2.20E+3   4.07E+2
W BODY        4.75E+3   8.79E+2
TESTES        7.51E+3   1.39E+2
OVARIES       1.15E+3   2.21E+2
      4    2     1.000    3650.     3650.     2400.       5.0       5.0
CS-134         .164      .0547
LUNG          7.31E+4
T MARROW      7.34E+4
SKELETON      7.24E+4
T E C L       7.24E+4
ST WALL       8.34E+4
SI+CONT       9.09E+4
ULI WALL      8.96E+4
LLI WALL      9.33E+4
THYROID       7.33E+4
OTHER         7.08E+4
W BODY        7.14E+4
TESTES        8.55E+4
OVARIES       7.55E+4
```

Figure C.2 (Cont'd)

CS-137	.250	.0835				
LUNG	5.59E+4					
T MARROW	5.61E+4					
SKELETON	5.56E+4					
T E C L	5.56E+4					
ST WALL	6.13E+4					
SI+CONT	6.39E+4					
ULI WALL	6.39E+4					
LLI WALL	6.64E+4					
THYROID	5.55E+4					
OTHER	5.45E+4					
W BODY	5.49E+4					
TESTES	6.15E+4					
OVARIES	5.70E+4					
SR-89	.0136	.0068				
LUNG	5.81E+2					
T MARROW	5.26E+3					
SKELETON	1.19E+4					
T E C L	1.20E+4					
ST WALL	3.12E+3					
SI+CONT	5.45E+3					
ULI WALL	2.91E+4					
LLL WALL	8.53E+4					
THYROID	5.81E+2					
OTHER	5.81E+2					
W BODY	1.91E+3					
TESTES	5.81E+2					
OVARIES	5.81E+2					
SR-90	1.340	0.669				
LUNG	3.18E+3	5.50E+2	1.80E+1			
T MARROW	2.08E+5	5.25E+4	1.29E+4	1.00E+4	3.10E+3	3.103+3
SKELETON	6.15E+5	2.57E+5	9.81E+4	1.09E+5	4.30E+4	4.30E+4
T E C L	5.27E+5	1.93E+5	6.77E+4	7.20E+4	2.76E+4	2.76E+4
ST WALL	4.05E+3	5.50E+1	1.80E+1			
SI+CONT	5.28E+3	5.50E+1	1.80E+1			
ULI WALL	2.11E+4	5.00E+1	2.00E+1			
LLL WALL	8.12E+4	5.00E+1				
THYROID	3.18E+3	5.50E+1	1.80E+1			
OTHER	3.18E+3	5.50E+1	1.30E+1			
W BODY	5.52E+4	2.03E+4	7.44E+3	8.08E+3	3.13E+3	3.13E+3
TESTES	3.18E+3	5.50E+1	1.80E+1			
OVARIES	3.18E+3	5.50E+1	1.80E+1			
10	11	0.333	365.	10950.	3285.	5.0	25.0

```
CO-58
CO-60
NB-95
ZR-95
RU-103
RU-106
I-131
CS-134
CS-136
CS-137
SCALE              36    NO
1.    EO2.    EO3.    EO5.    EO7.    EO1.    E12.    E13.    E
5.    E17.    E11.    E22.    E23.    E25.    E27.    E21.    E
2.    E33.    E35.    E37.    E31.    E42.    E43.    E45.    E
7.    E41.    E52.    E53.    E55.    E57.    E51.    E62.    E
3.    E65.    E67.    E61.    E7
RESULT              19    NO
```

Figure C.2 (Cont'd)

```
ACUTE FATALITIES
ACUTE INJURIES
FATAL RADIUS(MI)
INJUR RADIUS(MI)
ACU BMR DS-INT 2                    1.0E-02
ACU BMR DS-INT10                    1.0E-02
ACU BMR DS-INT14                    1.0E-02
ACU BMR DS-INT18                    1.0E-02
ACU BMR DS-INT20                    1.0E-02
ACU BMR DS-INT24                    1.0E-02
ACU THY DS-INT 2                    1.0E-02
ACU THY DS-INT10                    1.0E-02
ACU THY DS-INT14                    1.0E-02
ACU THY DS-INT18                    1.0E-02
ACU THY DS-INT20                    1.0E-02
ACU THY DS-INT24                    1.0E-02
TOT WBODY MANREM                    1.0E+02
INTERD AREA
DECON AREA
OPTIONS                      NO
                   -1
END
 RUN NO.5, CASE2A, 90-DAY DECAY, 100% RELEASE
EVACUATE                  1
     1.0                                                                    1.0
         .67        1.0        .5       .67       .32       .5      .05     .32
    2.66E-4    2.66E-4   1.33E-4   2.66E-4
       8045.       90.       95.        3.    1
END
```

Figure C.2 (Cont'd)

137

1 REPORT NUMBER (Assigned by TIDC add Vol No, if any)
NUREG/CR-4982
BNL-NUREG-52093

2 TITLE AND SUBTITLE	3 LEAVE BLANK		
Severe Accidents in Spent Fuel Pools in Support of Generic Safety Issue 82			
	4 DATE REPORT COMPLETED		
	MONTH		YEAR
	June		1987

5 AUTHOR(S)	6 DATE REPORT ISSUED	
V.L. Sailor, K.R. Perkins, J.R. Weeks and H.R. Connell	MONTH	YEAR
	July	1987

7 PERFORMING ORGANIZATION NAME AND MAILING ADDRESS (Include Zip Code)	8 PROJECT/TASK/WORK UNIT NUMBER
Brookhaven National Laboratory	
Upton, NY 11973	9 FIN OR GRANT NUMBER
	FIN A-3786

10 SPONSORING ORGANIZATION NAME AND MAILING ADDRESS (Include Zip Code)	11a TYPE OF REPORT
Division of Reactor and Plant Systems	
Office of Nuclear Regulatory Research	
U.S. Nuclear Regulatory Commission	b PERIOD COVERED (Inclusive dates)
Washington, DC 20555	

12 SUPPLEMENTARY NOTES

13 ABSTRACT (200 words or less)

This investigation provides an assessment of the likelihood and consequences of a severe accident in a spent fuel storage pool - the complete draining of the pool. Potential mechanisms and conditions for failure of the spent fuel, and the subsequent release of the fission products, are identified. Two older PWR and BWR spent fuel storage pool designs are considered based on a preliminary screening study which tried to identify vulnerabilities. Internal and external events and accidents are assessed. Conditions which could lead to failure of the spent fuel Zircaloy cladding as a result of cladding rupture or as a result of a self-sustaining oxidation reaction are presented. Propagation of a cladding fire to older stored fuel assemblies is evaluated. Spent fuel pool fission product inventory is estimated and the releases and consequences for the various cladding failure scenarios are provided. Possible preventive or mitigative measures are qualitatively evaluated. The uncertainties in the risk estimate are large, and areas where additional evaluations are needed to reduce uncertainty are identified.

14 DOCUMENT ANALYSIS - a KEYWORDS/DESCRIPTORS	15 AVAILABILITY STATEMENT
Spent fuel pools, generic safety issue, probabilistic risk assessment, PWRs, BWRs, Zircaloy oxidation, seismic hazard, fragility fission products, consequences, failure propagation, oxidation rate, SFUEL, CRAC2, ORIGEN2, decay heat	Unlimited
	16 SECURITY CLASSIFICATION
b IDENTIFIERS/OPEN ENDED TERMS	(This page) Unclassified
	(This report) Unclassified
	17 NUMBER OF PAGES
	18 PRICE